ANNUAL REPORT 2006

Asociación EURATOM-CIEMAT para Fusión

INDICE:

I. INTRODUCTION 1

II. TJ-II ENGINEERING AND OPERATION 4

II.1. Operation of TJ-II during 2006 4

II.2. Basic Machine Engineering 5

II.2.1. Introduction 5

II.2.2. Technical operation of the TJ-II 5

II.2.3. Power supply 6

II.2.3.1. Study of a new generator's mode of operation 6

II.2.3.2. New current measurement system in the Active Filter of TJ-II 6

II.2.4. Control system 7

II.2.4.1. Protection against NBI breaks 7

II.2.4.2. Java application for the timers of the diagnostic section 7

II.2.4.3. Event-oriented data base 7

II.2.4.4. New ground loop supervision system 8

II.2.5. International collaborations 8

II.2.5.1. Monitoring of the ENSA contract for IPP 8

II.3. ECR Heating 8

II.3.1. ECRH system routine operation and improvements 8

II.3.2. Design and manufacture of a new high voltage power supply 9

II.3.3. ECCD experiments 10

II.3.4. Experiments in Heliotron-J 10

II.3.5. Status of the Electron Bernstein Waves heating project 11

II.3.6. Electron Bernstein waves emission diagnostic 11

II.3.7. Influence of the controlled modulated power reflected back to the gyrotron 11

II.3.8. Participation in design and the testing of the remote steering upper launcher of the ECRH system for ITER 12

II.3.9. New developments on the High Critical Temperature Superconductor. 12

II.4. Neutral Beam Injection 13

II.4.1. Injector #1 13

II.4.2. Injector #2 14

II.5. Data acquisition Unit (DAQU) 15

II.5.1. Intelligent data retrieval methods 15

II.5.1.1. Entire waveform approach 16

II.5.1.2. Patterns in waveforms approach 16

II.5.2. Remote participation 16

II.5.2.1. Software architecture for remote experimentation 16

II.5.2.2. Access security 16

II.5.2.3. Message oriented middleware 17

II.5.2.4. Shared data access system 17

II.5.3. Data compression 17

II.5.4. Real-time event detection 17

II.6. Electronics and Diagnostic Control 17

II.6.1. Diagnostic Control System (DCS) architecture 18

II.6.2. New diagnostics 18

II.6.2.1. Internal mirror of the Electron Bernstein Waves 18

II.6.2.2. Automated system for control of the vacuum diagnostic system for the TJ-II 18

II.6.2.3. 6.2.3. Control system of four Li ovens 18

II.7. Plasma -wall activities 19

II.7.1. Activities in TJ-II. 19

II.7.1.1. 7. 1 .1 Hydrocarbon injection 19

II.7.1.2. He beam diagnostic 19

II.7.1.3. EIRENE simulation of neutral profiles 20

II.7.1.4. Neutral density studies 21

II.7.1.5. Wall Conditioning 22

II.7.2. Activities in H retention control 22

II.7.2.1. Scavengers 22

II.7.2.2. Plasma and HT Oxidation 23
II.7.3. Other activities 24
II.7.3.1. ITER Pressure Gauges 24

III. PHYSICS STUDIES 25

III.1. INTRODUCTION 25

III.2. Confinement and electric fields in ECRH and NBI plasmas 25

III.2.1. Global and local transport studies 25
III.2.2. Electric fields in ECRH and NBI plasmas 26
III.2.3. Kinetic studies 26
III.2.4. Statistical description of transport 27

III.3. Transitions and magnetic topology 28

III.4. Plasma rotation and momentum re-distribution mechanisms 29

III.4.1. Comparison of impurity poloidal rotation in ECRH and NBI plasmas 29
III.4.2. Edge sheared flows in TJ-II: 2-D visualization of edge turbulence in the TJ-II stellarator 29
III.4.3. Edge sheared flows: relaxation of electric fields 30
III.4.4. Edge sheared flows: comparison between model and experimental results 31
III.4.5. Edge sheared flows: Energy transfer between flows and turbulence 32

III.5. MHD studies 32

III.6. Diagnostic development 33

III.6.1. Diagnostic neutral beam injector (DNBI) 33
III.6.2. Hydrogen pellet injector 35
III.6.3. Neutral Particle Analyser Systems 35
III.6.4. Thomson scattering 36
III.6.5. Microwave reflectometry in TJ-II 37

III.6.6. Two colour infrared interferometer 37

III.6.7. Spectroscopy..... 38

III.7. JET activities..... 38

III.7.1. Inboard-Outboard pedestal temperature measurements in JET using ECE diagnostics 38

III.7.2. Upgrade of the heterodyne radiometer at JET 39

III.7.2.1. Test Camera system (within FC7 Enhancement Project) and experimental results in JET 39

IV. THEORY AND SIMULATION 40

IV.1. Grid Computing Research 40

IV.1.1. Grid computing for fusion..... 40

IV.2. Transport..... 40

IV.2.1. Dynamics of recycling and density control 40

IV.2.2. Experimental Electron Heat Diffusion in TJ-II ECRH plasmas..... 41

IV.2.3. One-dimensional model for the emergence of the plasma edge shear flow layer with momentum conserving Reynolds stress..... 42

IV.2.4. Fractional generalization of Fick's law..... 42

IV.2.5. The effect of electric field on ion orbits in TJ-II stellarator 42

IV.2.6. Ion transport in tokamaks 43

IV.3. Plasma Heating..... 43

IV.3.1. Relativistic effects on electron Bernstein Waves (EBW) heating in TJ-II Stellarator 43

IV.3.2. Calculation of the fully relativistic dielectric tensor 44

IV.3.3. ECRH induced Pump-out in plasma devices 44

IV.4. EQUILIBRIUM AND MHD 44

IV.4.1. Equilibrium criticality, diamagnetism and phase transitions 44

IV.4.2. ELM studies at JET 45

IV.4.3. Equilibrium reconstruction in tokamaks 45

V. MATERIALS PROGRAMME 46

V.1. Irradiation Effects in Ceramics for Heating and Current Drive, and Diagnostics 46

V.1.1. Radiation induced absorption and luminescence of selected alternative radiation resistant glasses (TW5-IRRCER D4) 47

V.1.2. Radiation enhanced incorporation of hydrogen isotopes in silicas and aluminas: optical, electrical, and dielectric effects (TW5-IRRCER D6) 47

V.1.3. Radiation enhanced diffusion of hydrogen isotopes in silicas and aluminas (TW5-IRRCER D7) 48

V.1.4. High temperature annealing on induced voltages (TIEMF) in copper and SS cored MI cables (TW5-IRRCER D8)..... 51

V.1.5. Resistive type bolometers using alumina, aluminium nitride, and silicon nitride substrates temperature and ionization effects (TW5-IRRCER D10)..... 52

V.1.6. Irradiation testing of a prototype radiation-hard capacitive bolometer assembly based on PZ ferroelectric material (TW5-IRRCER D13)..... 54

V.1.7. Coatings for mirrors resistant to radiation enhanced corrosion, dose and temperature effects (TW5-IRRCER D14)..... 55

V.1.8. Dielectric loss at 1 MHz during irradiation of RF source insulation. Assess possible breakdown (TW5-IRRCER D15)..... 57

V.1.9. Radiation induced conductivity for potential commercial insulators for NBI bushings (TW5-IRRCER D16) 57

V.1.10. TW5/6-IRRCER Underlying Technology..... 58

V.1.10.1. Study of Radiation Induced Electrical Currents for Hydrogen Isotopes and Helium at Low Residual Pressure and Effect on Insulating Surfaces 58

V.1.10.2. Study of thermally–induced electrical signals (TIEMF) in coated cables for in-vessel coils..... 59

V.2. Radiation Tolerance Assessment of RH Components 60

V.2.1. Gamma irradiation and subsequent testing of the hydraulic seal carriers: Progressive gamma irradiation of hydraulic seals (TW5/6-RADTOL) 61

V.3. Structural reduced activation and advanced materials, and blanket / tritium cycle..... 62

V.3.1. Structural materials: High performance steels (TW5-TTMS-006 D6) 62

V.3.2. Advanced materials: Divertor and plasma facing materials (TW6-TTMA-002 D1, D4, D6) 63

V.3.3. Structural materials: Modelisation of Irradiation Effects. (TW6-TTMS-007 D5, D12) 64

V.3.3.1. Modelling He effects in irradiated iron 64

V.3.3.2. Atomistically-informed Dislocation Dynamics in fcc crystals 65

V.3.3.3. Synchronous Parallel Kinetic Monte Carlo for Continuum Diffusion Reaction Systems 66

V.3.4. Tritium breeding and materials: HCLL (TW6-TTBC-005 D2) 67

V.3.5. TW5/6-Underlying Technology 67

V.3.5.1. Metallurgical Characterization of experimental ODS steel 67

V.3.5.2. Production, and mechanical and microstructural characterization of Y_2O_3 ODS EUROFER/UC3M 69

V.3.5.3. He Bubble Formation in Liquid Metals 69

VI. TECHNOLOGY WORK UNDER EFDA 74

VI.1. Introduction 74

VI.2. Physics Integration 74

VI.2.1. ITER Diagnostic Equatorial Port Plug Engineering and Integration. 74

VI.3. ITER In-vessel systems 76

VI.3.1. Ultrasonic Examination of the Divertor mock-ups. 76

VI.4. ITER site studies 78

VI.4.1. Subtask SL53.2: Safety Operational limits and correlation of the experimental programme 79

VI.4.1.1. Safety important components classification 79

VI.4.1.2. Operational Limits and conditions 79

VI.4.2. Subtask SL53.4a: Outline description of the maintenance programme 80

VI.4.3. Subtask SL53.8b: Hotcell and Radwaste. Functions during ITER dismantling and phases of Hotcell and Radwaste dismantling 81

VI.5. IFMIF 81

VI.5.1. Cost Evaluation and Time Schedule of the Superconducting DTL alternative for IFMIF (deliverable 5 of task TW5-TTMI-001)..... 81

VI.5.2. Assessment of the state of development and cost of alternative RF power sources for the IFMIF accelerator. Solid State Technology (deliverable 1b of task TW6-TTMI-001) 82

VI.5.3. EFDA TASK TW5-TTMI-002 Deliverable 5: IFMIF: Parametric study of fluiddynamics characteristics of Li-jet under deuteron load. 84

VI.6. Systems and Plants 85

VI.6.1. EFDA TASK TW5-TRP-008, Deliverable 1: Non-Electricity production applications for Fusion Power: state of the art of high temperature innovative processes for Hydrogen production. 85

VI.6.2. Power conversion cycles for DEMO. EFDA Reference: TW5-TRP-006 86

VI.6.3. Energy Storage System for a Pulsed DEMO 89

VI.7. Socioeconomic Studies 90

VI.7.1. Improving the global multi-regional EFDA-TIMES model: revision and update of the data included in the power generation sector of the model 90

VI.7.2. Improving the global multi-regional EFDA-TIMES model: revision and update of the data included in the residential and commercial sectors of the model 90

VI.7.3. EFDA-TIMES Model: Resource Potential Update 91

VI.7.4. Social Perception of Large R&D Programmes (TW5-TRE-FESS/C) . 91

VI.7.5. Investigating lay understanding and reasonning about fusion technology by means of a group-based methodology suitable to take lay participants through a learning process about fusion (TW6-TRE-FESS-B1) 92

VII. INERTIAL FUSION ENERGY KEEP-IN-TOUCH ACTIVITIES 93

VII.1. TARGET DESIGN AND RADIATION FLUID DYNAMICS 93

VII.2. ATOMIC PHYSICS 94

VII.2.1. Simulation and Code Development. 94

VII.3. Safety and Environment 94

VII.3.1. Impact of activation cross section uncertainties on the waste management performance of irradiated steels under different neutron environments of IFE Thick-Liquid Concepts. 95

VII.3.2. Safety and environmental considerations for laser IFE chambers.. 95

VII.3.3. III.3. Comparison of Monte Carlo neutron transport codes and Nuclear Data Libraries for neutron calculations in different IFE concepts 95

VII.4. IFE REACTOR CHAMBERS 96

VII.4.1. Materials Damage: Multiscale Modeling 96

VII.4.2. TRITIUM: Environmental impact in IFE reactors 97

VII.5. ALTERNATIVE CONCEPTS FOR IFE - INTENSE NEUTRON SOURCES 98

VIII. PUBLICATIONS 100

VIII.1. Journals, books and technical reports 100

VIII.1.1. Journals 100

VIII.1.2. Books 106

VIII.1.3. Technical reports 107

VIII.2. Conferences and workshops 107

VIII.3. Ph. D. Thesis and master diplomas 111

VIII.3.1. Thesis 111

VIII.3.2. Master Diplomas (Diploma de Estudios Avanzados) 112

VIII.4. Publications on Inertial Fusion 112

VIII.4.1. Chapter in Books 112

VIII.4.2. Articles in refereed International Journals: 113

VIII.4.3. Communications to refereed International Conferences 116

VIII.4.4. Invited Communications to International Conferences 117

I. INTRODUCTION

As it happened in the previous years, the scientific exploitation of the TJ-II stellarator has been the focal point of the association programme during 2006.

In parallel, following the evolution of the European Fusion Programme towards ITER and the increasing role of Fusion Technology research, the association has increased significantly its effort in technology tasks, oriented towards ITER and DEMO.

Concerning the TJ-II programme, 2006 had a shorter experimental period than usual, due to the replacement of the H.V power supply for ECRH, a necessary refurbishment that required the cancellation of the traditional autumn campaign. A number of other upgrades was carried out, in particular the new active filter for better control of the coil currents, the Li coating system (tested at the end of the campaign with plasma operation on Li wall), the diagnostic NBI, the step tuneable heterodyne reflectometer and the new system for high accuracy spectroscopic measurement of plasma rotation.

The spring (Jan-Jun) campaign devoted a substantial part of the experiments to the improvement of performance in NBI discharges. The highlights in the TJ-II physics programme were:

- Global confinement studies: contributions to the international stellarator database.
- Role of electric fields
- Role of magnetic topology: rationals, confinements transitions
- Momentum transfer, plasma rotation. Observation of fast changes in edge rotation.
- Wall conditioning by Li coating
- Hydrocarbon erosion & redeposition

Theory and simulation development included TJ-II specific physics, general stellarator studies and basic plasma physics work, applicable to tokamaks as well:

- Electric field and ion orbits in TJ-II
- Dynamics of recycling and density control in TJ-II
- Heat diffusion in ECRH plasmas in stellarators
- Non Gaussian statistical description of transport

- Shear flow generation in magnetic confinement devices
- Plasma heating by Electron Bernstein waves
- Computational tools: GRID computing for Fusion

The second branch of the association activity on plasma physics was the participation to the JET experiments and enhancements. It is worth to mention the work on equilibrium reconstruction, the simultaneous inboard and outboard pedestal Te measurements with ECE, the upgrade of the heterodyne ECE radiometer or the installation of a fast camera for edge turbulence studies. This later development was a consequence of the interesting results obtained with a similar system on TJ-II.

In the field of technology activities, CIEMAT has continued its traditional line of development in testing and characterization of functional materials under irradiation. Those materials, mainly ceramics, are of capital importance for the diagnostics, remote handling, blanket modules or heating and current drive systems in ITER.

Structural materials for DEMO o for the ITER Test Blanket Modules is an area of growing activity both from the experimental and the theory/simulation sides.

As explained above, CIEMAT is making an effort to broaden the range of its activities in technology for ITER and DEMO. New areas of work included:

- Diagnostic port engineering
- Divertor component tests by Ultrasonic techniques
- ITER safety studies, within the EISS project
- IFMIF developments on several areas: accelerator (superconducting DTL option, RF solid state sources) and target: Li fluidynamics.
- Systems & plants studies, focused on three areas: hydrogen production from fusion reactors, high efficiency energy conversion cycles for Fusion and energy storage technologies for pulsed reactors.

Preliminary work has also been done for NBI components (ion dumps, RH & maintenance systems), diagnostics (Reflectometry, LIDAR, IR view, pressure gauges and magnetics), TBMs (diagnostics, simulation tools), and CODAC (remote access tools, pattern recognition and data mining), but the tasks will be mainly performed in 2007

As a part of the EFDA Technology programme, CIEMAT has also continued its effort on socioeconomics studies, which basically involve two lines:

Improvement of the EFDA-TIMES model for analysis of the role of Fusion in the overall energy supply with horizon 2100.

Studies on social perception of large R&D projects, in particular Fusion.

Concerning educational activities, The CIEMAT team, in close cooperation with Spanish universities, was directly involved in European Fusion Education activities in the framework of the Erasmus Mundus "European Master in Nuclear Fusion Science and Enginering Physics" educational network which started in 2006.

II. TJ-II ENGINEERING AND OPERATION

This chapter covers the description of all the activities related to TJ-II operation during 2006, including the highlights of the experimental sessions, the main engineering activities, the work done by the plasma heating groups and the research and developments implemented by the data acquisition, electronics and diagnostic control and plasma wall groups. It is organised according to the following structure:

- 1 Operation of TJ-II during 2006
- 2 Basic Machine Engineering
- 3 ECRH Heating
- 4 Neutral Beam Injection
- 5 Data acquisition
- 6 Electronics and Diagnostic Control
- 7 Plasma wall activities

II.1. OPERATION OF TJ-II DURING 2006

The 2006 spring campaign took place between January and June, with 56 days of operation and 2247 shots. A summary of the experimental sessions performed, along with the number of shots allocated to each experiment/activity, is listed below:

- Start-up, commissioning of control and data acquisition systems and diagnostics: four sessions, 103 shots
- ECRH studies: calibration, power deposition profile (modulation) and ECCD experiments: seven sessions, 210 shots
- Rotational transform and plasma volume scan: eight sessions, 283 shots
- NBI plasmas (experiments devoted to optimize the coupling of the neutral beam to the ECH target plasma: working gas, magnetic configuration and plasma volume scans, ECH providing on/off axis heating, electrode biasing, etc): fourteen sessions, 364 shots
- Electron ITB´s and low order rationals: six sessions, 141 shots
- Plasma-wall studies: erosion and deposition of C on graphite: five sessions, 216 shots

- Comparison of profiles measured with different diagnostics: one session, 45 shots
- Electrode biasing and electric fields: seven sessions, 205 shots
- Direct losses of trapped electrons: three sessions, 89 shots
- Power/density scan: two sessions, 69 shots
- He plasmas: two sessions, 55 shots
- Kinetic studies: heating power, density and polarization: one session, 41 shots
- Lithium coating of the vacuum vessel: one session, 35 shots

The usual TJ-II autumn campaign had to be cancelled because the old ECH high voltage power supply had to be disassembled to make room for the new one, which was due to be installed by December 2006.

II.2. BASIC MACHINE ENGINEERING

II.2.1. Introduction

The engineering group of TJ-II has performed during the year 2006 tasks related with the operation and maintenance of TJ-II device, control and instrumentation systems, maintenance and repairs in the buildings, auxiliary systems, improvements in the present electrical distribution system, technical support for heating systems and diagnostics, and the actions required to preserve the safety of personnel, equipments and overall installations. The relevant tasks are hereafter described.

II.2.2. Technical operation of the TJ-II

So far, the plasma pulses in TJ-II have been produced during a magnetic field "flat top", with constant currents in all the coils. The TJ-II Physics Group has formulated new requirements in terms of the operation of the machine. This new mode of operation, called "Mode C", should allow the variation of rotational transform or magnetic well during the plasma pulse. In TJ-II, the strong magnetic coupling between the central (circular and helical) coils makes this mode of operation quite complex. The requirements, works, modifications and tests carried out in the different systems to enable this mode of operation are described in the reference [ENG 1].

II.2.3. Power supply

II.2.3.1. Study of a new generator's mode of operation

Since 2003 the power supply generator had been able to work in two different modes of operation: the first one is the impulse way of operation in which the generator works with no-load and with a low output voltage (1.5 kV) in between TJ-II shots. Before each shot the generator increases the voltage to its nominal value (15 kV) during a few seconds and provides all the output power to TJ-II. In the second mode of operation the pulse generator only provides energy to NBI (it is not compatible with TJ-II shots) and it maintains an output voltage of 9 kV during more than one hour.

During 2006 a third mode of operation is being developed. In this new mode the pulse generator should maintain continuously its nominal output voltage (15 kV) during the whole eight hours of the working day and it should be able to provide the required electrical energy for the TJ-II shots and for the NBI conditioning pulses. It is clear that this type of operation has a big impact in the whole installation: it affects the generator from the electromagnetic and also the thermal points of view and it also affects the excitation, cooling and protection systems and the DC pony motor among others.

Due to the fact that the motor-generator cooling system will have to dissipate a higher thermal power and in order to know in detail the current dissipation power, the water flow levels through the different heat exchangers have been measured with an ultrasound system. This measurement has demonstrated that the heat exchangers are currently dissipating less power than they are able, so the cooling system has some margin, but still is uncertain whether this reserve is enough for the new type of operation. To know in detail the new expected thermal losses, a large number of calculations of the behaviour of the machine under the new conditions will be done.

II.2.3.2. New current measurement system in the Active Filter of TJ-II

The total current in the Hard Core coils contains a DC component and a wide spectrum of harmonics (current ripple) due to the commutation of the thyristor rectifier and also due to the operation of the current controller. Depending on the plasma discharge scenario, the DC and the AC components can be up to 11kA and 70A peak to peak respectively. The active filter, connected in parallel to the CC or HX coils, should keep this current ripple within 4A peak to peak respect to the DC reference value. To ensure reliable work of the active filter, it is necessary to use a high precision current detector.

In the tests carried out during 2005-2006, the current through the coil (DC and AC component) was measured by a zero flux current transformer, with accuracy better than

70 ppm. It was observed, that in many cases the useful signal of the AC component of the current was practically comparable with the electrical noise and it resulted in an unstable operation of the filter. In order to solve this problem, the zero flux current transducer was replaced by a Rogowski coil that measures only the AC component of the current. Recent tests with the new current detector have shown that the operation of the active filter is correct and its output parameters are within the specified values.

II.2.4. Control system

The main activities have been concentrated in the system maintenance and upgrade areas [ENG 2].

II.2.4.1. Protection against NBI breaks

It has been observed that some strong breakdowns in the NBI ion sources during the pulse cause large electrical interferences, which, in turn, trigger protective actions of the control system and produce a sudden conclusion of the experiment. In order to avoid this fast termination a real time algorithm has been developed. It can differentiate between current peaks depending on their duration - the big inductance of the coils makes impossible very fast variations- and distinguishes between real dangerous current variations and spurious interferences.

II.2.4.2. Java application for the timers of the diagnostic section

An easy-to-use Java-based user interface for the TJ-II Timing System has been designed and implemented. Compared to the previous version, new additional features have been introduced, so any timing setting change produced in the system is notified to the application in automatic way, simultaneous visualization of the channels setting and information about real-time experiment status are also provided. The software has been designed according to client-server architecture based on the TCP/IP and UDP protocols. A web server running under OS9 operating system provides access to the application.

II.2.4.3. Event-oriented data base

A new event-oriented database for continuous data flows in the TJ-II control system has been designed and implemented in collaboration with the Data Acquisition Group. An event is defined as any occurrence relevant to the TJ-II environment. The control system is presently being upgraded to work in all the states of TJ-II exploitation, including operation, maintenance, assembly and testing of new components. In consequence, it will enable continuous monitoring of certain parameters. The software applications that

register locally events and data are being modified to allow the storage of this information centrally in this database. The ground loop supervision system (GLSS) is the first subsystem that has been upgraded to incorporate event-oriented data base capabilities. In addition, libraries for registering data/events in the database from different subsystems based on OS9 and VxWork have been developed.

II.2.4.4. New ground loop supervision system

Throughout the year 2006 the development of the new ground loop supervision system have been completed. The new system has increased the number of monitoring channels from 8 to 16. The new design facilitates the identification of the ground loop location and adds the possibility of measuring the impedances with different frequencies, allowing the measure of both real and imaginary components of the loop impedance.

II.2.5. International collaborations

II.2.5.1. Monitoring of the ENSA contract for IPP

The tasks developed during 2006 are related to the close monitoring of the manufacturing of the support structure of the coils during the summer. An engineer from Ciemat has been present at the manufacturer's workshop, for three weeks, during the last steps of the manufacturing process of the first module of the structure. No other activities have been carried out after this period.

II.3. ECR HEATING

II.3.1. ECRH system routine operation and improvements

The TJ-II experimental campaign lasted from January to June and the ECRH system was working with its two gyrotrons, which delivered a maximum power of ≈ 400 kW when they were working at the same time.

As the high voltage power supply continued with a lot of problems due to the spurious overcurrent interlocks that appear at the beginning of the pulse, and the limitation in current was reducing the power of the gyrotrons, it was decided to design a new one to replace it as soon as possible.

The mechanical system that allows the poloidal movement of both internal launchers was broken during the ECCD experiments. This problem caused a loss of only two days in the operation.

The remote control of the superconducting magnets power supplies was tested successfully in normal operation [ECRH1]. Improvements in the modules of the anode modulators were designed in order to implement new software to allow the remote control of the filament current power supply and the voltage of the anodes in the next future.

The cooling system was working properly and the annual maintenance was carried out during the summer.

II.3.2. Design and manufacture of a new high voltage power supply

The high voltage power supply was designed in 1987 to work with one gyrotron of the TJ-IU. Afterwards, in 1990, it was upgraded to supply in parallel the present gyrotrons of the TJ-II. These modifications were not able to reach the required current for both gyrotrons. During the last years the failures are affecting seriously the TJ-II operation and the ECRH system is not longer reliable enough. Moreover, the ripple of the output voltage had increase up to 10%, which means a modulation of the gyrotron power and a widening of its frequency spectra. Under those conditions the ECRH operation could continue, but the reliability and the quality of the microwave launched power could not be guaranteed.

A new high voltage power supply has been design with the following main characteristics: maximum output voltage: -80 kV, maximum output current: 50 A, maximum switch-off time in case of a short-circuit: 5 ms, output voltage ripple: 1%, optimal regulation of the voltage in the connection and disconnection of the loads to avoid over-voltages and over-currents.

The design is based on high frequency commutation techniques for high voltage power supplies. All the components are solid state and the active ones are placed in the low voltage section.

To fulfill the requirements, the components of the new high voltage power supply are the following: a transformer, which provides the isolation between the AC input and the DC bus and the voltage needed for the rectifier, a SCR rectifier with 12 pulses, which supplies a DC stabilized voltage of 700 V, a DC filter at low voltage, 32 IGBT´s that generate a high frequency chopped wave, which are connected to the primary of 32 high

voltage transformers and whose secondary is connected to a rectifier diode bridge, 64 high voltage rectifiers connected in series to provide the required DC voltage and finally, an output filter to reduce the ripple.

II.3.3. ECCD experiments

Electron Cyclotron Current Drive (ECCD) experiments were carried out in the TJ–II stellarator. The second–harmonic ECRH power was launched on-axis from two low–field side stellarator symmetric positions. To investigate the ECCD properties of the device, the dependence of the total toroidal plasma current on the launching direction of both ECRH beams at fixed density conditions, and on the line average density for some fixed launching configurations, was determined. In the launching direction scan, only discharges with similar density and temperature profiles were studied, in order to avoid strong modifications of the bootstrap current contribution and the refraction properties of the plasma. Moreover, the measurements of the toroidal plasma current and the plasma profiles were taken at the end of the discharge, when approximately steady–state conditions were achieved. Using the normalized current drive efficiency as defined by $h_{ECCD} \equiv \langle n_e \rangle I_{ECCD} R / P_{ECRH}$ we have obtained values up to $h_{ECCD} \approx 0.001 \times 10^{20} AW^{-1} m^{-2}$. [ECRH2].

This work has been carried out in the frame of the collaboration with the Kyoto University (Japan).

II.3.4. Experiments in Heliotron-J

Control of non-inductive current drive has been demonstrated in Heliotron J. The different contributions to the total current (Bootstrap and ECCD) were separated by means of field reversal experiments. Clear changes, in agreement with the theoretical predictions, were observed for different magnetic configurations with variable fraction of trapped particles and different confinement properties [ECRH3]. Moreover, the transmitted power measurements for oblique ECRH power propagation were find to be in good agreement with the theoretical ray tracing calculations [ECRH4].

In relation with the breakdown experiments, the previous studies carried out in three different devices (TJ-II, Heliotron J and CHS) were compared and the common features of the breakdown process were highlighted [ECRH5]. The importance of non-linear wave-particle interactions and the earlier breakdown for X-mode launching was clearly demonstrated. Finally, the spatial structure of the breakdown process was investigated

for the on-axis and off-axis cases using a multichannel array (32 chords) of H_a detectors [ECRH6].

This work has been carried out in the frame of the collaboration with the Kyoto University (Japan)

II.3.5. Status of the Electron Bernstein Waves heating project

Heating the TJ-II plasmas with electron Bernstein waves has several objectives: to reach high density plasmas and investigate higher collisionality regimes, to build a denser target plasma for good NBI power coupling and to investigate the current drive by electron Bernstein waves. A complete system (gyrotron, transmission line, launcher) has been specifically designed, fabricated and installed for EBW heating by O–X–B mode conversion.

The problems with the high voltage power supply for the 28 GHz – gyrotron were not solved and have delayed the scheduled start of the experiment. High power testing of the main components (gyrotron and transmission line) will be done during 2007. The new date to start operation is 2008.

II.3.6. Electron Bernstein waves emission diagnostic

The diagnostic for measuring the EBW emission from the TJ-II stellarator was designed and tested on the bench. It uses a section of corrugated waveguide and a glass lens to focus the emission from the plasma into the aperture of a dual-polarized quad-ridged horn. Horn-to-lens spacing and lens-to-waveguide spacing has been optimized for the experimental conditions in TJ-II [ECRH7].

The diagnostic was delivered to CIEMAT in December 2006.

This work has been carried out in the frame of the collaboration with the Oak Ridge National Laboratory, Oak Ridge, TN USA

II.3.7. Influence of the controlled modulated power reflected back to the gyrotron

The experiment performed with the gyrotrons of the TJ-II ECRH system to influence the microwave output radiation with a relatively weak wave returned from an external

mechanically modulated reflector was continued. An original method was found for directly measuring the wavelength of electromagnetic radiation in the free space. [ECRH8].

This work has been carried out in collaboration with the Institute of Applied Physics (Russian Academy of Science), Moscow and Nizhny Novgorod, Russia

II.3.8. Participation in design and the testing of the remote steering upper launcher of the ECRH system for ITER

Steering of the mm-wave beam of the upper-port launcher is required to use ECW for localized heating and current drive over a large range of plasma radii in ITER. The alternative solution, Remote Steering has been studied to avoid moving components at the plasma-facing. The design work has demonstrated the feasibility of the remote-steering approach and to validate it a full-scale mock-up line at 170 GHz was built and tested both at low power and at high power levels. The ECRH group has participated in both testing. [ECRH9].

This work has been carried out in collaboration with the EURATOM-FOM Association

II.3.9. New developments on the High Critical Temperature Superconductor.

The system under study is a GYCOM gyrotron used in the ECRH system. A Nb-Ti solenoid produces a uniform magnetic field of 2 T in a 150 mm warm bore. The magnet is cooled down at 4.2 K by continuous supply of expensive liquid helium and nitrogen in mobile tanks. The new magnet is made of BISSCO-2223 tapes operating at 20 K. It is a cryogen-free device, cooled down by a Gifford-McMahon cryocooler.

The manufacturing techniques have been improved by the fabrication of smaller coils. Finally, two large size prototype coils have been successfully fabricated and tested at different temperatures, both in a liquid nitrogen bath and in a specially-developed cryostat with a cryocooler. [ECRH10, ECRH11]

This work has been carried out in collaboration with the Superconductivity Unit of CIEMAT.

II.4. NEUTRAL BEAM INJECTION

The activities of the group during the first semester were focused on the conditioning and operation of Injector #1. Beams of 28 keV and 60 A were reliably injected into TJ-II plasmas from mid April to the end of the experimental campaign in June.

The Target Calorimeter of Injector #1 was installed and operated along the campaign, allowing the first beam power density profiles to be obtained.

Injector #2 underwent the last commissioning phases along the year. First plasmas in the Ion Source were obtained in May. Work on the High Voltage Power Supplies continued throughout the year.

II.4.1. Injector #1

Injector #1 Power Supplies: work was carried out on the Decel Supply, and on the switching circuitof the Accel tetrodes. The crowbar circuits were debugged allowing reliable crowbar operation. The first snubber was receptioned, but installation was postponed.

Injector #1 Control System: a new Timing interface was installed, tested and set in operation [ENG_3]

Injector #1 Ion Source: at the end of the experimental campaign, the ion source was tested for vacuum leaks in the water circuits, the Copper-button circuit was found to be clogged.

The ion source was dismounted and carried to the NBI laboratory, were it was fully refurbished.

The grids were carefully characterized (Gaps, alignment, curvature). It was found a significant gap non-uniformity due to heavy grid deformation. A bad misalignment was also found between the Ground Grid and the other two grids (Plasma Grid and Decel Grid). Both faults were found to be consistent with the beam assymetries detected by thermocouples and calorimetry in the injector. They can also affect the beam transmission, through an anomalous halo power, as observed with the Target Calorimeter [ENG_5]

The grids were carefully cleaned, X-rayed, re-curved, re-gapped (accel gap =6 mm), and re-aligned.

After assembly, the ion source was leak tested.

The alignment of the beam source as a whole was found to be defective. The Ion source was displaced with respect to the neutralizer, and the beam box was inclined with respect to the duct. Both defects were corrected.

The used BaF2 Filaments were removed and new ones mounted on the filament flange. They were subjected to phase I conditioning in the NBI laboratory, and phase II conditioning in the Ion Source.

Injector #1 Gimbal: the horizontal steering mechanism did not operate reliably. By design, the ion source weighs in the gimbals, thwarting their proper course. A strong spring was inserted to equalize the two ends of the gimbal course. Tests show the correct operation of the upgraded mechanism.

Injector #1 Target Calorimeter and Infrared Camera: the Target Calorimeter was first operated in February, allowing the thermal print of the neutral beams to recorded and subsequently analysed using the thermographic tools provided by the infrared camera [ENG_4].

The Target Calorimeter proved to be a powerful tool for the "in situ" characterization of the neutral beams [ENG_5].

Injector #1 Vcuum System: the vacuum instrumentation was upgraded, and made exactly equivalent to that on injector #2. A new Rotary pump was installed.

II.4.2. Injector #2

The Beam Vessel commissioning proceeded from January to March [ENG_6], when the four titanium gettering pumps were installed, the vacuum system was started, and the pressure reached 5x10-6 mbar. Vacuum leak tests showed that the Bending Magnet bellows leak was finally healed, making auxiliary vacuum in the bellows unnecessary.

All the subsystems were tested: the Gimbal, the V-calorimeter, the cooling system, the Titanium pumps and the Bending Magnet.

The vacuum instrumentation was installed and tested in April.

The 30 cm neutralizer: the copper tube and large flange are manufactured, the cooling circuits are being welded at an external company.

The Ion Source was mounted and tested during April-May.

The gas injection system was commissioned in May-June.

The first Arc in the Ion source was obtained in July.

The first control system tests were carried out in June, the system was fully operative in November.

The High Voltage Power Supplies were commissioned from April throughout December. The main problems encountered were unwanted RF oscillations at High Voltage onset, and bad voltage regulation at the decel Power Supply.

The beam duct was mounted in October, leak tests were satisfactory. The duct instrumentation was installed and cabled in November.

The target calorimeter: the coupling piece was installed in November

II.5. DATA ACQUISITION UNIT (DAQU)

During 2006, the work was focused on four different lines: intelligent data retrieval methods, remote participation, data compression and real-time event detection.

II.5.1. Intelligent data retrieval methods

Long pulse conditions and the associated large volumes of data need automated and efficient processes to identify similar structural shapes (*i.e.* similar physical behaviours) in waveforms. The classical paradigm of shot number for input and signal samples for output must be replaced. Instead, the input parameter for data retrieval should be a temporal evolution signal segment (pattern) and the outputs should be the shot numbers and the temporal intervals where the pattern appears in the database. A pattern to search can be either an entire waveform or a particular segment inside a waveform. Both

cases are solved in different ways in order to optimise the efficiency and the use of computational resources.

II.5.1.1. Entire waveform approach

This approach for data retrieval uses the structural forms of the signals to search for similar complete waveforms within the database. It is a very efficient and general purpose searching system [DAQU_1].

II.5.1.2. Patterns in waveforms approach

This technique allows seeking for patterns within waveforms instead of searching for entire waveforms [DAQU_2].

II.5.2. Remote participation

Activities on remote participation were centred on several aspects related to the distributed nature of experimental and databases systems. The aim was to contribute to the development of secure, standard and scalable solutions for user interactions from remote locations. Research lines can be summarized in four points: software architecture for remote experimentation, access security, a middleware for message distribution and contributions to help in the development of a shared data access system.

II.5.2.1. Software architecture for remote experimentation

The TJ-II model for remote experimentation is based on thin client environments as an easy, inexpensive and powerful solution to remote experimentation requirements. It implies the generation of a multi-tier software architecture based on three layers: user interface layer, security layer and data management layer [DAQU_3].

II.5.2.2. Access security

Security is an essential element in remote participation. The interplay environment between users and systems is a distributed one and therefore only distributed authentication and authorization systems can handle security requirements in a proper way. An ad-hoc meeting to discuss related issues was held in Culham. General ideas were presented [DAQU_4] and also the TJ-II experience with PAPI was shown [DAQU_5]. As a result of the meeting, it was agreed to create a federated security infrastructure between EFDA sites and to analyse the intercommunication between different federated systems, in particular PAPI and Shibboleth.

II.5.2.3. Message oriented middleware

Distributed message systems are key components for remote experimentation. A specific development for the TJ-II stellarator was put into operation. It is based on a publish/subscribe architecture with http tunnelling to avoid the issues of firewalls [DAQU_6].

II.5.2.4. Shared data access system

A common software layer for data access between end-users and laboratories was proposed by A. Neto et al. It means the creation of a software abstraction layer between users and databases to facilitate data retrieval in a common way. To this end, the XML-RPC protocol was used. Our contribution was to secure the data access with PAPI [DAQU_7].

II.5.3. Data compression

When managing a big volume of information and handling billions of bits per second like in ITER, data compression seems a useful candidate to prevent the waste of resources in communication and storage systems. Data compression should address the questions of '**what**' (several data sources), '**where**' (application scenarios), '**why**' (benefits), '**when**' (on-line or off-line) and '**how**' (specific techniques) data should be compressed. A new real-time compression technique (cyclic delta) based on delta compression was proposed [DAQU_8]. This reference, on the one hand, shows capabilities of the new technique for real-time waveform compression. On the other hand, it compares compression rates in JET and TJ-II databases with the cyclic delta technique and the ones used in JET and MDS+.

II.5.4. Real-time event detection

Long pulse operation requires the detection of interesting events in continuous data flows. A neuro-fuzzy model for real-time event detection was presented in the 16th HTPD Conference [DAQU_9].

II.6. ELECTRONICS AND DIAGNOSTIC CONTROL

During the year 2006 the Electronic and Diagnostic Control Group has continued the development of the electronics and control of the new diagnostics that have been installed in TJ-II, as well as the improvement and maintenance of those already existent.

II.6.1. Diagnostic Control System (DCS) architecture

The DCS is integrated in the "TJ-II Remote Participation System ", and it consists , so far, of 19 systems, namely:

- 9 PLC´s Simatic S5 and S7 (Siemens).
- 4 I/O Ethernet (National Instruments and W&T).
- 11 Positioning Control Units (Maxon).

The access to monitor/program of each diagnostic can be done from any web browser,and computer platforms. After introducing the corresponding username and password it allows access to the web page where the diagnostic status is visualized on line.

II.6.2. New diagnostics

II.6.2.1. Internal mirror of the Electron Bernstein Waves

The corrugated waveguide of electron Bernstein wave has an internal movable mirror inside the vacuum chamber to focus the beam, located at top D6TOP port. This mirror has two freedom degrees, poloidal an toroidal. The control electronic and the used motor allows an angular resolution of 0.1 degrees.

II.6.2.2. Automated system for control of the vacuum diagnostic system for the TJ-II

These systems are part of each diagnostic and their control has been integrated into a PLC S7200 (Siemens) that carries out this task. All the controls are connected through a ASi network, so as to interchange data between the general system of TJ-II.

II.6.2.3. 6.2.3. Control system of four Li ovens

Four ovens of Li have been installed in TJ-II located at A1TANG, B1SIDE, C1TANG and D1TANG. The temperature is controlled with PID controllers.

II.7. PLASMA -WALL ACTIVITIES

II.7.1. Activities in TJ-II.

II.7.1.1. 7. 1 .1 Hydrocarbon injection

Hydrocarbon fuelling experiments have been performed in ECRH TJ-II plasmas by injecting methane and ethylene, representing the main hydrocarbon species released by the chemical sputtering of carbon materials. The puffing is delivered at several radial positions into the edge plasma, and it is made through a gas injection port located on a poloidal, diagnosed carbon limiter. Another identical limiter is located at 180º toroidally, and it is used for reference. The edge parameters and their possible change during injection were monitored by atomic beams and Langmuir probes. Particle balance for the injected H atoms indicates that cracking of ethylene convey a high retention of this species into the film, and only a 10% of the injected H is recovered into the gas phase after discharges. The experiments were then focused on the erosion by the plasma of the deposited films on the limiter. Thus, comparison between erosion of the "clean" and contaminated carbon limiters allowed the identification of the specific effect of the deposited layer. The insertion of the gas-injection limiter into the plasma leads to enhanced carbon contamination, as a consequence of the local deposition of hydrocarbon films. Erosion of the deposited films by the plasma and by local puffing has been compared. The direct data indicate that plasma erosion is more efficient than local puffing for the removal of the films. However, the contribution of other parts of the vessel also contaminated could mask the expected enhancement due to FC and CX neutrals. The spectroscopic signatures of the injected molecule were also recorded. Ethylene yields only a 15% of Ha photons per injected molecular H atom when compared to H_2 fuelling. Also, the ratio of CH/Ha photons delivered upon molecular cracking at the edge is a factor of three higher for ethylene than for methane under the edge conditions (~30-50 eV, 2.10^{12} cm^{-3}) of the plasmas under study [ENG 7].

II.7.1.2. He beam diagnostic

A fairly strong effort has been devoted to the improvement of the supersonic He beam diagnostic and its interpretation during 2006. On the instrumental side, a completely new set-up for the detection of the He lines has been built and tested. Modifications were required in order to get a more reliable alignment of the optical system and to avoid the vignetting effect of some parts of plasma. In addition, the characterization of beam geometrical parameters, in particular its divergence was carried out in situ. Respect to

the model validation, two important aspects were addressed. First, the self-consistency of the profiles, tested through the attenuation of the beam according to the reconstructed profiles, was checked. A reasonable agreement between predicted and observed attenuation of the beam was found. Moreover, the density and temperature profiles found are in very good agreement with other edge diagnostic data in TJ-II (reflectrometer, Langmuir probes, Li beam…)

Laser Induced Fluorescence is been implemented for the direct detection of excited states in the He beam. The validation of the C-R model by this method, however, is far from trivial, mostly due to the large number of states involved in it and their mutual collisional coupling. A method was envisaged, that combines the information from both diagnostics [ENG 8]. So, the parameters obtained through the atomic beam emission spectroscopy are used in the modeling of the time evolution and amplitude of the laser perturbed populations for some selected transitions. In particular, laser pumping of the 3^1P (501 nm) and 3^3D (507.7 nm) states followed by detection of the Dn=0 collisional induced emission lines was simulated in order to test the sensitivity of the method to the assumed rate constant values. A procedure to fully test the assumed values of the main rate constants involved in the population of the excited states monitored in the He beam diagnostic was produced after extensive modeling of the expected LIF signals. Contrary to other proposed schemes for He CR model validation, the one proposed here doesn't rely on the data provided by other edge diagnostics and represents an internal test of the model.

II.7.1.3. EIRENE simulation of neutral profiles

The emission profiles of the neutral He lines typically used in the supersonic He beam diagnostic, i.e., the 667 and 728 singlet and the 706 nm triplet lines from the n=3 excited He atoms have been recorded in ECRH helium plasmas, with minor contamination from H. Line integrated values at the edge were recorded and compared with EIRENE code predictions. While the central values of the density and temperature profiles corresponding to the Thomson Scattering data for the analyzed discharges were used in the simulation, some freedom on the corresponding values at the edge was allowed, and the measured values in similar H plasmas by the supersonic He beam were used as starting guess. The neutral code EIRENE has been adapted to the geometrical conditions of the TJ-II stellarator. For these simulations, inclusion of the He emmisivities at the selected wavelengths, which were absent in the original version of the code, has been made. In order to attain a statistical uncertainty of less than 5%, 9.6 million trajectories were required.

Good fitting was found in the simulations under these assumptions [ENG 9]. A maximum difference of 16%, with an average value of 7%, between the experimental and simulated intensity ratios was achieved. No effect of parameters such as the assumed ion temperature profile, the ratio of HeII to HeIII ions or wall temperature on the quality of the simulation was seen. Conversely, a high sensitivity to the exact profiles for the electronic parameters at the edge was evidenced. The fitting shows high sensitivity to the atomic velocity of the recycled He atoms. Thus, for atom energies above 2eV, to be expected for high energy reflection coefficient of the He ions at the typical edge temperatures assumed and for the boronized wall conditions, or below ~0.1 eV (thermal) a measurable deviation from the observed signals should be seen, in particular for the line ratios 667/728 and 728/706 used in the beam diagnostic. Moreover, the computed ratio of edge to central neutral density was found extremely sensitive to the particular value of the atomic velocity within the valid range of energies. Finally, absolute calibration of the detectors is presently underway. Thus, the evaluation of the excited He atom density at the edge will be used as input for the verification of the code predictions. EIRENE is presently being adapted to allow for this type of comparisons.

II.7.1.4. Neutral density studies

Hydrogen recycling and puffing through a hole in a poloidal limiter of TJ-II is studied by spatial resolved H_a emission spectroscopy with a CCD camera. Very different emission profiles are obtained depending on whether the hydrogen enters the plasma when recycling at the carbon limiter or whether it is puffed through a hole in the limiter directly inside the last closed flux surface of the plasma. From the emission profiles the neutral density profile of the H_a emission precursor is deduced. This is the basis for the analysis of the atomic and molecular mechanisms responsible for the excitation, dissociation and ionization of the hydrogen neutrals entering in the plasma in front of a limiter where the electron temperature is relatively high (T_e > 30 eV). If the puffing rate is very strong the plasma can be locally perturbed and the electron temperature decreased, this affecting the neutral reaction processes. With the help of a simple model, which is adjusted to the experimental profiles, the hydrogen neutral energy is estimated and the atomic and molecular reactions can be deduced. It is shown that the way the hydrogen molecule is dissociated and ionized in the plasma, which depends on the electron temperature especially in the range of 10 eV – 30 eV, will have a strong influence on the neutral density radial profile. The analysis of the emission profiles together with the simple model confirms that for T_e > 30 eV, the hydrogen atoms produced from molecular dissociation have very low energies of typically 0.3 eV, as was observed in other fusion devices with the Doppler-line broadening technique. This energy is a factor of about ten lower than that predicted by simple Franck-Condon dissociation and was attributed to

strong vibrational excitation of the molecules. In this context it is discussed here if surface phenomena can influence the excitation state of the molecule when being desorbed [ENG 10].

Total neutral pressure during discharges has been recorded by a conventional ionization gauge at < 1m from the main plasmas. Good correlation between electron density, particle fluxes (as deduced from Ha and Langmuir probe signals) and neutral pressure was found, except for the cases of cut-off, in which neutral pressure largely overcomes the rise in electron density. Calibration of the system in the presence of the field has allowed the quantitative analysis of the signals, yielding typical neutral densities at the port location in the range of $10^{11\text{-}12}$ cm^{-3}. The results will be cross-checked with Eirene simulations of H and He plasmas, presently underway [ENG 11].

II.7.1.5. Wall Conditioning

Lithium coating of the inner wall of TJ-II has been attempted for the first time. A set of effusive ovens, either fixed or mobile, together with a devoted control system were built during 2006 and finally applied to the lithiumization of TJ-II. 4 g were delivered into the vacuum vessel and a Glow Discharge of Ne was simultaneously run to help in the uniform distribution of the coating. Due to accidental venting of the chamber with nitrogen (which readily reacts to form a Li nitride with the coating) no test of plasma performance under the expected low H recycling characteristics of the coating were made. Improvement of the oven design and development of other techniques to enhance redistribution of the Li after its deposition have been addressed afterwards, and will be tested upon re-start of operation [ENG 12].

II.7.2. Activities in H retention control

II.7.2.1. Scavengers

Activity in the field of in-situ inhibition of re-deposited CH films by scavenger injection has been mainly devoted to the characterization of the underlying mechanism. For this, experiments at the CIEMAT in a Glow Discharge reactor were undertaken. A new method to discriminate the reactive species coming out from the plasma in the presence of methane, nitrogen and hydrogen was developed. It is based in the condensation of the pumped gases in a liquid nitrogen trap, followed by thermal release under programmed heating. The technique has been labeled as Cryotrap Assisted Mass Spectrometry (CTAMS) Good discrimination between HCN and ethylene, with strongly overlapping mass spectra, was possible by this simple method [ENG 13]. The results indicate a very

important contribution of ethylene and acetylene to the reaction products, in stark contrast with the conspicuous formation of HCN and C_2N_2 molecules driven by strong ion bombardment. A systematic comparison of complimentary plasmas was undertaking by using the CTAMS technique. The conclusion of these studies is that the scavenger effect is directly associated to the interaction of nitrogenated surfaces with the incoming plasma radicals. Some hints of the formation of an intermediate product, which could poison the surface preventing the film growth, were deduced from the CTAMS data [ENG_14, ENG_15].

II.7.2.2. Plasma and HT Oxidation

Alternatives to direct oxidation of the carbon films created in ITER under carbon divertor scenarios by pure oxygen are strongly needed. This is mainly due to the required high temperatures found for fast oxidation, well above the maximum 540 K allowed by the water circuit to be used for machine heating. Some alternative concepts have been tested at CIEMAT, in collaboration with two groups from the CSIC, the Catalysis and Petrochemistry group and the Surface Engineering group, both at Madrid. Carbon films produced at CIEMAT in a glow discharge reactor, with a H/H+C ratio of 0.4, and flakes from the ALT limiter at TEXTOR and from the divertor region of Asdex Upgrade were analyzed and exposed to reactive gases. Oxidation by NO was tried as alternative to Oxygen and direct or catalyzed isotope interchange, using hydrogen peroxide as a catalyst, was attempted. While no conclusive statement can be made at this stage, it was found that exposing the flakes (with intrinsic high porosity) to pure hydrogen in a continuous flow reactor can lead to the release of deuterated species at temperatures slightly higher than those required for the full oxidation of the films with pure oxygen, thus alleviating the side effects of unwanted oxidation of the reactor components and time consuming plasma recovering [ENG_16].

For carbon areas exposed to the main plasmas, glow discharge in He/O_2 mixtures has proven effective. Nevertheless, there are some scenarios, likely to be found in real operation in the presence of several types of first wall materials, under which the removal by this technique becomes very slow or impossible. This is the case originated by material migration into gaps (as those present in the macrobrush design of the divertor modules) or the space between plasma-exposed components, making tritium release impossible by direct ion impact. In order to find alternative solutions for this problem, a metal grid with 1mm gaps of 4 mm depth was built. A heater element (Thermocoax) in winded at the bottom of the gaps, and it is first exposed (unshielded) to a carbon deposition plasma. The removal of the carbon by a He/O_2 glow discharge plasmas under this geometry, aimed at simulating the macrobrush structure, was

investigated by thermal desorption spectrometry. Efficient removal of the carbon film at the bottom of the gaps was achieved by a 30' exposure to a He/O_2 GD. A fast rate, of the order of 50 times higher than previous reports, was seen in the unshielded films. Also, the removal rate was insensitive to the plasma current. These facts suggest that atomic species, rather than ions, are responsible for the film erosion [ENG 17]. He/O_2 and H_2/N_2 glow discharge cleaning techniques were tested and compared resulting a high cleaning efficiency of 12 nm/min and 3,6 nm/min respectively On the other hand, boron-containing films show lower reactivity to the cleaning techniques studied, maybe due to conversion from sp^2 to sp^3 hybridization in the presence of B [ENG 18].

II.7.3. Other activities

II.7.3.1. ITER Pressure Gauges

During the fall of 2006 CIEMAT has joined the DIADES Task on Bolometry and Pressure Gauges for ITER, being responsible for the assessment of the later. The possibilities to adapt presently existing gauges to the ITER peculiarities and the possible development of specific new designs, together with cabling and space requirements are included in the Task as CIEMAT duties.

III. PHYSICS STUDIES

III.1. INTRODUCTION

This section describes physics studies in the TJ-II stellarator and JET tokamak during 2006.

The magnetic topology is an important ingredient of plasma confinement in magnetic traps. Plasma flows also play a crucial role in transport in magnetically confined plasmas, and clarifying the contribution of neoclassical effects and turbulence to flows is a key outstanding issue. Due to the flexibility of stellarator devices, like TJ-II, these are ideal laboratories to study the relation between magnetic topology, electric fields, flows and transport. In addition, recent improvements in plasma diagnostics have led to a better understanding of the confinement properties of TJ-II.

Physics activities in JET were focussed in the in-out pedestal temperature measurements and upgrade of JET plasma diagnostics including heterodyne radiometer and fast visible cameras.

III.2. CONFINEMENT AND ELECTRIC FIELDS IN ECRH AND NBI PLASMAS

III.2.1. Global and local transport studies

TJ-II data on global energy confinement, extracted from the temperature and density profiles, have been included in the International Stellarator Confinement Database (ISCDB). This Database has been used in 2006 to continue the assessment of global Stellarator confinement [PHYS 1].

Interpretative transport has been used to revisit the global scalings of TJ-II ECRH plasmas from a local perspective. Density, rotational transform and ECRH power scans were analysed based upon Thomson Scattering data (electron density and temperature) in steady state discharges. A simple formula to obtain the thermal conductivity, χ_e,

assuming pure diffusion and negligible convective heat fluxes was used in a set of 161 discharges. All the analysis was performed with the ASTRA transport shell.

The density scan indicates that inside ρ=0.4 there is no significant change of χ_e with density in the range studied (0.4≈<ne>(1019m-3)≈1.0), while in 0.5<ρ<0.8 approximately, χ_e decreases with density. In the rotational transform scan it is found that the values of χ_e when a low order rational of the rotational transform is present locally seem to be smaller for the corresponding range, although it is apparent a general tendency of χ_e to decrease with increasing rotational transform, suggesting a general beneficial effect of the corresponding change in magnetic structure. Finally, in the ECRH power scan, χ_e is found to have an overall increment in 0.2<ρ<0.6 when QECH increases from 200 to 400 kW, although it is less significant in the density gradient region (ρ≈0.7) [PHYS 2].

III.2.2. Electric fields in ECRH and NBI plasmas

The direct measurement of the electric potential and its fluctuations in the core plasma is of primary importance to understand the mechanisms of confinement improvement and the role of the electric field in plasma confinement. A Heavy Ion Beam Probe diagnostic (Cs+ with energies up to 125 keV) was used to study the plasma electric potential directly, with a good spatial (~1 cm) and temporal (~2 μs) resolution. It is well known that the plasma potential in stellarator devices (and the electric field) changes from positive to negative values as the density is increased. Recent TJ-II experiments have investigated (shot by shot in stationary plasmas, as well as dynamically) the evolution of plasma potential profiles versus plasma density in a systematic way. The smooth change from positive to negative plasma potential in the core plasma region is now known to be a systematic feature, not dependent on TJ-II configuration [PHYS 3].

(In collaboration with Institute of Nuclear Fusion, RRC Kurchatov Institute,123182, Moscow, Russia and Institute of Plasma Physics, NSC KIPT, Kharkov, Ukraine)

III.2.3. Kinetic studies

Studies on generation and dynamics of suprathermal electrons have been continued during the last campaign. The spatial distribution of the ripple-trapped suprathermal electron losses has been monitored in "continuous mode" through the bremsstrahlung

emission from the vessel wall [1]. The characteristic energy of the lost electrons is derived from the spectrum of the photons emitted by the limiter in the soft x-ray range.

Both "spontaneous" and forced changes of escaping particle dynamics have been monitored through i) their effect on the 2-D plasma emissivity distribution [PHYS_4] and ii) the behaviour of global radiation asymmetries with respect to central plasma potential.

The concomitant effect of suprathermal electrons and rational surfaces/magnetic islands on impurity transport has also been deduced from the detection of high-energy impurity emission lines at very low-temperature plasma regions [PHYS_5].

[1] F Medina et al "Spatial distribution of lost ripple-trapped suprathermal electrons" 32nd EPS Conference on Plasma Phys. Tarragona, ECA Vol.29C, P-5.026 (2005)

III.2.4. Statistical description of transport

The traditional description of transport in fusion plasmas by means of effective diffusivities and convective terms is unsatisfactory in the sense that a number of interesting and remarkable phenomena (e.g. profile stiffness, profile peaking during off-axis heating, power degradation, non-diffusive scaling of confinement with system size, rapid transport phenomena) are difficult to understand and model in this framework. In recent years, the foundations of the diffusive description have been re-examined, and it was found that some assumptions underlying the standard description are violated in the extreme conditions of (non-equilibrium) fusion plasmas.

An alternative description, based on the Continuous-Time Random Walk and the Master Equation, was therefore developed. When incorporating a critical transport mechanism, the above unusual phenomena could all be reproduced in the framework of a very simple numerical model. Recent work includes a study of the propagation of perturbations in this model [PHYS_6], and a discussion of the mathematical and physical consequences of incorporating a critical mechanism in transport models [PHYS_7], showing that some common naive assumptions regarding the behaviour of such models (including other models than our specific model) are unjustified.

Our model involves the use of non-Gaussian Lévy probability distributions to simulate a rapid super-critical transport mechanism. While most of the cited phenomena do not depend critically on this ingredient, it is nevertheless likely that such a mechanism should be operative in plasma turbulence with e.g. radially elongated 'streamers'. In [PHYS_8],

we have studied how such an effective transport mechanism could arise from underlying microscopic motion.

It has been observed that the ion temperature profile of low density ECR heated TJ-II plasmas is almost flat and that energetic ions are present well outside the last closed magnetic surface. Ion trajectories with different pitches and starting points have been calculated. The trajectories of ions in TJ-II are computed by considering the actual 3D geometry and the usual drifts due to electric field and gradient of magnetic field are considered. It has been found that a feasible explanation for such a flat mean energy profile is that ion orbits are wide enough to communicate distant radial parts of the plasma, thus giving an effective flat ion temperature profile for low density plasmas. The distribution function is also obtained without considering collisions and non-Maxwellian features are found. The experimental data show that the ion temperature shows a gradient in NBI plasmas in which plasma density and collisionality are higher. In this situation, the electron temperature decreases and approaches the ion value. As both temperatures approach, the energy transmission between both species becomes more efficient, so ion orbits will have less importance for transport and more peaked ion temperature profiles are expected, in accordance with experimental results.

III.3. TRANSITIONS AND MAGNETIC TOPOLOGY

Transitions to improved core electron heat confinement are triggered by low order rational magnetic surfaces in TJ-II ECH plasmas [PHYS_9]. Experiments have been performed to study the influence of the magnetic shear on CERC formation keeping the order of the rational surface (n/m=3/2) and changing the magnetic shear by the induction of Ohmic current. The results indicate that the rational surface n/m=3/2 triggers the transition within the studied range of magnetic shear. In these experiments the ECH power is modulated to explore transport properties of plasmas with CERC. The improvement in the electron heat confinement is reflected by the delay of the heat pulse propagation. Within the accuracy of the experiments, the heat confinement improvement is independent of the magnetic shear [PHYS_10]. Transitions triggered by the rational surface n=4/m=2 show, in addition, an increase in the ion temperature synchronized with the increase in the electron temperature. Ion temperature changes had not been previously observed either in TJ-II or in any other helical device. Aside from a simultaneous change in electron and ion transport, a possible mechanism to explain the ion temperature change would be linked to the resonances of the radial electric that modify the ion orbits and ion confinement. SXR tomography provides a tool to identify

the presence of the magnetic island linked to the rational surface 4/2. These experiments show that, under some circumstances, the island precedes and provides a trigger for CERC formation.

III.4. PLASMA ROTATION AND MOMENTUM RE-DISTRIBUTION MECHANISMS

III.4.1. Comparison of impurity poloidal rotation in ECRH and NBI plasmas

The poloidal rotation of C V ions has been deduced from spectral line shifts measured using a high spectral resolution spectrometer and a nine fibre channel system. For ECRH plasmas with densities below 0.7 −1×1019 m-3 the radial electric field is positive. Analysis of the data obtained has shown that a change of sign of the poloidal rotation direction occurs that depends abruptly on plasma density, no matter the heating method. Whereas in low-density plasmas the poloidal direction corresponds to a positive radial electric field, at higher densities negative radial electric fields are deduced from the measured poloidal rotation. These measurements, consistent with HIBP results, are in qualitative agreement with neoclassical theory calculations that predicts that the change of sign of the radial electric field is mainly due to a change in the ratio of the electron to ion temperature [PHYS 11]. The influence of rotational transform on poloidal rotation has been investigated in the iota range 1.6 – 2.2. There is a small but systematic dependence of core rotation on iota.

III.4.2. Edge sheared flows in TJ-II: 2-D visualization of edge turbulence in the TJ-II stellarator

Edge turbulence has been visualized in 2-D by means of Ultra Fast Speed cameras [PHYS 12]. Bright, long-living structures are frequently seen with a spatial extent of few centimetres. Those structures, previously referred to as “blobs”, show predominant poloidal movement with typical speeds in the range of 103 - 104 m s-1, in agreement with the expected ExB drift rotation direction. At plasma densities near the threshold value, evidence of inward radial electric fields has been observed at the plasma edge, whereas in the plasma core the radial electric field remains positive.

An image analysis method based on two-dimensional continuous wavelet transformation is used to localize structures (blobs) in the images and to extract their geometrical characteristics (position, scale, orientation angle and aspect ratio). We study the impact of edge shear layers on these geometrical aspects of blobs. Results show a reduction in the angular dispersion of blobs as the shear layer is established in the boundary, as well as an increase in the elongation of these structures. This result is consistent with a basic prediction of the shear decorrelation model (put forward more than 15 years ago).

During improved confinement regimes the number of detected blobs decreases. Some indications are found suggesting that the turbulence reduction could be scale-selective in the biasing-induced improved confinement regime of TJ-II stellarator. Perpendicular flow reversal is visualized with the cameras and the time scales for flow reversal are found to be less than 50μs. Radially propagating structures are found in the SOL with velocities in the range ~1000 m/s and with a poloidally asymmetric spatial distribution.

(In collaboration with Princeton Plasma Physics Laboratory, Princeton, New Jersey, USA and Association Euratom/IST, Centro de Fusão Nuclear, Instituto Superior Técnico, Lisbon, Portugal).

III.4.3. Edge sheared flows: relaxation of electric fields

The role of neoclassical mechanisms to explain poloidal flows is an open issue in the fusion community. Recent experiments support the idea of a non-neoclassical origin of the poloidal flow. The universality of the observed characteristics of sheared flows points to a unique and general ingredient (e.g. turbulence) to explain the damping/driving mechanisms of these flows development in the plasma boundary region of fusion devices. Experiments in the TJ-II stellarator showing that the generation of spontaneous sheared flows at the plasma edge requires a minimum plasma density or density gradient **[2, 3]**, that depends on the magnetic configuration and on the plasma volume (ripple) [PHYS 13], open a unique possibility to characterize the dynamics of sheared flow development in fusion plasmas.

The perpendicular viscosity at the plasma edge can be deduced by means of the decay rate of the perpendicular flow measurement once the driving force has been removed. To understand the viscous damping mechanisms, changes in the plasma rotation and turbulence have been studied when an electric field is externally applied at the plasma

edge. The modifications in the plasma properties induced by electrode biasing depend on several parameters as the biasing voltage, the electrode location and the plasma density. The response of the plasma to bias is different at densities (or gradients) below and above the threshold value to trigger the spontaneous development of ExB sheared flows. Two different time scales arise in the relaxation of externally induced electric fields in TJ-II: a fast time scale and a slow time scale, being this in the range of the particle confinement time (tens of milliseconds) and evolving with plasma density. The fast time evolution of floating potential signals, when biasing is switched-off, can be fitted to an exponential function from which the relaxation time is deduced. Experimental results show that the characteristic time decay of the fast scale is in the range of 10 - 40 μs (of the order of a few turbulence correlation times).

The influence of plasma density on the fast relaxation time scales has also been investigated in TJ-II. Results suggest an increase in decay times above the critical value of the control parameter (i.e. the local density gradient) once edge perpendicular sheared flows are fully developed.

The result of the experiments carried out in TJ-II stellarator can help to understand and quantify the importance of anomalous versus neoclassical mechanisms on the damping physics of radial electric fields and flows in fusion plasmas.

(In collaboration with Association Euratom/IST, Centro de Fusão Nuclear, Instituto Superior Técnico, Lisbon, Portugal)

[2] C Hidalgo et al. "Experimental evidence of coupling between sheared-flow development and an increasein the level of turbulence in the TJ-II stellarator". Phys. Rev. E 70, 067402 (2004)

[3] M A Pedrosa et al, "Threshold for sheared flow and turbulence development in the TJ-II stellarator" Plasma Phys. Control. Fusion 47 777 (2005)

III.4.4. Edge sheared flows: comparison between model and experimental results

In the mid 90's, a simple model was proposed to explain the transition from low (L-mode) to high confinement mode (H-mode). This model predicts two successive

transitions as the pressure increases. The first one is a second-order transition controlled by the poloidal shear flow and leads to a reduction of the turbulence level. The second is a first-order transition controlled by the pressure gradient that leads to the suppression of turbulence. This second state seems to describe well the H-mode state. The first transition (the second-order one) has the characteristic properties of the emergence of the sheared flow layer. We have used the transition model to compare the predictions of this first transition with the experimental results of the formation of the sheared flow layer observed in TJ-II. Comparisons between the model and experimental data show that in spite of the simplicity of the model, it captures the qualitative features of the transition near the critical point. It should be taken into account that the model has no free parameters once the position of the critical point is determined. Of course this comparison does not confirm the exact values of the power dependences, but it shows that they are compatible with the data. We have considered plasmas with more complicated density evolutions than a simple ramp and results are also in good agreement with experiments [PHYS 14].

III.4.5. Edge sheared flows: Energy transfer between flows and turbulence

Experimental results have shown significant parallel turbulent forces (proportional to quadratic terms in fluctuating velocities) at plasma densities above the threshold value to trigger perpendicular ExB sheared flows [PHYS 15]. A new method has been applied for the quantification of the local energy transfer between flows and turbulence, by computing the production term (P). The radial-parallel contribution to the turbulence production term is proportional to the radial derivative of the mean parallel velocity and the radial-parallel component of Reynolds stress. Experimental results show that turbulence can act both as an energy sink and an energy source for the mean flow near the shear layer. These parallel turbulent forces are mainly localized at the radial location where sheared flows develop. TJ-II results show that shear flow physics involves 3-D physics phenomena in which both perpendicular and parallel dynamics play a role.

(In collaboration with Association Euratom/IST, Centro de Fusão Nuclear, Instituto Superior Técnico, Lisbon, Portugal)

III.5. MHD STUDIES

MHD activity in the TJ-II stellarator has been experimentally characterized with magnetic probes for ECRH and NBI plasmas and a wide range of magnetic configurations [PHYS 16]. It has been found to depend on rotational transform as well as operational parameters (line-averaged density and heating power). The magnetic activity in the ECRH scenario is consistent with pressure driven instabilities at frequencies 5<f<70 kHz. In NBI heated plasmas high frequency Alfven waves (150-400 kHz), with footprints of Global Alfven Eigenmodes (GAEs), are observed.

Previous experiments have shown an increase in fluctuation levels in configurations with magnetic hill in the plasma edge region. However, although the magnetic well is the main stabilizing mechanism in TJ-II, plasma profiles are not dramatically affected when the magnetic well is removed in the plasma edge. This result, consistent with recent findings in the LHD stellarator, calls into question stability calculations based on the assumption of smooth pressure profiles.

ELM-like events have been reported in TJ-II magnetic configurations with rational magnetic surfaces (3/2, 5/3, 8/5) in certain plasma parameters windows (e.g. high density). An analysis of ELM-like events, based on the coupling of ion-temperature-gradient modes to Alfvén and acoustic modes has been made [PHYS 17].

III.6. PLASMA WALL INTERACTION STUDIES IN TJ-II

See Chapter II.7

III.7. DIAGNOSTIC DEVELOPMENT

III.7.1. Diagnostic neutral beam injector (DNBI)

A dedicated diagnostic neutral beam injection (DNBI) system as well as a charge-exchange spectroscopic diagnostic were developed and commissioned on the TJ-II. This installation will permit localised charge-exchange recombination spectroscopy (CXRS) and neutral particle analysis (NPA) measurements to be made in the TJ-II. In this way, spatially resolved measurements of ion velocities and temperatures, with spatial

resolution of the order of 1 cm, can be obtained for studies on confinement, plasma poloidal and toroidal rotation.

The DNBI selected for TJ-II was a compact DINA-5 (manufactured by the Budker Institute of Nuclear Physics in Novosibirsk, Russia). Its main parameters include a 10 to 30 keV beam energy, a 2.5 A of neutral hydrogen current and a 1/e beam radius at focus of 21 mm. The DNBI, together with its power supplies and control systems, was delivered to CIEMAT in May 2004, when experts from Novosibirsk reassembled and tested the complete system (on a test bed) during a two-week period. During 2005, a mobile cradle and support structure were manufactured and installed on TJ-II for the DNBI ion source and neutraliser. During 2006 the DNBI was vacuum coupled to the TJ-II, vacuum and control systems were installed, and the first successful diagnostic neutral beam injections into TJ-II plasmas were performed. Initial testing revealed a slight toroidal misalignment of the beam with respect to the TJ-II. This has been corrected.

Work on a charge-exchange recombination spectroscopy (CXRS) system for obtaining multiple (up to 36) spectra was completed during this period. This diagnostic includes focussing lenses and fibre bundles for collecting and transferring charge-exchange emissions of C VI to the input of a high-throughput spectrograph equipped with a back-illuminated CCD camera [PHYS 18]. The focussing lenses were installed outside vacuum window assemblies on the top and bottom viewports of sector A7. Multiple fibre-optic arrays were positioned at the focal plane of these lenses. The 12-way fibre bundles, which connect to a single 36-way fibre bundle, guide the light collected to the spectrometer input. The spectrometer chosen was a high-throughput model equipped with a high-dispersion transmission grating. In addition, a high-efficiency (~95% at 529 nm) back-illuminated CCD camera was fixed at the focal plane of the spectrometer. Finally, other components such a narrow bandpass filter, a fast shutter and multiple slits were also procured, or manufactured, and subsequently installed. This system was tested and operated during early 2006 as a passive diagnostic. The system permits multiple spectra centred about the C VI emission line at 529 nm to be collected every 50 ms along a TJ-II discharge [PHYS 19]. System calibration is made using a pencil lamp (Neon) in the light collection pathway.

Work also begun during 2006 on a semi-automated spectral line analysis code. It permits the multiple spectra to be analysed simultaneously. It permits, by using calibration spectral lines as reference, obtain line widths and line displacements for all 36 channels.

Also, analysis of CXRS spectra is done by the automatic removal of passive (beam off) C VI signal from passive & active (beam-on) C VI signal.

III.7.2. Hydrogen pellet injector

Work is in progress to provide a pellet injection system and associated diagnostics systems for TJ-II. Such a system consists of a cryostat and cold finger for creating hydrogen pellets, propulsion mechanisms for accelerating the resultant pellets, guide tubes for directing and delivering them and inbuilt diagnostics for determining the size and velocity of the pellets entering the plasmas. The injector is being built in collaboration with the Fusion Energy Division at Oak Ridge National Laboratory (ORNL). The provision of this active diagnostic will provide a new tool for studying several key physics issues of interest for the TJ-II programme. These are stability and transport, magnetic configuration, and non-thermal electron studies.

Preliminary studies were carried out during 2004 to evaluate the benefits of installing a pellet injector in the TJ-II and to define the pellet sizes and velocities best suited to ECRH and NBI plasmas in TJ-II. The ranges selected then were pellet diameters between 0.4 and 1 mm and velocities between 150 and 1000 m s-1. During 2005 the design of key components was begun at ORNL and key components were procured or manufacture during 2005/2006. Also during 2006, a closed circuit cooling system for the cryocooler controller was installed at Ciemat. The cryocooler will provide 4 watts of cooling capacity at 10 kelvin, sufficient to produce up to 4 pellets per TJ-II discharge.

III.7.3. Neutral Particle Analyser Systems

The TJ-II is equipped with four neutral particle analyser (NPA) systems for obtaining ion temperature profiles. Two of these systems, type Acord-12, are located in port A-8 and scan the plasma poloidally. Another, a Compact Neutral Particle Analyzer (CNPA), developed by the IOFFE Physical Technical Institute of Russian Academy of Science and St. Petersburg State Technical University, is located in the tangentially viewing B-1 port. It is an energy and mass spectrometer of reduced size. Significant reductions of spectrometer size and weight were achieved by employing a thin diamond-like carbon foil instead of the traditional stripping gas for stripping and using a high field permanent magnet instead of the traditional electromagnets for the generation of the analysing magnetic field. It is designed to study high-energy tails of the distribution function of escaped H0 atoms in the range 0.8 to 40 keV. Finally, a 24-channel, upgraded Acord-24

NPA is also located on port B-1. In both cases, the lines-of-sight are almost tangential to the magnetic axis.

During 2006 the control and data collection systems of the CNPA and Acord-24 were improved as part of the collaboration with IOFFE. In addition, work was carried out to synchronize and calibrate these new systems with the DNBI system.

III.7.4. Thomson scattering

Some hardware replacements/improvements have been performed during 2006.

A broken Printed Circuit Board (PCB) camera has been changed for a new one, helping with the routine diagnostic alignment.

A laser energy monitor signal (ELASER) has been included in the TJ-II database. The peak amplitude of the signal is proportional to laser energy, and its steep leading edge marks the time where the laser is actually fired. This signal helps the routine operation of the diagnostic, assessing the quality of the laser shots.

A new, both sides antireflection coated BK7 window has been substituted for the old, uncoated output window, increasing the overall transmission of the system in a few percent.

A technique using vibrational Raman scattering in different gases (CO2, Ethane and SF6 at several tens millibars) has been implemented in TJ-II as an aid to the density calibration of the diagnostic. In TJ-II Thomson Scattering system, vibrational Raman Scattering may have some advantages over rotational scattering in N2 or H2 due to the fact that the notch filter of the system attenuates (or in some cases, eliminates) rotational lines close to the ruby exciting wavelength, but has much less effect on vibrational lines. As a by product of these experiments, some nonlinear effects associated with the high power ruby laser/high gas pressure have been observed, like enhanced antiStokes lines from CO2 or supercontinuum emission from SF6. More work is needed to compare this technique with Rayleigh scattering and eventually produce from both techniques an absolute density calibration.

A newly bought Sun workstation (Sunblade 1500) has been installed (with its corresponding operating system) as a replacement for the old one. A new IDL license has been acquired, and a copy of the whole file system of the old workstation has been transferred to the new one. It remains to re-install/re-compile and update the old programs to work in the new machine. To this end, the collaboration of our colleagues of the FOM Institute for Plasma Physics (who developed the running version of the software) will be essential.

The police of buying spare parts for the system, as well as the maintenance visits for the ruby laser have been continued.

III.7.5. Microwave reflectometry in TJ-II

A broadband fast frequency hopping reflectometer designed for measuring plasma turbulence is in operation at TJ-II. The reflectometer allows to probing several plasma layers within a short time interval during the discharge. The asymmetric turbulence spectra measured using the reflectometer allow us to measure changes in the perpendicular rotation velocity of the turbulence at the plasma edge and their dependence on plasma conditions [PHYS 20]. The interpretation of these experimental results has been crosschecked with results obtained using a two-dimensional full-wave code [PHYS 21]. Numerical results reproducing the experimental measurements demonstrate the capability of the reflectometer to measure the velocity shear layer with good spatial resolution. The code has been also used to study the Doppler reflectometry capability to measure the perpendicular velocity of the density fluctuations. Accurate Doppler measurements can be obtained using high directivity Gaussian beam antennas with optimum beam waist in slab plasmas and also in plasmas with high curvature. Antenna systems with wide beam divergence should be avoided even in plasmas with very low-curvature cut-off layers.

III.7.6. Two colour infrared interferometer

A study of reliability has been performed and new improvements proposed and initiated. To eliminate thermo-optical effect, one ZnSe window has been removed and substituted by an in vessel Cu mirror with an "ad hoc" designed holder. Also HeNe laser 633 nm second wavelength has been changed to a Nd-YAG laser1064 nm one. CO2 laser source for 10,6 μm first wavelength has been substituted by a stabilized one. Study of under-sampling, noise and noise reduction applied to our phase measurement has been done.

The activities have complemented those into the cooperation project with IPP in the field of development and construction of a multi-channel CO2-Interferometer for W7-X [PHYS_22].

III.7.7. Spectroscopy

A method for measuring absolutely calibrated rotation velocities in fusion plasmas by means of passive spectroscopy, using a single plasma view, has been implemented in TJ-II. The method consists of simultaneously recording the emission lines from the plasma and from a calibration lamp by means of a double fiber-fiber guide. A software simultaneously analyzes the plasma and calibration lines, which are obtained with a high-resolution spectrometer equipped with an intensified linear detector array, and provides absolute rotation measurements. Experimental results of carbon impurity ion rotation measured in the TJ-II stellarator demonstrate than accuracy better than 0.3 km/s can be achieved. [PHYS_23].

III.8. JET ACTIVITIES

III.8.1. Inboard-Outboard pedestal temperature measurements in JET using ECE diagnostics

The characterization of the pedestal electron temperature (Te) profiles in JET has been expanded in 2006 by using a new set of measurements obtained using electron cyclotron emission (ECE) radiometry at both, the high-field-side (HFS) and low-field-side (LFS) midplane. This is possible because the existing radiometer can be set up to measure either 1st harmonic/O-mode or 2nd harmonic/X- mode electron cyclotron emission. Whereas for second harmonic X-mode the maximum radius at which reliable temperature measurements can be obtained is limited to R>2.6 m (due to harmonic overlapping), for first harmonic O-mode polarization this limitation does not exist. The good temporal (typically 0.3 ms and up to 2 ms for faster studies) and spatial (3-6 cm) resolution of the radiometer makes it an ideal diagnostic to measure fast, spatially localized phenomena, such as ELMs.

Data in different plasma scenarios (different configuration, density, q95, ...) have been collected during the 2006 campaigns. In order to calibrate HFS data, two independent

methods has been developed: cross-calibration with Michelson interferometer using specific toroidal field ramp pulses and comparison to the data measured at the plasma LFS during L-mode (assuming that Te is constant on the same flux surface). The initial comparative analysis of the inboard and outboard pedestal temperature show very good agreement between HFS and LFS Te pedestal profiles. Given the relative novelty of the technique, most of the effort this year has been devoted to the validation of the new HFS data and the identification of the limitations of the measurements and the data analysis. Further data collection and analysis will be carried during 2007.

III.8.2. Upgrade of the heterodyne radiometer at JET

A second enhancement of the heterodyne radiometer at JET was approved in 2006 with CIEMAT as the leading Association. The main purpose of this enhancement is to extend the spectral coverage of the radiometer, in order to allow X-mode second harmonic measurements at all magnetic fields (1.7 T < BT < 4 T) used in JET (currently central Te data in X-mode is limited to BT < 2.5 T). This upgrade will bring an increase in the associated cut-off densities, with the cut-off density for the second harmonic X-mode being twice that of the first harmonic O-mode. The detailed design of the system was approved in March 2006. The different contracts were awarded by the commission at the end of 2006. The manufacturing of those components is under way with the goal of finishing the installation and commissioning of the new system by the end of 2007.

III.8.2.1. Test Camera system (within FC7 Enhancement Project) and experimental results in JET

A fast (test) visible Photron APX-RS camera (on loan from CIEMAT) has been installed, commissioned and operated on JET during campaign C17 (2006) and later on during C18 and C19 (2007). The camera is located near the equatorial plane and uses the visible port of the KL7 endoscope designed for infrared imaging (same field of view). It uses a CMOS detector with a maximum recording speed of 250 kHz and a minimum exposure time of 1 us. In the present set-up no interference filters are used. The camera was tested against high radiation fluxes and rapidly varying magnetic fields. The integrated neutron fluence in the camera position after four months of operation is in the range of 4x1010 n/cm2. So far there is no evidence of permanently damaged pixels. Several disruptions were recorded, the camera withstanding field variations of up to 4 T/s.

The test camera system has proven to provide useful information to study different fusion plasma relevant issues including plasma wall interaction, ELMs and disruption physics.

IV. THEORY AND SIMULATION

IV.1. GRID COMPUTING RESEARCH

IV.1.1. Grid computing for fusion

During the year 2006, several activities have been developed on grid computing for fusion. The Fusion-VO, which is the name of the virtual organization inside EGEE infrastructure, has reached a peak power of about 1 Tflop [TH_1]. Several applications are running in this virtual organization [TH_2]. The first one, devoted to Kinetic Transport is in production phase and relevant physical results are obtained. The second one is devoted to ray tracing foe electron Bernstein Wave heating in stellarators, which is being submitted to a benchmark. The third one is devoted to the stellarator optimization and is based upon a genetic algorithm.

IV.2. TRANSPORT

IV.2.1. Dynamics of recycling and density control

Density control is a relevant aspect in the experimental campaigns of the TJ-II Heliac. Based on a simplified model for kinetic equation (the one included in the ASTRA package [1], the electron source distribution has been studied in typical TJ-II plasmas depending on the recycling conditions. To this aim, we act on the boundary conditions of the kinetic model as follows: based on pressure measurements in the vacuum chamber of the TJ-II [2], we change the neutral density in the plasma boundary depending on puffing and transport outflows. The resulting electron sources allow us analysing the sensibility of the plasma to cold gas puffing depending on the recycling conditions. The problem of density control actually found in the experiments is thus modeled by the numerical calculations, which allows studying the ratio between recycling and gas-puffing flows towards the plasma in typical Electron Cyclotron Heated discharges of the TJ-II stellarator. For densities below ECH cutoff, density control via gas puffing is difficult because the range of stable densities in the presence of a limiting wall is small. In the plasmas heated by energetic neutral beam injection, the experimentally observed increments in plasma density respond to strong additional particle sources not accounted by the neutral beam

itself. These studies have provided a first stage of understanding before, in a next exercise, we adopt a more complete numerical routine to evaluate the particle source from gas-puff and recycling [TH 3].

[1]: G. V. Pereverzev, P. N. Yushmanov, ASTRA Automated System for TRansport Analysis, Max-Planck-Institut für Plasmaphysik, Rep. IPP 5/98, Garching, February 2002.

[2]: F. L. Tabarés, D. Tafalla, J. A. Ferreira, Neutral pressure measurements in TJ-II plasmas, 6th Iberian Vacuum Mtng. (VI RIVA), WS-18-MoM-OR.3, Salamanca, June 26-28, 2006.

IV.2.2. Experimental Electron Heat Diffusion in TJ-II ECRH plasmas

Interpretative transport has been used to revisit the global scalings of TJ-II ECRH plasmas [3] from a local perspective. Density, rotational transform and ECRH power scans were analysed based upon *Thomson Scattering* data (electron density and temperature) in steady state discharges. A simple formula to obtain the thermal conductivity, χ_e, assuming pure diffusion and negligible convective heat fluxes was used in a set of 161 discharges. All the analysis was performed with the ASTRA transport shell [4].

The density scan indicates that inside ρ=0.4 there is no significant change of χ_e with density in the range studied ($0.4 \approx \langle n_e \rangle (10^{19} m^{-3}) \approx 1.0$), while in $0.5<\rho<0.8$ approximately, χ_e decreases with density. In the rotational transform scan it is found that the values of χ_e when a low order rational of the rotational transform is present locally seem to be smaller for the corresponding range, although it is apparent a general tendency of χ_e to decrease with increasing rotational transform, suggesting a general beneficial effect of the corresponding change in magnetic structure. Finally, in the ECRH power scan, χ_e is found to have an overall increment in $0.2<\rho<0.6$ when Q_{ECH} increases from 200 to 400 kW, although it is less significant in the density gradient region ($\rho \approx 0.7$) [TH 4].

*[3] E. Ascasíbar, et al., Nucl. Fusion, **45**, 276, 2005.*

[4] G. V. Pereverzev, P. N. Yushmanov, ASTRA Automated System for TRansport Analysis, Max-Planck-Institut für Plasmaphysik, Rep. IPP 5/98, Garching, February 2002.

IV.2.3. One-dimensional model for the emergence of the plasma edge shear flow layer with momentum conserving Reynolds stress.

We have formulated a one-dimensional version of the second-order transition model based on the sheared flow amplification by Reynolds stress and turbulence supression by shearing. We have included a form of the Reynolds stress which explicitly conserves momentum. After performing a linear stability analysis of the critical point, we have studied the dynamics of weakly unstable states, which is determined by a reduced equation for the shear flow. In the case in which the damping term is diffusive, the stationary solutions of the reduced equation are those of the Ginzburg-Landau equation.

IV.2.4. Fractional generalization of Fick's law.

In the study of transport in inhomogeneous systems it is common to construct transport equations using the inhomogeneous Fick's law. The validity of this approach requires that at least two ingredients be present in the system. First, finite characteristic length and time scales associated to the dominant transport process must exist. Secondly, the transport mechanism must satisfy a microscopic symmetry usually known as global detailed balance. However, many complex systems have been shown to lack these characteristic scales. We have shown how to construct a generalization of the inhomogeneous Fick's law that does not require the existence of characteristic scales while still satisfying global detailed balance [TH 5].

IV.2.5. The effect of electric field on ion orbits in TJ-II stellarator

The ion confinement is studied in TJ-II by estimating a large number of orbits. Typically 10^7 particles and launched following the experimental density and temperature profiles and their orbits are estimated using the guiding centre approximation. No collisions are considered for the moment and the effect of the electric field on the orbits is estimated by comparing the results of following particles without and with electric field. This one is considered similar to the experimental one in TJ-II, as measured by heavy ion beam

probe. Beyond the confinement enhancement in the presence of the field (which is not surprising) interesting results are obtained form this model as the asymmetries on particle density in the toroidal as well as in the poloidal direction [TH 6]. Due to the absence of collisions, only limited statements can be extracted on the real kinetic transport. Collisions will be included in the future [TH 7].

IV.2.6. Ion transport in tokamaks

We have adapted the Monte Carlo method described in [TH 7] to a Tokamak geometry, in order to manage with analytical electromagnetic fields and include ITER profiles in the near future. The collision operator is exactly the same as in the former reference, but deterministic drift equations are modified because plasma currents are not negligible. We have also included the linearized wave-particle operator in the evolution equations, so ICH effects are taken into account [TH 8]. The aim of this work is to compare the particle and heat fluxes in presence of ICH.

Solving numerically these equations require large supercomputers. Most of the simulations have been performed in the Fusion-Grid computers, as well as in the BIFI cluster (www.bifi.unizar.es). The Fusion Grid is a new supercomputing cluster that joins many medium size clusters all over Europe and allows the user to submit processes when some CPU's are unnocupied.

IV.3. PLASMA HEATING

IV.3.1. Relativistic effects on electron Bernstein Waves (EBW) heating in TJ-II Stellarator

Previous works have shown that the most suitable scheme for EBW in TJ-II is the O-X-B1 that has acceptable efficiency heating for central densities above 1.2 x 10^{19} m^{-3}, and frequency heating of 28 GHz . Non relativistic ray tracing calculations were performed using the code TRUBA to estimate the EBW heating properties of such a scheme. Based on such calculations it was possible to optimize the launching position and, hence, to design the hardware system. During this time, a weakly relativistic dispersion relation valid for any angle and refractive index value, has been developed. Thus the relativistic effects are included both in ray trajectory and absorption for EBW. The relativistic results

are compared with the non-relativistic ones and the results show that those effects are not negligible either on heating or current drive [TH 9].

IV.3.2. Calculation of the fully relativistic dielectric tensor

The fully relativistic dielectric tensor is calculated extended the concept of the plasma dispersion function to the fully relativistic case. This estimation allows to perform calculations for burning plasmas for which the temperature will be high enough to make the raltivistic effect non negligible. The comparison with the weakly relativistic calculations has been carried out showing the range of parameters for which the weakly relativistic approximation is still valid [TH 10].

These calculations allow the extension of the relativistic tensor to the case of complex frequencies, which will be useful to study plasma instabilities.

IV.3.3. ECRH induced Pump-out in plasma devices

A linear simplified model based on Langevin equations [TH 8] is developed to estimate the radial flux induced by ECRH in plasma devices. In tokamaks and stellarators, low density ECRH plasmas are characterized by having a hollow density profile and a peaked temperature one. The first observation can be explained in terms of the creation of a outward flux induced by microwaves. In this work, this flux is estimated by considering the flux of particles in the loss cone in the velocity space. It is assumed that all the particles that enter in the cone are instantaneously lost [TH 11].

IV.4. EQUILIBRIUM AND MHD

IV.4.1. Equilibrium criticality, diamagnetism and phase transitions

The conjecture that transport barrier formation is preceded by a critical equilibrium (due to a degenerate zero of the poloidal current density profile) remains to be tested. Updates on this work include a study of the evolution of current profiles in tokamaks. Even in a simple cylindrical model it is apparent that the natural evolution of the plasma

equilibrium is towards criticality and the formation of diamagnetic regions in the plasma, given localised non-inductive current drive (such as bootstrap or auxiliary current drive).

IV.4.2. ELM studies at JET

The possibility of matching ITER pedestal and edge parameters in JET plasmas was studied. High edge electron temperature and low plasma resistivity lead to essential differences in plasma current profiles, which can have a fundamental effect on ELMs in ITER. An experimental proposal was developed to study hot edge plasmas, in a large ELM regime. In particular such target plasmas would be useful to test ELM control and mitigation techniques to be for ITER. [TH 12]

Further, data analysis confirmed earlier results, showing that ELM arrival may not always occur outboard first. [TH 13]

IV.4.3. Equilibrium reconstruction in tokamaks

The equilibrium code EFIT, used to reconstruct equilibrium at JET, is being updated. There is now a unified version of the code, EFIT 2006, written in Fortran 90 and C++ (tasks ITM-05-IMP1-T2 and ITM-05-IMP1-T7 of the project IMP-1 of the European Integrated Tokamak Modelling Task Force). Exact numerical agreement between the old JET version and the new fortran 95 version was reached for reconstructions with external magnetic measurements and kinetic measurements, so far only with polynomial description of the profiles. Input structures of the ITM can now be used, via IDAM, as well as JETPPF input/output and namelists. [TH 14, TH 15, TH 16, TH 17].

V. MATERIALS PROGRAMME

During 2006 the association has been involved in three main materials fields:

- Ceramic insulators for heating and current drive and diagnostic systems.
- Radiation tolerance assessment of standard components for remote handling.
- Structural reduced activation and advanced materials, modelling, and blanket/tritium cycle.

V.1. IRRADIATION EFFECTS IN CERAMICS FOR HEATING AND CURRENT DRIVE, AND DIAGNOSTICS

Within theses tasks CIEMAT has been responsible for 9 deliverables related to:

- Radiation induced absorption and luminescence of selected alternative radiation resistant glasses
- Radiation enhanced incorporation of hydrogen isotopes in silicas and aluminas: optical, electrical, and dielectric effects.
- Radiation enhanced diffusion of hydrogen isotopes in silicas and aluminas.
- High temperature annealing on induced voltages (TIEMF) in copper and SS cored MI cables
- Resistive type bolometers using alumina, aluminium nitride, and silicon nitride substrates temperature and ionization effects.
- Irradiation testing of a prototype radiation-hard capacitive bolometer assembly based on PZ ferroelectric material.
- Coatings for mirrors resistant to radiation enhanced corrosion, dose and temperature effects.
- Dielectric loss at 1 MHz during irradiation of RF source insulation. Assess possible breakdown.
- Radiation induced conductivity for potential commercial insulators for NBI bushings.

V.1.1. Radiation induced absorption and luminescence of selected alternative radiation resistant glasses (TW5-IRRCER D4)

KU1 (high OH content) and KS-4V (low OH content) are high purity silicas that are being considered as main candidates for use in ITER as windows and optical components since they exhibit very good behaviour when exposed to a radiation field particularly in terms of radioluminescence and radiation induced optical absorption. A study of the radiation induced absorption and luminescence of two types of alternative multicomponent glasses has been carried out at CIEMAT. The samples were provided by SCK-CEN and the nominal composition of both types of glasses in weight percentage is 75% SiO_2, 22% Na, 3% CaO. One of the types was 0.05% Cerium doped while the other type was undoped.

The two types, Ce doped and undoped, materials have been studied in terms of radioluminescence, photoluminescence, and radiation induced optical absorption. In order to perform such a study the samples were irradiated with 1.8 MeV electron at 15, 100, and 200ºC up to a dose of 190, 60 and 60 kGy respectively and during irradiation radioluminescence and optical absorption measurements were performed at different doses. In addition, for all the samples; before and after electron irradiation; photoluminescence and optical absorption spectra were taken making use commercial spectrophotometers.

The results show that both types of glasses are highly sensitive to radiation, particularly in the case of the radiation induced optical absorption. Some improvement is observed when these glasses are irradiated at 200ºC. However even at this temperature the material behaviour is much worse than in the case of KU1 or KS-4V. [MAT1]

V.1.2. Radiation enhanced incorporation of hydrogen isotopes in silicas and aluminas: optical, electrical, and dielectric effects (TW5-IRRCER D6)

Oxides will be used in ITER in heating and current drive and also diagnostic systems where they will play important roles as electrical insulators and optical components.

These materials will be subjected to neutron and gamma irradiation, and additionally to bombardment by low energy ions and neutral particles. These low energy particles will deposit most of their energy at or very near the surface and hence the local damage and/or degradation of the physical properties at the vacuum surface could be very high. Previous works have shown severe electrical and optical degradation with a marked temperature dependence. The dependence on ion mass, energy, and dose rate, together with the evolution of electrical degradation as a function of ion dose has been studied.

KS-4V (SiO_2) samples, 10x10x0.9 mm^3 in size, were implanted with low mass ions at different energies and dose rates. To compare different low mass ions, the samples were implanted with 54 keV He^+, H^+, H_2^+ and D^+ at 50 ºC up to a dose of 10^{17} ions/cm^2. In analogous way, to compare different energy ions, the samples were implanted with 27 and 54 keV helium at 50 ºC up to a dose of 10^{17} ions/cm^2 . And finally, to compare different dose rates the samples were implanted with 54 keV helium at 450 ºC up to doses of 10^{17} ions/cm^2 and 10^{18} ions/cm^2, at 0.5 μA and 5 μA respectively.

The degradation curves (surface electrical conductivity as a function of ion dose) exhibit two separate stages: an initial rapid electrical degradation during the first stage, followed by a second stage where the rate of degradation is much more moderate. The SiO2 surface electrical degradation depends strongly on the implanted particle energy. The electrical conductivity degradation is higher for the higher energy. Initially, for low dose, the dependence on ion energy is less marked. However, for higher dose the trend to saturation occurs much more rapidly for the lower energy implantation. A clear dependence on ion mass has been observed, with the degradation occurring much more rapidly for heavier ions. No dependence on dose rate was observed implying that the fundamental processes related to surface electrical degradation must take place on a very short time scale. [MAT2, MAT3, MAT4, MAT5]

V.1.3. Radiation enhanced diffusion of hydrogen isotopes in silicas and aluminas (TW5-IRRCER D7)

The objective of this task is the assessment of radiation enhanced diffusion of tritium through candidate insulator materials, and the potential effects on the material properties relevant for the application. Sapphire, aluminas, BeO, Macor, Viton, Diamond

were studied. Deuterium permeation and absorption measurements under 1.8 MeV electron irradiation have been performed. In order to carry out the experiments an special chamber was fabricated and mounted at the end of a Van de Graaff accelerator. The irradiation chamber, was divided in two smaller chambers: the pressurized deuterium chamber and the vacuum chamber. The samples studied were circular in shape, 30 mm in diameter and 1 to 3 mm in thickness. The samples were placed between the two cells and Viton O-ring seals were used to isolate them. One of cells could be gas pressurized meanwhile the other was kept in vacuum and connected to a Helium/Deuterium leak detector. Hence one side of the sample was exposed to pressurized deuterium meanwhile the other was kept in vacuum and receiving directly the electron beam.

More specific deuterium permeation and absorption measurements were performed for Deranox 995 alumina: One Deranox 995 sample was mounted at the irradiation chamber, the deuterium cell was kept in vacuum and the sample was electron irradiated at 100 Gy/s. Irradiation temperature was kept below 50 C. A deuterium signal around 10-11 mbar l/s was measured during irradiation, it reached a maximum and then decreased with dose. This signal was due to the 0.016% natural proportion of deuterium associated to either hydrogen or moisture present on chamber walls and sample surface. Then the deuterium cell was filled with deuterium at 1bar. Before irradiation no signal was measured but with irradiation a leak signal of around 10-11 mbar l/s was observed. In this way the sample was irradiated and at the same time deuterium loaded at 100 Gy/s during 1.5 hours. Once the irradiation was finished the sample was reversed: the deuterium loaded face was exposed to both the electron beam and helium/deuterium detector. Immediately after mounting a signal of about 10-9 mbar l/s was measured indicating that deuterium was being spontaneously released from the alumina surface, the signal decreasing with time. Once irradiation started the leak value increased about 40%. A similar experiment was performed but in this case the deuterium loading was performed without irradiation. The deuterium loading performed during irradiation was much higher, about 20 times, than when loading without irradiation.

No conclusive radiation enhanced permeation of deuterium has been observed. However clear radiation enhanced absorption has been observed to occur for Deranox 995 alumina. Some of the deuterium absorbed on the surface is released spontaneously at room temperature however the experiments clearly show that an important part of the deuterium is trapped at rather stable sites and that ionizing radiation is necessary in

order to release them from traps. Further experiments are necessary in order to quantify and clarify all these phenomena not only for Deranox 995 but also for the other ceramics.

In addition to the experimental work on tritium diffusion, the problem has been addressed theoretically. Ceramic insulators will be used in the ITER Heating and Current Drive and Diagnostics (H&CD/D) systems as optical and RF vacuum windows (VW) or as feedthroughs. Their performance as materials could come modified by the intake of deuterium-tritium which might be enhanced by ionizing radiation effects. Physical operational conditions of a generic alumina VW of ICRH system in ITER have been analysed. A phenomenological release rate transport model has been formulated and adapted to TMAP7 1-dimensional finite modelling tool. Precise values for permeation fluxes and inventories are provided from solution of mass transport equations. Experimental priorities are seen to be concentrated in precise quantifications of radiation enhanced diffusion and trapping defects phenomena with the mastering of surface roughness characteristics.

Main results

The results show how combined surface/radiation-rate regimes determine the species transport behaviour in the VW. These depend on the characteristic times, both diffusion and recombination, of the processes: respectively (Figure 10). Radiation-enhanced diffusion "through" competes with radiation enhanced diffusion "back" with shorter pathways for recombination-desorption along the transmission line.

General Conclusions

As has been shown, refined tritium transport release-rate models together with detailed parametric studies can make assessments more precise. In addition such modelling can serve as conceptual framework to quantify the impact of underlying phenomena (e.g. radiation enhanced diffusion or potential effects of radiation damage on tritium transport through the VW) and its final impact on main transport parameters of interest for VW design: permeation flux and D/T inventories. In the present work it has been shown how, for implantation of ionized D,T in the VW being the major source for isotopes intake, a hybrid *recombination/radiation enhanced diffusion* regime determine H-isotopes transport kinetics in the window. No matters of Tritium and Deuterium transport through ICRH VW in ITER with safety. Intake and transport of DT in the window may have an impact on the modification of the physical (electronic) properties, not considered here.

Further work for this task

The present refined release rate models are useful to establish, through sophisticated numerical analyses, the prospective targets of experimental activity generating the inputs needed in appropriate ranges. For the identified hybrid *recombination/radiation enhanced diffusion* regime main parameters of interest for experimental studies are: the final range of radiation enhanced diffusion factor enhancement, material surface constants (disassociation and recombination) entering in recombination rate constants (*s*: sticking coefficient), nominal values for radiation-induced trap concentrations c_T and trapping well energies E_T. Correlations between known possible radiation-induced defect structures in Al_2O_3 and related E_T values seem of theoretical interest for near term investigations. Such correlations can also be established through well known procedures by transient experiments. According to ranges such experiments are very demanding in terms of experimental precision. The type of test and experimental capabilities needed will be detailed investigated in the near future. The maximum design precision of inputs for D/T release rate can be obtained through the use of advanced computing tools. MCNPx tools (providing detailed neutron and charged particles transport analyses) are used to precise input values for precise damage computation at the Al_2O_3 VW using actual design inputs in ITER. A net computation of c_T value is in the short term scope of this work. As an extension to the work is expected to analyze the window infringed damage under radiation conditions in the operation time; evaluating with the neutron transport tool, MCNPX, the possible interactions with the alumina lattice and obtaining the consequences with SRIM2003 code. The developed release-rate model and its implementation for the analysis of other VW/H&CD systems (ECRH, LHRH feedthroughs) is expected for the near future. Use of phenomenological release rate model to model real fusion data (real data is available from D/T experiments at JET and TFTR fusion machines) can be considered as medium term activity. [MAT6, MAT7]

V.1.4. High temperature annealing on induced voltages (TIEMF) in copper and SS cored MI cables (TW5-IRRCER D8)

After initial experiments mainly at CIEMAT proving the existence of TIEMF (Thermally Induced Electromotive Force), CIEMAT and SCK-CEN were devoted to the study of these thermoelectric effects. One possible reason for TIEMF would be based in the fact that cold-work induces changes in thermoelectric power in Cu. Therefore it could be possible

to eliminate this specific TIEMF cause by thermal annealing. The purpose of this task therefore, has been to examine the effect of high temperature on the voltage between the ends of the central conductor of MI cable leads (TIEMF), and examine the possibility of thermally annealing the phenomenon, thus giving more details about the TIEMF origin.

Two MI cables were studied with different inner wire; one based on Cu plated SS and the second only 304L stainless steel, both with SS sheath and 1 mm outer diameter.

A thermal scan was firstly used to detect the regions of the cable with maximum and minimum TIEMF effect. The existence of TIEMF peaks was then used to study the maximum sensitivity points more in detail, as previously done in several Cu based cables. The main conclusions are:

- Using a higher temperature gradient we have detected the existence of TIEMF in the steel cable and evaluated this effect as a function of temperature.
- Different behaviour of TIEMF as a function of temperature has been measured in copper and stainless steel MI cables. As previously estimated it values are much lower in SS (0.020 μV/ºC max) than in Cu MI cables (0.080 μV/ºC max). In the SS case, values of T > 170 ºC during thermal scanning were necessary to obtain a signal/noise ratio acceptable. The peaks in general were fewer and broader than in Cu based MIC.
- Short times treatments at temperatures around 500 ºC did not change noticeably the TIEMF values of the two cables studied.
- The annealing of copper is complex but there is quite a lot of information in the bibliography. Therefore some estimations can be made to compare with results obtained for effect of temperature on TIEMF. Cold work does not seem responsible of TIEMF. This indicates that TIEMF is probably due to impurities located inhomogeneously.

[MAT8, MAT9, MAT10, MAT11]

V.1.5. Resistive type bolometers using alumina, aluminium nitride, and silicon nitride substrates temperature and ionization effects (TW5-IRRCER D10)

In order to find an alternative to mica, the technical feasibility of producing sufficiently thin substrates from more radiation resistant materials with adequate thermal and dielectric properties was examined. Alumina, aluminium nitride, silicon nitride, silicon dioxide, and CVD diamond were examined, all these materials having the added advantage of considerably increasing the upper temperature limit for continuous use above the 500 ºC recommended for mica. Using Pt instead of Au as metal sensor will present reduced transmutation due to comparable lower low energy neutron capture cross section. Initial trial results led to the conclusion that substrates of Al_2O_3, Si_3N_4, and AlN are perfect alternative candidates to mica substrates. The electrical resistance of deposited Pt tracks of initial and improved bolometer series was characterized as a function of temperature and ionizing radiation. Under electron irradiation at 400 ºC, an induced resistance increase of about 0.13 % / MGy was measured and considered tolerable for the ITER design application. Some were sent to the SCK-CEN experimental reactor, where irradiation was performed in vacuum up to 500 ºC to a total fast neutron fluence of $1.3x10^{19}$ n/cm^2 (about 0.013 dpa). After the experiment, no substrate swelling and no distortion of the resistance strips could be observed, but some of the electrical connections were lost during testing due to a weak union between the Pt wire and the Pt sputtered film. Here we report on an improved prototype, with reduced meander area, enhanced Pt film quality and adhesion, and better electrical connections.

The present devices are being fabricated with a more realistic complex meander Pt sensor in which the conductor length has been increased, while keeping the sensing area dimensions constant. The meander deposited substrate was sandwiched between two Macor frames, the best version having the electrical terminals of Pt wires attached to SS screws which allocate Cu strips in contact with the substrate.

The bonding and stability of the meander was considerably improved by e-beam evaporation of 100 nm Pt + 6 nm Ti sensor onto polished surfaces of AlN and Al_2O_3 substrates. The thermo-mechanical response of the Pt-ceramic interface was enhanced by annealing the bolometer in vacuum at 400 ºC for 2 hours. Sputtered and evaporated Ti/Pt thin films suffer from thermal degradation, as observed during in-situ sample heating by using ESEM. When submitted to temperatures above 600 ºC in air, the metal film became dull and rough in appearance due to the formation of metallic microclusters while the measured electrical resistance increased. It is therefore recommended to avoid temperatures above about 500 ºC.

After vacuum annealing at 400C, these new prototypes were electrically characterized. The linear temperature behaviour is independent of the following parameters: the depositing substrate, the design of the meander-like sensor, and the deposition method. The measured thermal coefficients of resistance (around 0.0006) are well below that of the bulk Pt (0.0038), explained in terms of the important contribution of defects, which dominates the thin film resistor (Mathiessen law). The Al_2O_3 and AlN bolometers were irradiated with ionizing dose rates up to 200 Gy/s for about 7.5 and 11.5 h at 203 ºC and 450C to total doses of 5 and 8.4 MGy, respectively. Resistance variations (≤ 0.5 and ≤ 1 %, respectively) over periods of time far greater than one ITER shot can be accommodated.

Also in this task a complete bolometer prototype fabricated at IPP Garching with 300 and 500 nm thickness Pt sputtered meander tracks onto a 1.5 μm thickness, insulating layer of Si_3N_4 was electron irradiated at CIEMAT in preparation for neutron irradiation in BR2. The bolometer was irradiated in the temperature range 189 to 194 ºC at ionizing dose rates from 10 to 200 Gy/s, up to 2 MGy. Ionizing radiation due to electron irradiation has no measurable effect on the sensor resistance values, although the present organic materials must be substituted by inorganic alternatives.

[MAT12, MAT13, MAT14]

V.1.6. Irradiation testing of a prototype radiation-hard capacitive bolometer assembly based on PZ ferroelectric material (TW5-IRRCER D13)

Objective: The development of radiation resistant active diagnostic components, namely radiation-hard capacitive bolometers based on multilayered ferroelectric material structure. Ferroelectric bolometer prototype stage development brings together material studies and more detailed prototype engineering aspects including the optimisation of mutilayered structure of selected sensing layer and substrate, buffer layers, bottom /top electrodes and carrier film layouts compatible with existing bolometer head assemblies. It was expected to test various detailed aspects of material performance and prototype in specific radiation environment at test sites of association members – including CIEMAT- according to particular stage of development. Tests include basic electric performance characterization, thermal heating and thermal stimulus response measurements with or without irradiation. Pulsed laser deposition, sol-gel technology, photolithographic layout

patterning and shadow masking sputtering will be used to produce of thin film multilayers.

Unfortunately, samples have so far not been delivered to CIEMAT for this irradiation testing and therefore no new results are available concerning the radiation hardness.

V.1.7. Coatings for mirrors resistant to radiation enhanced corrosion, dose and temperature effects (TW5-IRRCER D14)

Radiation enhanced degradation of reflectivity of different commercial mirrors as a function of irradiation temperature and time (dose) in different environments (vacuum, nitrogen, air), as well as enhanced corrosion in a humid environment are being studied. It has been observed that the SiO protective layer is unstable. SiO converts to SiO_2 in the presence of ionizing radiation and oxygen in the air causing the coating to crack due to swelling, and render the mirror susceptible to corrosion in the presence of water vapour. Furthermore it has been observed that some mirrors, although nominally identical, are more susceptible to corrosion than others.

During this work some problems have been encountered with the as-received commercial mirrors concerning reflectivity and overcoating. Mirrors provided as identical, in the same batch by the manufacturer (Coherent), have very different reflectivity in the UV range. Analysis of the surface material has shown varying amounts of SiO and SiO_2 for nominally SiO overcoating. In another case the specified coating (MgF_2) for an UV enhanced mirror (Newport) was observed to contain Hf, neither Mg nor F were found. Hf is commonly used to enhance the reflectivity in the UV spectral range, but Hf has a large low energy neutron capture cross section and may cause problems due to transmutation. It is therefore very important to analyse the composition and measure reflectivity of all commercial mirrors before use in ITER, as commercial specifications are not completely reliable.

For some commercially available mirrors, and two prototype Al on Pyrex glass mirrors made at CIEMAT, overcoated with SiO_2 and Al_2O_3, reflectivity changes after gamma irradiation up to 40 MGy in dry nitrogen at 170 and 250 ºC were examined. In dry nitrogen, for UV enhanced mirror little or no measurable degradation of reflectivity in the VIS-NIR range is observed, however below about 400nm, radiation produces a clear

decrease of reflectivity. For the Al_2O_3 overcoated mirror the decrease is larger at 250ºC than at 170 ºC, whereas for the UV enhanced mirror the decrease is similar at both temperatures. Corrosion susceptibility, (irradiation in a humid atmosphere up to 0.5 MGy and 250 ºC temperature) were examined for nominally MgF_2 and the Al_2O_3 overcoated mirrors. At this dose no measurable degradation of reflectivity in the UV-VIS range occurs in a humid atmosphere.

New commercial mirrors of two types have been acquired from Thor. The manufacturer specifications are: general broad band use mirrors (4 mirrors), with SiO overcoating and reflectivity >90% from 400 nm to 10 μm. and UV enhanced (4 mirrors), with MgF_2 overcoating and reflectivity >90% from 250 to 400 nm. Taken into account the problems encountered previously with the as-received commercial mirrors concerning reflectivity and overcoating, reflectivity measurements and XPS analysis of the surface material of as-received mirrors were carried out.

SiO overcoated mirrors provided as identical show two different reflectivities: one group (2 mirrors) have similar reflectivity and another group (2 mirrors) have similar reflectivity. The XPS spectra are different. In one group Thorium (Th) and Fluorine (F) are present (not referenced by the manufacturer), and it is present SiO and SiO_2. The other group shows that is completely SiO_2 overcoated not as nominally (SiO overcoated). UV enhanced (4 mirrors) nominally MgF_2 , show similar reflectivities, but Mg and F were not found, only SiO2 is present, that it is not the specified coating.

Within the TW6 part of the mirror task (TW6-IRRCER-D4), several mirrors are being prepared to study the effect of neutron irradiation. Two different substrates with guaranteed radiation resistance have been chosen. These are KU1 and KS-4V high purity silicas, that are considered for optical components in ITER. Three discs of the KU1 silica of 30 mm of diameter and three of KS-4V of 37 mm of diameter have optically polished. The thickness for both materials is 2mm. Aluminium will be supported by high irradiation resistance silica substrates and afterward will be SiO2 overcoated. The coatings will be obtained by the sol-gel technique and after heat-treated at about 300ºC for fixing together. Pre- and post gamma irradiation reflectivity measurements from 250 to 2500 nm of these mirrors will be studied. The gamma irradiations will be done at different temperatures.

[MAT15, MAT16, MAT17]

V.1.8. Dielectric loss at 1 MHz during irradiation of RF source insulation. Assess possible breakdown (TW5-IRRCER D15)

Objective: The alternative NBI RF source will require insulation for the RF coil which will operate at about 1 MHz, 60 kV. The chosen insulation will be subjected to high temperature, voltage and radiation and therefore its behaviour must be assessed.

Due to the high voltage the existing irradiation chamber has been modified for higher safety and a new oscillator of 1 MHz and 1000 V pp has been designed and tested.

An alumina with high performance as a dielectric was selected and the high purity grade "Deranox 99.9%" was purchased from Morgan Advanced ceramics. Unfortunately there was a long delay for delivery. When received and after first strange experimental results it was confirmed that instead of Alumina the samples were Zirconia, with a high dielectric constant and higher loss. This error has caused another long delay to discuss with the company and to get the "real" Deranox 999" samples.

Their dielectric properties (permittivity and dielectric loss) have been measured in an extended frequency range to asses the effect of posterior radiation and high voltage. The loss has acceptable values at 1 MHz - between 3.10^{-4} and 5.10^{-4} depending on the sample (of the same batch)- being quite flat down to 1 kHz, but increasing rapidly at higher frequencies and reaching almost 10^{-2} at 100 MHz.

V.1.9. Radiation induced conductivity for potential commercial insulators for NBI bushings (TW5-IRRCER D16)

The aim of this task is the measurement of Radiation Induced Conductivity (RIC) in insulating materials candidates to be used in Neutral Beam Injectors. These insulators should fulfil with the requirements of big size, should be commercially available and should support a high voltage (1 MV) with a minimum of conductivity under irradiation. Neutral Beam Injectors must face at the plasma and therefore a high radiation field is expected in this area. At present the best candidates for this application are porcelains and some ceramics.

During the last period any new material has been required to be measured. This period has been used in the improvement of the measuring system. The X-ray installation where the RIC measurement system was set up is not involved in the Fusion Technology Programme but in the calibration of instrumentation for measurement of ionising radiation. When the RIC measurement system was set up in this laboratory there was a reasonable availability to allow this task to be performed. The work load in this installation during the last two years has let to a few chances for our experiments. In fact during the last year the measuring system has not been into the installation allowing us at least to make some experiments without radiation.

Several actions have been performed in order to move the measurement system to a new X-ray installation with a very low work load. This change has also allowed some improvements required for measurement of low conductivity materials under irradiation and some modifications to avoid problems related to conduction through the residual gas (ubiquitous problem in this kind of experiments).

V.1.10. TW5/6-IRRCER Underlying Technology

V.1.10.1. Study of Radiation Induced Electrical Currents for Hydrogen Isotopes and Helium at Low Residual Pressure and Effect on Insulating Surfaces

Severe surface electrical and optical degradation has recently been observed when oxide materials are implanted to low doses (10^{19} ions/m^2) with keV H and He ions at 50 to 450 C[. Similarly ITER ceramic insulators and windows may also degrade, as they will be bombarded by energetic H isotope and He ions due to ionization of the residual gas by gamma radiation and acceleration by local electric fields. To assess this potential problem one must determine the magnitude of radiation generated ion currents at low residual gas pressures.

Experiments were performed in a chamber mounted in the beam line of a Van de Graaff accelerator. H, D, and He gases at a controlled pressure were irradiated through an aluminium window with 1.8 MeV electrons. Within the chamber a guarded volume between copper electrodes with a voltage applied, permitted the electric current flowing through the ionized gas to be measured. In this way radiation induced ion currents have

been measured at gas pressures between 10^5 and 10^{-2} Pa, dose rates of 20 Gy/s, and applied voltages up to 1500 V (10^5 V/m). As anticipated a decreasing ion current was observed on lowering the pressure. However the measured current reached an unexpected constant saturation level for pressures below 10 Pa. The electrically insulated irradiation chamber permitted polarization of the chamber relative to the guarded volume. This allowed one to demonstrate that the saturation was due to a radiation induced dark current of electrons rather than ions. With the modified system it was possible to suppress most of this dark current and measure ion currents down to 10^{-2} Pa. At this pressure the radiation induced ion currents were about 10^{-6} A/m^3/Gy/s, i.e. potentially high ion currents for large systems.

Dark currents occur in large high voltage systems under vacuum, and can produce Bremsstrahlung (X-ray) radiation. In some cases they have been observed to degrade insulation performance in NBI test systems. To date radiation enhanced dark currents have not been considered as a potential problem. However the results obtained indicate that currents of the order of 10^{-7} A/m^2/Gy/s may be generated from metal surfaces.

[MAT3, MAT4, MAT5, MAT18, MAT19]

V.1.10.2. Study of thermally–induced electrical signals (TIEMF) in coated cables for in-vessel coils

Present results obtained in Mineral Insulated (MI) cables indicate that temperature gradients (Inherent to reactor operation) generate signals along the central conductor of MI cables in the range of μV's (TIEMF). The effect of such an induced voltage is of serious concern for the proposed ITER magnetic diagnostic coils, as it will introduce an error signal impossible to differentiate from the required information. In previous tests it was found that the TIEMF can even be larger than the radiation induced RIEMF. This effect has been found in all the MI cables studied. The purpose of this task therefore, was to examine the possibility of using other cable types, at least partially.

One cause for TIEMF effect would be based in the fact that cold-work induces changes in thermoelectric power in Cu. Therefore several alternative candidate cables have been identified in the main plasma sprayed and similar coated cables which should have suffered less from this effect.

Finally two of these ceramic coated cables (5 and 7 m long) have been available for study, one based in a Ni-Cu core (from Ceramawire) and the other in SS (manufactured by California Fine Wire) both purchased by Consorzio RFX (Padova) in the framework of the EFDA Task TW5-TPDS-DIADEV. This allows us to compare quite easily with the previous studied MI cables based also in Cu and SS conductors.

A new oven of very small dimensions and well controlled temperature and movement has been used to reveal the spatial details of TIEMF with high resolution. The main conclusions are:

- Using the air flow method, the results for Ni Cu coated cable gives better results than Cu MI cables, but clear TIEMF peaks have been also observed. This together with the problems observed in RFX concerning the insulation coating makes this cable unsuitable for magnetic diagnostics or at least shows no great advantages over a mineral insulated Cu cable.
- The use of the new oven reveals very clearly the existence of the TIEMF peaks and their spatial structure.
- Using the air flow method, the results for SS cable indicates rather low TIEMF, but again problems were observed in RFX concerning the lack of insulation with temperature and voltage.
- The use of the new oven for SS cable has shown very clearly the existence of the TIEMF peaks and their fine structure spatial structure, being much narrower than in CuNi.
- Although there are large differences in manufacture and origin, the differences between the two ceramic coated cables are in general agreement with the differences observed in Cu and SS mineral insulated cables and the expected reduction of TIEMF is not enough taking into account the insulation problems.

[MAT8, MAT9, MAT10, MAT11, MAT20**]**

V.2. RADIATION TOLERANCE ASSESSMENT OF RH COMPONENTS

Within this task CIEMAT has been responsible for 1 deliverable, as follows:

- Irradiation and subsequent testing of the hydraulic seal carriers: Progressive gamma irradiation of hydraulic seals.

V.2.1. Gamma irradiation and subsequent testing of the hydraulic seal carriers: Progressive gamma irradiation of hydraulic seals (TW5/6-RADTOL)

The main CIEMAT contribution to the present task centred on irradiation of a number of seal carriers developed jointly by IHA (Finland) and Gradel (Luxembourg). Each stainless steel seal carrier comprised a UHMW Polyethylene seal (from Busak+Shamban's (Z-80)) with a conventional NBR O-ring underneath, and a closed stainless steel ring around the seal representing the cylinder bore. The seal assembly was designed to be fitted (after irradiation) to a specially modified piston which was then pushed carefully into the cylinder of a hydraulic test rig (developed by IHA) such that there was minimal manipulation strain to the seal itself. A total of 10 seals carriers were assembled by IHA and sent to CIEMAT where they were irradiated in the Nayade facility to total doses from 100 kGy to 10 MGy and at the dose rate of about 6 Gy/s and 323 K. During irradiation, tensile specimens and other samples of the seal and O-ring material were placed in the empty core of the seal assembly to allow basic mechanical tests and inspection to be carried out following irradiation.

Following irradiation the mechanical test samples were dried for 48 hours in an oven at 45 ºC. Even before mechanical testing could be performed all the specimens showed a high level of permanent residual deformation after the drying, mainly due to warping. The warping was more severe for the NBR material than for the Z-80. Also it was possible to observe defects due to mechanization on the edges and, in some cases also cross-sectional warping with the consequent distortion of the geometry of specimens. For some of the samples cracks of up to 5 mm or more appeared aligned along the greater dimension of the specimen.

Main results:

Seals (Z-80): With increasing dose they change colour, becoming browner. But they are still flexible, even by 10 MGy. The gamma irradiation modifies specially their ability for straining that decreases dramatically from about 450 MPa in the as received material to almost 4.5 for that irradiate at 20MGy. However, the strengths remain in the same range for all the studied doses. As the dose is enhanced it is possible to appreciate that the specimens tend to break at the yield point

O rings (NBR): 2 MGy still elastic, slightly deformed by the pressure (normal behaviour), however at 5 and 10 MGy hard and brittle. The results obtained for the standard rubbers nitrilo-type indicated that they have low tolerance to the gamma radiation. It has only been possible to obtain values for 5 and 10 MGy doses. Above these doses the specimens are so fragile that they are broken by the handling before testing.

[MAT21, MAT22, MAT23**]**

V.3. STRUCTURAL REDUCED ACTIVATION AND ADVANCED MATERIALS, AND BLANKET/TRITIUM CYCLE

Within these tasks CIEMAT has been responsible for 6 deliverables related to:

- Characterisation of reference EU ODS-EUROFER batch (Charpy and FM).
- W alloys; production, joining, and basic studies.
- Modelling of radiation effects
- HCLL; LiPb, He

V.3.1. Structural materials: High performance steels (TW5-TTMS-006 D6)

Characterization of reference EU ODS-EUROFER batch: Charpy and FM

The charpy properties of the EU ODS-EUROFER steel, normalized in Ar at 1100°C/30'plus tempered in Ar at 750°C/2h/air cooled, have been studied in two products forms: plate of thickness 16 mm (Heat HXX1115) and rod of diameter 20 mm (Heat HXX1116). The impact characteristics of this alloy have been investigated in the TL and LT orientation for the plate and L orientation for the rod. The DBTT has been calculated as the temperature corresponding to USE/2.

The EU ODS-EUROFER has shown the following DBTT values: -38°C for the TL orientation, -24°C for the LT orientation and -2.6°C for the rod. These values mean a significant shift of the DBTT compared with the Eurofer'97 (DBTT = -107°C). The difference of the DBTT between the orientation and the product form could be attributed

to the fitting procedure. The USE decreased, compared with the Eurofer'97, by 15% for the rod and around of 40% for the both orientations of the plate.

In addition, the charpy properties of the EU-ODS EUROFER steel have been completed with factographic examinations. Both product forms (plate and rod) exhibit brittle fracture by cuasi-clivage in the ductile-brittle transition region. No intergranular fracture has been observed in any specimen. However, the fracture surface of some specimens present cracks that seems to indicate material de-cohesions. These features have been detected in the plate (TL and LT orientations) and in the rod (L orientation). The cracks are perpendicular to the fracture surface plane for both orientations of the plate while they present circumferential orientation for the rod.

Turning next to the fracture toughness properties of EU ODS EUROFER, this steel are being testing in both product forms and in the same orientations that in the charpy tests. The first results seem to indicate that the application of the master curve will not be possible. The fractographic examination shows that many ductile areas are present in the fracture surface of the specimens and then the rupture is not pure cleavage, even at very low temperatures. In general the fracture toughness obtained present small variations in the lower shelf, but there is a suddenly shift up to the upper shelf where the behaviour is ductile. Due to this jump in a very short temperature interval the Master Curve does not represent the real behaviour of the material.

[MAT24].

V.3.2. Advanced materials: Divertor and plasma facing materials (TW6-TTMA-002 D1, D4, D6)

D1: Production of small laboratory batches of improved W alloys for characterization

Pure tungsten and tungsten alloys having 0.5 wt % Y_2O_3, x wt % Ti and 0.5 wt % Y_2O_3+ x wt % Ti have been prepared by powder metallurgy; $0 \leq x \leq 4\%$. Elemental powders were blended or ball milled, canned, outgassed and finally consolidated by a two-stage HIP process under a pressure of 200 MPa. It is found that Ti addition favours the densification attaining a fully dense material, while pure W and W-0.5Y_2O_3 achieve 93% and 90% of theoretical density, respectively. XRD, SEM and TEM analyses of the material with Ti addition reveal the formation of a structure consist of tungsten particles embedded in a

W rich Ti matrix. Microhardness measurements and pin-on-disk wear tests have also been performed on these materials. [MAT26, MAT27].

D4: Joining techniques of ODS steel and W alloys

Dissimilar welds between pure tungsten and EUROFER have been made using two alternative welding procedures: 1) laser brazing applying a high temperature braze alloy wire of 80Ni-20Cr and 2) solid diffusion bonding by HIP using a pure copper as interlayer. Laser weldability tests showed metallurgical compatibility among selected brazing filler and both ferritic-martensitic steel and tungsten. Input energy densities applied for laser brazing were in the range 550-1000 W/mm^2 with travel speeds of 2.5-3.5 mm/s. Under these conditions, formation of brittle intermetallic compounds was not observed in any of the both welded interfaces and continuous joints free of porosity or fusion faults were obtained. However, as input energy was increased, the risk of cracking from W sheets towards the filler is promoted because the large mismatch in expansion thermal coefficients. First tests of diffusion bonding by HIP showed weldability problems associated both to the steel/copper and W/copper interface formation. Oxidation during diffusion bonding cycle limits metallic contact among parent alloys with interlayer. [MAT28].

D6: Fundamental studies on mechanical properties of W-alloy

The bending strength and toughness of these materials have been assessed at room temperature and analyses of the fracture surfaces have performed. A fracture toughness K_{IC} as high as 9.8 MPa $m^{1/2}$ have been measured for W-4Ti alloy. [MAT29, MAT30].

V.3.3. Structural materials: Modelisation of Irradiation Effects. (TW6-TTMS-007 D5, D12)

V.3.3.1. Modelling He effects in irradiated iron

We have developed a rate theory model for He diffusion in Fe based primarily on ab initio results for defect energetics. A good agreement between calculations and experimental results could be obtained by using effective values for the migration of V and binding energies of V to Hei and to Hes. The values found could be explained by invoking the presence of impurities in the experimental samples. One likely candidate, considering experimental observations and ab initio calculations, is carbon. In addition, our model reveals that several mechanisms govern He diffusion during isothermal annealing. In

particular, the model shows that self--interstitials clusters play a fundamental role in the diffusion of He in irradiated Fe.

In order to elucidate the contribution of each mechanism for He diffusion we have performed calculations using OkMC for different conditions of temperature and He to Vacancy ratio. We have observed that the contribution of the vacancy mechanism is only significant at low temperatures (400K) and He to V ratios of at least 10 V per He. On the other hand the presence of self-interstitials significantly alters He diffusion through the replacement mechanism at all temperatures. The effect of carbon on He diffusion is also being studied systematically. Carbon is included at different concentrations: 1 appm and 10 appm and results are compared with the case without carbon. In particular we have observed that the presence of carbon increases the total number of He jumps, and therefore affects He diffusion. The actual path resulting in this increased diffusivity of He in the presence of C still needs to be studied further.

Further information can be found in the report for task TW6-TTMS-007-D04. Three publications have resulted from this work, two on Physical Review B and one in Journal of Nuclear Materials. It should also be mentioned that the results of this work were highlighted by Anton Möslang and Thierry Wiss in a recent News&Views article of Nature Materials [Nature Materials, Vol. 5 (2006) 679]. It has also been presented in four international conferences.

[MAT31, MAT32, MAT33, MAT34].

V.3.3.2. Atomistically-informed Dislocation Dynamics in fcc crystals

We have extended the discrete dislocation dynamics methodology as developed by Arsenlis et al. (2007) and Bulatov et al. (2004) to fcc systems by explicitly considering all dislocation dissociations and reactions among partials [DDAtom_DENIM06]. To this end, we have derived simple continuity laws that enable the treatment of stacking faults and partial dislocation nodes. In addition, we have added appropriate topological rules to account for the specific transformations relevant to fcc slip, e.g., dislocation dissociation, junction formation, cross-slip, etc. Our dislocation dynamics methodology has been fitted to atomistic results in Cu, including core energetics, and has withstood the test of several simple validation checks. We show that, consistent with real crystals, the sole parameter needed to describe all dislocation dissociations and reactions is the stacking fault energy. We have obtained the dissolution strengths of the main four dislocation junctions in fcc metals, namely the Lomer-Cottrell, Hirth, co-linear and coplanar junctions, for the

straightforward geometry of perfectly-parallel initial dislocation segments. We find that, in agreement with the current state-of the-art in DD simulations, the co-linear junction is clearly the strongest. A full mapping of the junction strength as a function of the character of the reacting dislocations will be undertaken in future studies. We have characterized the four-dimensional cross-slip surface by mapping threefold stress subspaces and have extracted simple mathematical rules to implement the different cross-slip mechanisms considered. Based on atomistic simulations, our model does not include cross-slip into obtuse planes, as the stress required for this process is significantly larger than for the acute case. The thermally-activated nature of cross-slip has not been treated here and our stress surfaces provide a cross-slip map in zero-temperature equivalent conditions. Future work includes computing the cross-slip energy landscape as a function of the applied stress so that thermal effects can be accounted for. An extension of these models is actually being generated for taking into account the bcc materials such as Fe and its alloys by using empirical potentials incorporating magnetic effects.

[MAT35**].**

V.3.3.3. Synchronous Parallel Kinetic Monte Carlo for Continuum Diffusion Reaction Systems

We have developed a novel parallel kinetic Monte Carlo algorithm that promises to access time and length scales as-of-yet unexplored in kMC simulations [PKMC_DENIM_JCP06, accepted 2006 in J. Comp. .Physics]. Our algorithm is based on a perfectly-synchronous parallel decomposition of the master equation, to which it provides an exact solution for the case of independent walkers. The correct simulation of interacting systems is contingent on the rigorous treatment of boundary conflicts, which we will address in future publications. Regardless, in the limiting case of large problems (large number of particles, many PEs), our algorithm provides fairly accurate solutions for interacting systems. The efficiency of the method is dependant on the characteristics of the problem at hand and the optimization facilities of the decomposition chosen. We have shown the validity and performance of our algorithm in a few well understood diffusion problems, with reasonable scaling and excellent agreement between our computational results and analytical and serial cases. Due to its trivial implementation in parallel architectures, our algorithm suggests itself as a more practical alternative to other previously published parallel methods.

[MAT36**].**

V.3.4. Tritium breeding and materials: HCLL (TW6-TTBC-005 D2)

Experimental determination of reference Sieverts' constant and diffusivity values for tritium in Pb-Li.

The preparatory work related to the Absorption - Desorption experimental technique of the University of the Basque Country to determine the hydrogen transport properties of Sieverts' constant and diffusivity in the eutectic Pb-Li alloy has been concluded. This work consists of several tasks that are briefly commented below.

Pure tungsten crucibles (9 units) have been manufactured by Plansee following a precise design in order to hold the liquid alloy during the hydrogen absorption-desorption tests. This crucible minimises the contribution of the sample container to gas absorption and desorption. A quartz sample-holder has been adapted to hold the tungsten crucible with the liquid sample into the temperature controlled region. The necessary glass blowing work has allowed the precise connection of the experimental chamber to the gas analysing volume of the facility. Data acquisition system (National Instruments SC-2345) managed by Lab View software has been prepared to acquire all the test parameters (pressure evolution and temperature) with high frequency (200Hz). A new Bayard-Alpert gauge to measure the vacuum level in the facility and a new Quadrupole Mass Spectrometer to analyse the gas composition has been mounted in the gas analysing chamber of the facility. Two ingots of PbLi euthectic alloy with 0.62 – 0.68 wt% Li and max 100ppm impurities have been prepared and certified by GMH Jost- Hinrich Stachow GmbH to get the samples. The maintenance of the two ultra-high vacuum pumping units of the facility has been performed. A specific model has been developed to simulate absorption-desorption runs to derive transport parameters of diffusivity and Sieverts' constant. Currently the experimental campaign has begun and the first blank runs in the absence of samples have been obtained. [MAT37, MAT38, MAT39].

V.3.5. TW5/6-Underlying Technology

V.3.5.1. Metallurgical Characterization of experimental ODS steel

During 2006 CIEMAT has dedicated its Underlying Technology (UT) effort to determine the fracture toughness of the Eurofer'97 steel by testing small specimens in the ductile to brittle transition region, with the application of the Master Curve methodology, in order

to evaluate this method to assess the decrease in fracture toughness due to neutron irradiation.

It is worth to point out that it has not been possible to perform the CIEMAT investigations foreseen for the 2006 within the Underlying Technology, related to the metallurgical characterization of experimental ODS steels in collaboration with the Carlos III University, due to experimental problems in the ODS fabrication in the university.

The Eurofer'97 steel was tested using two different size of bend specimens: the standard charpy size (10x10x55 mm) denoted PCCV, and small-size bend specimens (3x4x27 mm) denoted KLST. These specimens were machined in the L orientation from the 100 mm bar. For comparison fracture toughness tests of compact tension specimens machined from the 14 mm plate in the TL orientation, previously studied, are also included. The value of the reference temperature T_0 (Table 1) was determined by the multi-temperature method included in the ASTM E1921-05 standard.

Heat	**Specimen**	**Orient.**	**Thickness, B (mm)**	**Width, W (mm)**	**T_0 (ºC)**	**n**	**r**
100 mm rod	PCCV	LT	10	10	-113	15	12
	KLST		3	4	-99	15	9
14 mm Plate	½TCT	TL	12.7	25.4	-129	11	9

Table 1: T_0 values for Eurofer'97.

The T_0 value obtained by testing KLST specimens presented here is higher than the other T_0 values. That means that KLST specimens show a lower fracture toughness value than other geometries, contrary to the specimen size effect on fracture toughness. This behaviour could be related, according to the literature, with that the 3x4 specimens have a tendency to yield higher T_0 values. Other reasons for the higher T_0 values with KLST specimens are related with the validity window of test results, and the low test temperature necessary for those specimens, which usually gives conservative estimate. **[**MAT40**]**

V.3.5.2. Production, and mechanical and microstructural characterization of Y_2O_3 ODS EUROFER/UC3M

Ingots of steel ODS EUROFER and non-ODS EUROFER have been produced by HIP and their microstructural and mechanical characteristics investigated [6]. Positron annihilation experiments performed on isochronally annealed ODS material reveal the formation of voids that are not annealed out at 1550 K. However, voids formed in the non-ODS material consolidated by HIP are unstable at temperature above 1325 K [7]. **[**MAT41, MAT42**]**

V.3.5.3. He Bubble Formation in Liquid Metals

D1: He bubble formation and potential impact on the design of fusion technology systems (HCLL channels, IFMIF target and LM plasma wall concepts)

The significance of He bubble production in NFT breeding systems has been established. For the role of helium at IFMIF Li-jet target the main underlying question is related with the possible helium bubble nucleation within the Li-jet residence time in the target. Precise quantitative answer to this question is provided by the comparison of characteristic times of He-nucleation rates (clustering rates for stable He-clusters in Li) with Li residence time in IFMIF target stripping surface. Characteristic times for helium clustering (bubble nucleation) under helium supersaturated conditions in lithium has been assessed by adapting Continuum Scale Nucleation Models in Solids developed for ^{3}He/tritides to He in Li. The residence time of 15 m/s Li-jet in the breeding area (length: L ~ 25 cm, assuming plate curvature) stripping target is also within the range of tenth ms (roughly 20 ms). Assessment of nucleation kinetics drives to slightly lower values of clustering characteristic times. In this sense, with a large probability, the He bubbles are formed out of stripping target in the concave plate and then with no major impact on target performances. Bubbles nucleating in the bottom part of the concave plate of IFMIF target would impact Li-jet hydrodynamic stability (Li jet versus Li-jet plus Helium bubbles) and must be considered for future (not present, other stability analyses are preferential) CFD refinements of jet stability analyses. Bubbles formed in form of small bubble (nano/micron) are transferred into the reservoir and flow through Li-loop channels. For DEMO-2003 Breeding Blanket /He-cooled Lithium-Lead blanket conditions and according with He atomic breeding and actual approximation for values of He Henry´s constant in Pb15.7Li, the LM is supersaturated in helium. The main question is if ionic breeding can create the local perturbation conditions (as cloud chamber in high energy physics) for He bubble nucleation. It can be assumed as reasonable that ion breeding in LM can create the microscopic conditions for bubble nucleation. Many direct and indirect proofs of it exist. In principle, bubbles might be nucleated with minimum

number of atoms. It is observed in diverse tritides. Following the available equation of state valid for native bubbles, the bubbles in LM need a larger number of atoms (n ~ 10^4) for high inner bubble pressures (100 MPa). Bubble nucleation process is fast enough. Nucleation can be considered instantaneous for technical BB design purposes. In HCLL channel conditions bubble formed are about diameter 20 nm. This value is based on liquid metal surface tension data and assessment made here for He solubility in LM. Bubble generation rates in HCLL have been obtained from atomic breeding and from the number of atoms per stable bubble created. The bubble concentrations and sizes allow to consider bubbles as independent with low coalescing probabilities. Proposed values for nano-bubbles are given. Small and independent nano-bubbles evolve stably in slow LM HCLL channels. The main important driving forces for bubbles are derived from the momentum transfers from LM, i.e.: viscous drag forces. Bubble Brownian diffusion overlaps this drag component. Thermal gradients can have an effect on bubble transport and can justify a transfer of bubbles to the interface between LM and CP and non-nucleated gas condensation. If such a regular and homogeneous interface is established it can justify a mass-transfer resistive mechanism for tritium transfer permeation into the CPs. Precise description of bubble plume transport can be numerically achieved from precise solution of fluid velocity fields accounting for both MHD and thermal convection effects. According to bubble sizes and distribution in channels the coalescing probability of bubble along HCLL channels is low. Simple approximations can be exploited to evaluate the final role of bred bubbles for the specific in the case of HCLL channels is the small size of bubbles and the low mass flow rates. Use of such approximations (assuming common reference values for the rest of parameters) permits one to justify POTENTIALLY LARGE IMPACT of bubbles on tritium transport. In a reference case values of natural extraction efficiencies of 0.27 (!) (as fraction of tritium transported by bubble) may be justified. This fraction, if confirmed, would mean an important impact on the conceptual design of tritium cycle technology for Fusion Reactor DEMO in many aspects: - relaxing or complementing requirement of tritium permeation barriers, - on design definition of tritium extraction systems, etc.

Developments towards the numerical implementation of 2-phase dispersion models for a bubble plume in LM conducts represents a major computational goal. Activities, on modelling and on definition the appropriate experimental programme (specific tests (CAVITEX) seem absolutely necessary) are ongoing in CIEMAT. For He bubble nucleation at FS/FW concepts, FS/FW concentrations are clearly above the He super-saturation limit in Li and the necessary super-saturation conditions for Helium bubble formation seem guaranteed. Helium bubbles are created with (~ tenths ms) kinetic with (tenths

nanometres) radii. A large number of bubbles (ratio between bred atoms and needed atoms per cluster) can be in principle justified and transfer of bred helium atoms in solution to bubbles can be justified as an efficient mechanism for bubble growth. According to surface tension values the bubble, sized in the range of nanometre would be stable against re-dissolution or implosion. Once created bubbles migrates stable in the FS/FW Li-flowing wall. A precise modelling of helium behaviour in FS/FW appears complex and requiring a large set of physical assumptions with simplification hypothesis (future work). Main assumptions are related with stability assumptions and thermal evolution field in the FW surface.

According to Diffusion coefficient data, the diffusion characteristic times of implanted helium atoms at 450 º C are extremely low ($t_c \sim Dx^2/6D \sim 10$ ns, Dx ~ projected range 0.068 mm, i.e.. shorter than typical He bubbles nucleation times. In this conditions the surface kinetics for free He atoms desorption (sweeping atoms into S-O-L vacuum) impose the He recycling kinetics at the FS/FW and He poloidal concentration evolution at the FS/FW is driven by free-surface sweeping. If (sub-micron) bubbles are nucleated (typical minimal nucleation times ~ 10 ms in Figure A3.6), diffusion characteristics times should be recalculated taking values close to of Brownian diffusion coefficient. Typical values at 450 º C range between 10^{-11} and 10^{-12} m^2/s and ($t_c \sim Dx^2/6D \sim$ 0.15 ms). If a thermal gradient is considered across the LM thickness (between the free surface and the solid back-plate wall), the mean time needed buy a bubble to diffuse from the implantation range into the free surface is, for nano-metric bubbles, something like a fraction of ms (shorter than typical bubble nucleation times assessed). In this sense, even if bubbles are formed He diffusivity in Lithium is so high, that He recycling is achieved with atoms. Most accurate picture of He behaviour in the flowing FS/FW concept is something like a continuous atomic sweeping of helium from plasma vacuum. According to last simple kinetic consideration, bubble nucleation is occurring from non-pumped amounts and the a detailed study of atomic He desorption kinetic in free surface of major interest. Even if bubbles can be formed, FS/FW seems robust for high He recycling. Such high He recycling would minimize He bubble on D(implanted)/T(implanted and bred) transport in the fluid.

[MAT43**].**

D2: Literature review on available Li-Li, He-He and He-Li interatomic potentials and achievements

In deliverable No.2 a rigorous and systematic literature review of inter-atomic potentials for Li-Li, Li-He and He-He system has been accomplished. Li-Li, He-He and He-Li inter-atomic potentials can be found in the literature, with only narrow margins of uncertainty for the obtaining by computational ways basic physical magnitudes in this system. These input on potentials have been reviewed so that an ab-initio simulation of the He/Li system with He super-saturation can be carried out in order to look for a visualisation of bubble nucleation in Li system.

From this review a large confidence on the available Li-Li, Li-He and He-He potentials for simulations can be concluded. Li-Li potentials and Li-He potentials have a large experimental (spectroscopic) validation. Among them DFT and in particular OF-AIMD potentials have shown the largest reliability to reproduce Li-Li neutron and x-ray diffraction experimental data (at lower k numbers) with relaxed computational costs. Another question is the computational costs for each type of potential and computational approach. This issue will be addressed in next deliverable 3 and 4.

Diverse potentials (Li-Li, Li-He, He-He) have proven large capabilities to reproduce bulk and physical magnitudes of systems and interaction properties. Potential are then available for the simulation and visualisation of He dynamics in liquid Lithium. Global representation of each pair potential (Figure 7) advances the possible He behaviour in Li-system: tendency of Li atoms to cluster at short distance, weakness of He-Li interaction and comparative stronger long-range He-He interaction. Such characteristics advance natural tendency of He atoms in liquid lithium for nucleation.

[MAT44**].**

D3: Generation of DFT potentials by SIESTA

In deliverable No.3, SIESTA DFT potentials have been produced. Such values are genuine products because DFT potentials for DFT system had never been produced before. Ways to generate directly He-Li simulations have been explored. Conclusion is that DFT are not useful for direct DFT/MD simulations of He-Li systems in order to visualize nucleation phenomena. Extra large computational demands would be needed according to reference values of He/Li solubility and number of atoms needed to constitute a bubble within the LM. Ways to do it using large Spanish supercomputing has been started. Pending answer.

D4: Development of a MD simulation of bubble formation (using MOLDY or MDCASK)

Alternatively, classical MD makes an accessible route to approach the problem and is assumed as the method for the final attempt. Computations are ongoing with MDCASK updates.

General Conclusions

Helium bubbles exist in LM breeding systems and have a major impact on NFT designs, in particular on tritium transport along LM BB channels. **[**MAT45, MAT46**].**

VI. TECHNOLOGY WORK UNDER EFDA

VI.1. INTRODUCTION

During 2006 CIEMAT continued its effort to increase the level of activity within the EFDA technology programme, in order to extend the capabilities beyond the traditional work on irradiation effects on functional materials, reported on chapter V.

Activities were undertaken in six different areas:

- Diagnostic design support: port engineering.
- Divertor component tests by Ultrasonic techniques
- ITER safety studies, within the EISS project
- IFMIF developments on several areas: accelerator (superconducting DTL option, RF solid state sources) and target: Li fluidynamics.
- Syetems & plantes studies, focused on three areas: hydrogen production from fusion reactors, high efficiency energy conversion cycles for Fusion and energy storage technologies for pulsed reactors.
- Socioeconomics studies: EFDA-TIMES model and social perception of Fusion research.

Other tasks of interest have been initiated by the end of 2006: ITER diagnostics (reflectometry, LIDAR, Infrared viewing) , NBI components (ion dumps, RH). Results on those areas will be reported in 2007 ´s annual report.

VI.2. PHYSICS INTEGRATION

VI.2.1. ITER Diagnostic Equatorial Port Plug Engineering and Integration

EFDA Technology Work programme 2005 (EFDA Reference: TW5-TPDS-DIASUP)

The objective of the engineering activities of the diagnostic port plug integration on ITER (EFDA TWP 2005 contract 05/1344) was to provide analysis and expertise on, mainly,

the following areas: engineering design including CAD effort, structural static analysis with combined loads and stresses, thermal analysis (including hydraulic and thermo-hydraulic calculations), provide assessment of relevant QA requirements and to contribute to the development of common standards and guidelines for design engineering and integration.

The two areas of CIEMAT activities were:

- Study of an improved Blanket Shield Module (BSM) attachment arrangement for the representative equatorial port plug. This study was based on a simple design concept develop by the ITER blanket team [Ref ITER BT]. CIEMAT have developed a particular support system design taking into consideration the BSM and Equatorial Port Plug (EPP) front frame design geometry. This design concept is derived from the limiter of FDR 2001 and from other special blanket modules.
- Hydraulic design analysis including draining and drying considerations for the representative equatorial port plug. A "reference" cooling circuit has been built coupling the EPP cooling circuits included in the CATIA model supplied by ITER to the BSM circuits developed in [Ref. BSM]. In addition, the needed modifications to accommodate this reference hydraulic circuit to the new BSM attachment arrangement have been studied. The hydraulic parameters of both circuits (flow distribution, pressure drop, temperatures, etc.) have been analyzed. From this analysis there will be improvements to the cooling circuit, mainly for a better equilibrium of temperatures and flow distribution.

The report was mainly divided in two parts, one devoted to the new BSM attachment analysis and the second one related to the hydraulic analysis of the entire Port Plug.

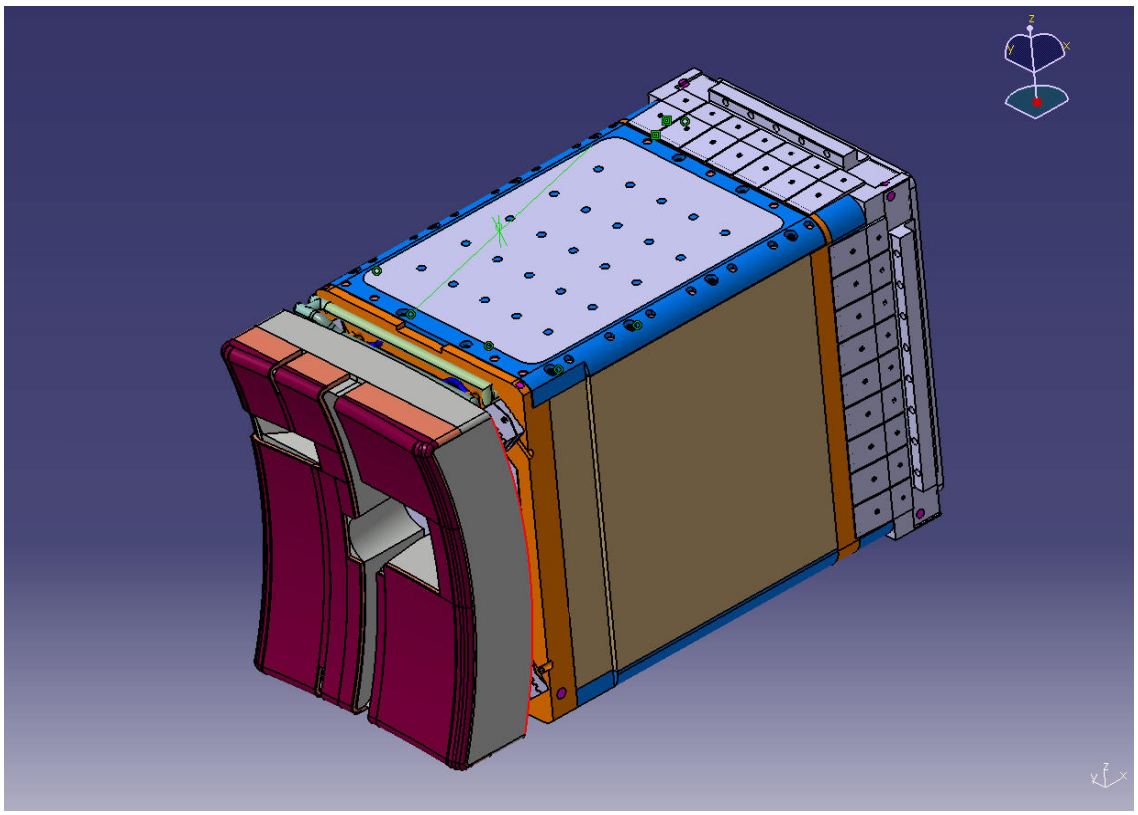

EPP CATIA model supplied by ITER drawing office

References

(Ref. ITER BT): "Design of the blanket shield module for the diagnostic plugs in the equatorial ports". F. Elio and X. Wang (ITER IT)

(Ref. BSM): "BSM Attachment Design Requirements", ITER_D_222SSC

VI.3. ITER IN-VESSEL SYSTEMS

VI.3.1. Ultrasonic Examination of the Divertor mock-ups.

EFDA Technology Work programme 2005 (EFDA Reference: TW5-TVD-FABCON)

The Divertor is one of the most challenging components of the ITER machine. It contains a high number of joints which failure could compromise its performance. There are tens

of thousands of joints in the divertor assembly, either carbon fibre composite (CFC) to copper alloy (CuCrZr) joints or tungsten (W) to CuCrZr joints.

The development of suitable non-destructive testing (NDT) methods of the heat sink to armour joints is an essential topic to be addressed. As NDT methods have been selected infrared thermography and ultrasonics.

The task is aimed at identifying a suitable NDT procedure for the final acceptance of the divertor PFC´s based on a data merging of the two techniques.

In order to test the performance and capabilities of the NDT methods a number of Divertor joint mock-ups containing artificial defects have been manufactured by European indutries using two different technologies.

The specific task assigned to Ciemat is the US examination of the 112 mock-ups manufactured with artificial defects, that will be inspected before and after being high heat flux tested. Ciemat has subcontracted these inspections to a specialized Spanish company (Tecnatom). The task started in June 2006 and will be finished at the end of this year.

During 2006 the examinations of two set of mock-ups have been completed. The results show the capabilities and appropriateness of the ultrasonic inspection method and suggest possible future tasks such as characterisation of the implanted defects, optimisation of the analysis criteria and assessment of the ultrasonic examination technique sizing capabilities.

Details can be obtained in the reports submitted to EFDA;

- Ultrasonic inspection of the W flat tiles mock-ups manufactured by Ansaldo
- Ultrasonic inspection of the CFC monoblocks mock-ups manufactured by Plansee

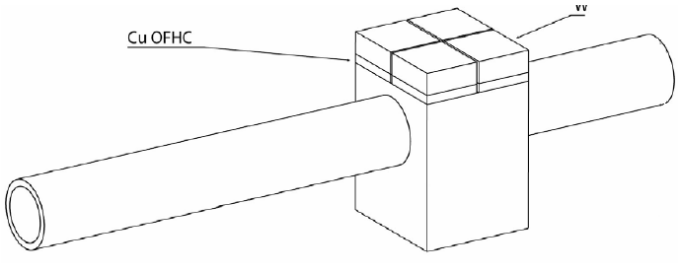

Figure 1: W flat tiles mock-ups

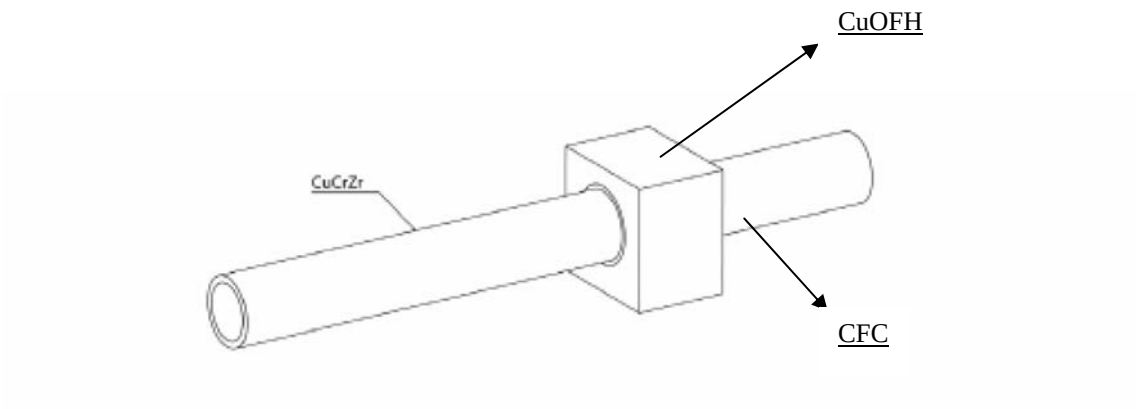

Figure 2: CFC monoblocks mock-ups

VI.4. ITER SITE STUDIES

EFDA Technology Work programme 2005 (EFDA Reference: EISS5-SL-53) EFDA Technology Work programme 2005 (EFDA Reference: EISS5-SL-53)

The EISS-5 project aims to complete a number of activities that shall allow the establishment of the ITER team and the start of ITER construction in Cadarache, utilising all the results of the previous stages of the EISS. As for the previous phases of EISS, the work is performed in cooperation between EFDA, ITER team, ITER-France team, the Euratom-CEA Association, other Euratom Associations and industry.

Following the French regulatory procedure, after "Dossier d'Options de Sûreté, DOS" a so-called "Rapport Préliminaire de Sûreté, RPrS" must be written in order to prepare the demand for construction of the installation, "Décret d'Autorisation de Création, DAC".

CIEMAT is responsible of three subtasks that belong to Task SL53: Studies in support of RPrS.

The tasks have been coordinated by a group of people composed by members of the Laboratorio Nacional de Fusión at CIEMAT, the spanish national waste management company ENRESA, and of the CIEMAT Safety Department. A specialized company with previous experience on ITER safety analysis has been subcontracted.

Several international meetings were held during 2006 for the development of the tasks:

- January 9th, Madrid. Kick off meeting for tasl SL53.2
- March 23rd, Garching. Kick-off meeting for tasl SL53.4
- June 8th , Cadarache. Progress meeting SL53.2
- October 25th-26th, Cadarache. Progress meeting EISS5 tasks

VI.4.1. Subtask SL53.2: Safety Operational limits and correlation of the experimental programme

Under this task, two different studies have been peformed:

- Safety importance components classification
- Operational limits and conditions

VI.4.1.1. Safety important components classification

The results of this work have been compiled in the final report of the task: EISS_01[1], which includes the list of safety-importance structures, systems and components (SIC) of the ITER design. The safety classification criteria used in the preparation of this list and the methodology followed are detailed in the report. The list includes also the seismic classification of each component and the applicable coes and standards. This information is prepared for subsequent inclusion in the RPrS (Rapport Préliminaire de Sureté).

A cross-checking with the reference sequences of the safety analysis has been performed with the aim of demonstrating that the list of the components classified as SIC is exhaustive. As a consequence of this study a few new SIC components were detected and included in the list. The methodology employed for this crosschecking and the results and explained in the last chapter of the task final report.

VI.4.1.2. Operational Limits and conditions

The purposes of this subtask have been

- To revise the complete list of the Operational Limits and Conditions using the current documentation and events sequence analysis
- To derive a minimum set of conditions which define the main safety parameters that should be retained with regard to the DAC (Décret d´Autorisation de Création), grouping various constraints as much as practical and reducing the current list

The results of the study are compiled in the final report of the task: EISS_02[2]. The starting point has been the document *"Definition of Authorized Operational Domain for ITER Licensing", March 2005 (Task order EFDA 93/851-JA).* This document has been reviewed taking into account the latest ITER design documentation (including accepted DCRs). The completeness of the resulting OLC list has been checked using the results of

[1] Safety Important Components. Final Report of EFDA task EISS5. SL53.2. CIEMAT. IN-IT-EISS-002. May, 2007
[2] Operational Limits and Conditions. Final Report of EFDA task EISS5. SL53.2. CIEMAT. IN-IT-EISS-003. May, 2007

the PIE-PITs analysis and selection of bounding event sequences as well as the rest of the sequences of the 25 reference events analyzed in chapter VII of the Generic Site Safety Report have also been reviewed. During this review, the pertinent OLCs have been extracted for each sequence, checking that they were included in the final list.

A summary table of all of the OLCs, classified according to French practice as limit de conduite (LC), limit de fonctionnement (LF), limit de sûreté (LS) and limit de dimensionnement (LD) has been elaborated.

Finally, a minimum set of conditions (top OLCs) which define the main safety parameters that should be retained with regard to the DAC (Décret d´Autorisation de Création) has been derived. To prepare this list, the OLCs of different systems have been grouped per parameter and using this analysis as a basis, the most significant parameters for safety have been selected.

VI.4.2. Subtask SL53.4a: Outline description of the maintenance programme

The objective of this task was to provide a breakdown of the scheduled hands-on maintenance operations that must be carried out on components/systems located in potentially radioactive/contaminated areas in the Tokamak Complex during normal plant operation.

The study refers not only to the maintenance of SIC components but also to the maintenance of any system or component located in an area with radiological monitors. The results are presented in the final report: EISS_03[3].

Each building of the Tokamak complex is dealt with in a specific chapter of this report. Each chapter lists the systems in each building, describing their general functions and safety functions. The information for each system is gathered in a table that shows its constituent components, their locations and the hands-on maintenance requirements. The details of each maintenance requirement such as task objective, system, frequency, initial conditions, assumptions, handling sequence, handling tools, outstanding issues, manufacturer requirements and references, are written in the form of task sheets, which can be common to different systems. For each step of the handling sequence an estimation of the time required has been performed. The expected times required for each elementary activity have been taken from a previous study performed by ENEA. All task sheets have been gathered in the document as an appendix.

[3] Outline Description of the ITER maintenance Program. Final Report of EFDA task EISS5. SL53.4. CIEMAT. IN-IT-EISS-001. May, 2007

Operator maintenance instructions will have to be provided in a later phase of the project by the component manufacturers. This document only provides guidelines to calculate the operator doses. The maintenance procedures have been prepared based on the ITER available information (DDDs, PID, Technical Review Meetings, Design Change Request…etc) and the authors´ previous experience in Nuclear Power Plants. Components still under design have been included in the document but no maintenance requirements have been specified for them. The document structure is such that it can be easily updated in the future as the design evolves.

VI.4.3. Subtask SL53.8b: Hotcell and Radwaste. Functions during ITER dismantling and phases of Hotcell and Radwaste dismantling

This subtask shall present the main functions of the Hot Cell and Radwaste Buildings to be performed during the dismantling phase and how the dismantling of the Hot Cell and Radwaste buildings themselves can be integrated in the dismantling phase.

As the hot cell design which is an input for this task, had not been fully approved during 2006, this work has been postponed. It will be performed during 2007.

VI.5. IFMIF

VI.5.1. Cost Evaluation and Time Schedule of the Superconducting DTL alternative for IFMIF (deliverable 5 of task TW5-TTMI-001)

This task was started at the end of 2005 and completed in 2006. Its objectives were to provide a detailed and realistic estimation of the cost of the design, construction and operation of a superconducting cavity based drift tube linac for IFMIF as well as of the differences in the costs of design, construction and operation of the whole sc-DTL based accelerator with respect to the reference option and to give a preliminary time schedule for the development and construction of such installation. As a detailed design including integration of the superconducting (sc) DTL was not available, before making the cost estimation it has been necessary to make a pre-design proposal for the elements whose

design is lacking. This predesign and the cost estimation based on it is described in the final report of the EFDA task: IFMIF_1[4] .

A second issue of this report: IFMIF_1b[5] was made in order to include modifications motivated by the comments of the ad-hoc group for the assessment of the superconducting alternative of the IFMIF accelerator (AHG) during its first meeting in Garching on 23-24 october 2006 and the results of the on-going design of the superconducting IFMIF option. This report includen an annex which studies the cost implications of a design modification proposed by the group of Frankfurt University consisting of splitting the first superconducting cavity.

The main conclusions of the study are the following:

- The operational costs are 7076 k€/year lower in the sc-DTL case than in the reference one. This saving represents a 9% of the total operational costs and is mostly due to the reduced electricity consumption.
- The net capital cost saving of the whole installation due to the use of a superconducting DTL instead of the reference one is around 60 M€-2003 (for the design with 7 sc-cavities), which represents around 20% of the total cost of the accelerator facility (311.6 M€). For the design with eight cavities the capital savings are around 45 M€.

With regard to the time schedule of the sc-DTL option, the critical path is not in the superconducting components, but in the sub-systems that are shared with the reference solution, i.e., the transmitters. Therefore no major impact on the schedule is expected in the case that the superconducting option is chosen after the EVEDA phase.

VI.5.2. Assessment of the state of development and cost of alternative RF power sources for the IFMIF accelerator. Solid State Technology (deliverable 1b of task TW6-TTMI-001)

[4] Cost evaluation and time schedule of the superconducting DTL alternative for IFMIF. IN-IF-ACEL-001, Issue 1. June, 2006.
[5] Cost evaluation and time schedule of the superconducting DTL alternative for IFMIF. IN-IF-ACEL-001, Issue 2. January, 2007.

This task consists on an assessment of the possibility of using RF power sources based on solid state technologies for feeding the IFMIF accelerator as an alternative to the present reference solution based on the use of a 50 kW vacuum tube and the 1 MW diacrode. The performed study is contained in the final report of the EFDA task: IFMIF_2[6]

To begin with, the state of the art of the RF power sources used in the different facilities has been reviewed with special emphasis in those using solid state technology. As a second step a search of commercial amplifiers (up to several tens of kW) has been made using available literature and consulting different companies of the radio/TV world. As the IFMIF application will require a specifically designed amplifier, a study of the characteristics of the main components (transistors, combiners, etc) available in the market has been performed.

With all this information, a feasibility study of the production of both a 50 kW and a 1 MW amplifier working at 175 MHz has been carried out. A pre-design of the amplifier based in elements presently available at the market has been undertaken including considerations about the type of transmission line, cooling options, combiners, power supply. A cost estimation for the proposed design is presented.

The main conclusions of the study are the following:

- There are commercially available solid state devices with powers up to tens of kW (for low and medium power TV transmitters). However it would be advisable to develop a specific optimized design for IFMIF. Efficiencies larger than 60% can be obtained.
- The feasibility of giving 1 MW at 175 MHz using solid state technology with an efficiency around 50% has also been shown. It must be noted that solid state amplifiers with powers of that order are currently feeding RF cavities in some facilities. Higher performance could be achieved in the future, after the development of basic modules with high efficiency. The efficiency of the combiners required in such designs is also essential, but nowadays there are commercial high power combiners with very low insertion losses.

[6] Assessment of the state of development and cost of alternative RF power sources for the IFMIF accelerator. SOLID STATE TECHNOLOGY. IN-IF-ACEL-002, Issue 1. June, 2007.

- The following considerations can be made when comparing vacuum tubes with solid state solutions for IFMIF RF amplifiers:

  - The availability of solid state devices is much higher than that of vacuum tube devices. Furthermore, as hundreds of solid state basic modules work in parallel to provide high output powers, the failure in some of them only involves a negligible reduction in power.

  - With regard to cost, manufacturing cost could be higher for solid state than for vacuum tube solutions. However, due to the longer lifetime of solid state components and the simpler power sources required, the maintenance costs are expected to be lower.

  - The inherent modularity of solid state amplifiers allows the fabrication of amplifiers with the required power for each cavity of the accelerator, decreasing the total investment cost.

Given the previous considerations and the fact that availability is an essential parameter for IFMIF, a thorough reliability-availability-maintainability analysis should be performed to assess the convenience of using solid state amplifiers. An intermediate solution with solid state technology up to 50 kW and a diacrode for the final stage could be also considered although in this case system availability would still depend on diacrode failures.

VI.5.3. EFDA TASK TW5-TTMI-002 Deliverable 5: IFMIF: Parametric study of fluiddynamics characteristics of Li-jet under deuteron load.

To remove the beam power deposited on the IFMIF liquid lithium target (up to 10 MW), the lithium jet must have a speed around 20 m/s, which may give rise to flow instabilities. However, a stable liquid free surface is a very critical requirement of the target system, otherwise the neutron field produced by the deuteron beams stripping

reactions in the target could be altered. Therefore the objective of the task is the study of the fluiddynamics characteristics (velocity profile, temperature and heat distribution, heat transfer coefficient to the backplate,..) of the lithium jet under the deuteron heat load, based on applications of the CFX 5.7 code, a commercial Navier-Stokes equations solver with specific modelling of turbulence, like the classical k-e among others.

A fine 2D dimensional mesh of the lithium target for CFX calculation has been developed along the longitudinal flow direction, with refined areas in the free surface and close to the wall regions. In order to support the results of the calculation, a model assessment has been done by taking relevant information from open literature concerning water experiments. As results of the calculations (Ref LiTarget_1) the behaviour of the free surface and the lithium jet thickness has been assessed considering the liquid fraction volume as a first rough indicator of the surface disturbance. The pressures and temperatures maps have been obtained and occurrence of cavitation has been assessed.

This task began in 2005 and has been completed in 2006. It has been developed in cooperation with Universidad Politécnica de Madrid.

VI.6. SYSTEMS AND PLANTS

VI.6.1. EFDA TASK TW5-TRP-008, Deliverable 1: Non-Electricity production applications for Fusion Power: state of the art of high temperature innovative processes for Hydrogen production.

The fusion reactor studies in Europe have focused on electricity production. There are, however, possible non electricity production applications, such as hydrogen production, as hydrogen is regarded as a major secondary energy medium that may have large market share (fuel for heat, transportation…). The objective of the task is therefore to review the high temperature innovative processes for hydrogen production using the process heat of fusion reactors.

The report submitted to EFDA provides an overview on the wide portfolio of thermochemical hydrogen production technologies, in particular those more acceptable for potential integration with future fusion reactors (thermochemical cycles and High

Temperature Electrolysis). The main conclusion is that the coupling of the even most feasible thermochemical cycles to fusion reactors require temperatures between 750ºC and 1000 ºC. This range of temperatures lead us to the most advanced designs of fusion blankets, with outlet coolants temperatures higher than 850ºC most of them, which are attractive but still require large R&D. Therefore, the development of a viable blanket can be seen as the central requirement for the successful application of the process heat from the fusion energy to the hydrogen production. In addition to this, it must be stressed the technical difficulty of the fusion reactor coupling with the chemical process, due to the complex chemistry, materials compatibility problems at the extremely high temperatures, inventories of hazardous materials, etc..

This task began in 2005 and has been completed in 2006. It has been developed in cooperation with CIEMAT Renewable Energies Department.

VI.6.2. Power conversion cycles for DEMO. EFDA Reference: TW5-TRP-006

During 2005, the Laboratory has gained several contracts for different tasks launched in the framework of the EFDA Technology Work programme 2005. Specifically, in the area of DEMO Conceptual study a series of scoping studies were launched with the aim of providing technical information focused on the selection of DEMO parameters.

The purpose of this particular task was the investigation of advanced power conversion cycles in order to get an improvement of the thermodynamic efficiency.

This task concluded in April 2006, was performed by a specialized Spanish company subcontracted by Ciemat.

The study was carried out based on the parameters of the HCLL (Helium Cooled Lithium Lead) model AB defined within a previous phase of - Power Plant Conceptual Studies - (PPCS). In the latter, model AB was coupled to a standard Rankine cycle showing a net efficiency around 28%. Two heat sources are present in the reactor: the blanket that provides 82% of the total thermal power with a moderate coolant temperature (300-500 ºC) and the divertor, with a more respectable coolant temperature (540-717 ºC) delivers 18% of the thermal power is considered a high-grade heat source.

Within this task different configurations of Supercritical (SC) Rankine and SC CO_2 cycles were coupled to model AB looking for improved values of the thermodynamic efficiency.

For the SC Rankine cycle different configurations were analysed: superheat (Figure 1), reheat and "improved cycle". The improved cycle aimed at optimizing the thermal exchange between primary and secondary circuits attempting a new Primary Heat Transfer System configuration. This case showed the best results with an increase in the net efficiency of more than 3 percentage points respect to the standard Rankine

Among the configurations studied for the SC CO_2 cycle, the recompression cycle yield the better option. This cycle improves the efficiency by reducing the heat rejection from the cycle introducing an auxiliary compressor, bypassing the main cooler, the main compressor and the low temperature recuperator. A reduced compression work is obtained taking advantage of the CO_2 inlet conditions close to the critical point at the main compressor, as well as the improvement of the performance of the recuperators by feeding to the auxiliary compressor with a certain flow fraction. Figure 2 shows the flow diagram of the recompression cycle considered in the study, with the secondary side of the heat exchanges of the blanket and divertor connected in series.

SC CO_2 , dual recompression cycles for the blanket and divertor yield net efficiencies comparable to the "improved" SC Rankine resulting an increase of 2.92 percentage points respect to the standard Rankine.

The results of the different SC cycles analysed are summarized in the next Table 1.

The Flow diagrams of the superheat SC Rankine and the SC CO_2 recompression cycle are shown in Figures 1 and 2 respectively.

Additional information is available at the EFDA report for this task.

	SC CO2 Brayton recompression	SC Rankine "improved"	Separate cycles: Rankine/ SC CO_2	Separate cycles: SC CO_2 / SC CO_2	Rankine standard
Fusion Power (MW)	4290	4290	4290	4290	4290
Thermal Power (MW)	5144	5144	5144	5144	5144
Blanket	4219	4219	4219	4219	4219
Divertor	926	926	926	926	926
Divertor Gross Power (MW)	---	---	531	527	---
Blanket Gross Power (MW)	---	---	1747	1928	---
Helium compressors (MW)	370	370	370	370	370
Auxiliary heating (MW)	477	477	477	477	477
Water pumps (MW)	---	88.32	40	---	47
Total Gross Power (MW)	2185	2566	2278	2455	2353
Total Net Power (MW)	1338	1629	1390	1608	1458
Cycle Gross Efficiency (%)	**42.49**	**49.88**	**44.29**	**47.73**	**45.74**
Cycle Net Efficiency (%)	**26.01**	**31.68**	**27.04**	**31.26**	**28.34**

Cycle Gross Efficiency = 'gross power' vs. 'thermal power'

Cycle Related Net Efficiency = 'net electrical power' vs. 'thermal pow

Table 1. Summary of the SC cycles analysed

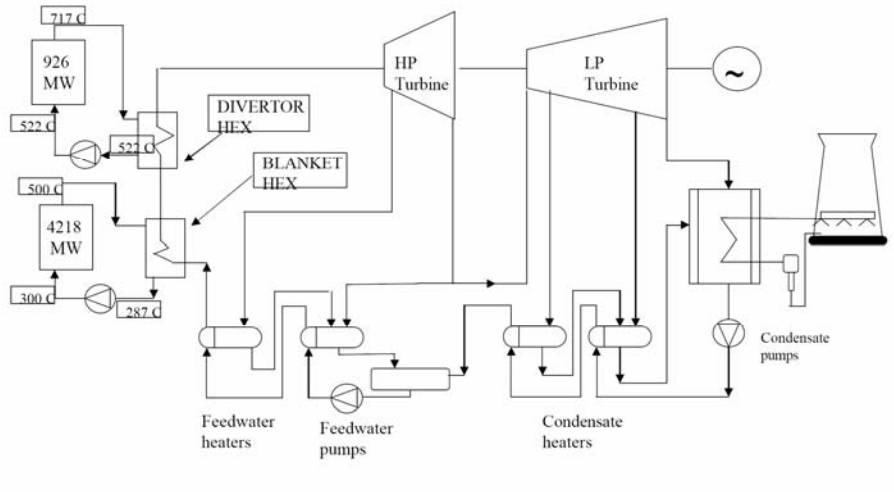

Figure 1 : Flow diagram of the superheat SC Rankine cycle

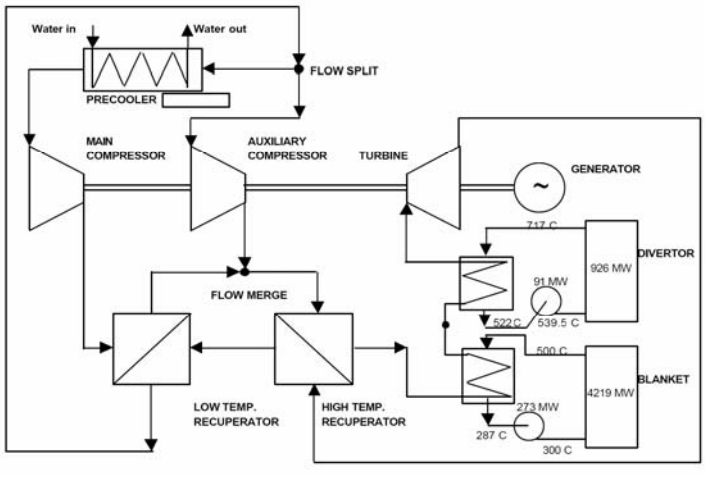

Figure 2 : Flow diagram of the recompression cycle

VI.6.3. Energy Storage System for a Pulsed DEMO

EFDA Technology Work programme 2005 (EFDA Reference: TW5-TRP-007)

DEMO studies contemplate a pulse mode of operation in addition to the steady state reference operation. This task considers DEMO as a pulsed device and studies how to provide a continuous electrical power distribution to the grid. In this situation, an energy storage system is needed in order to obtain this aim.

This task began in October 2005 and finished at the end of April, 2006. The task has being undertaken by Ciemat with a partial support from Elytt Energy Company.

The state of the art of energy storage systems have been reviewed in the first part of the task. In the second part, recommendations on possible systems for a fusion power plant operating in a non-steady state mode have been provided. For each of the recommended system(s) the main features have been described and a rough cost estimate has been obtained. The main DEMO characteristics to be considered are: 1 GW net electrical power output, pulse length between 4 and 8 hours with a dwell time between 5 and 20 minutes

Thermal energy storage, fuel cells and other hydrogen storage, compressed air storage, water pumping, batteries, flywheels and ultracapacitors are the most promising solutions to energy storage. Each one is detailed described in the task report showing its basis, features, advantages and disadvantages for this application.

The conclusion of the review is that, based on existing technology, thermal energy storage using molten salts and a system based on hydrogen storage are the most promising candidates to meet the requirements of a pulsed DEMO. These systems are investigated in more detail together with an economic assessment of each. Additional details in the EFDA task report.

VI.7. SOCIOECONOMIC STUDIES

VI.7.1. Improving the global multi-regional EFDA-TIMES model: revision and update of the data included in the power generation sector of the model

The EFDA-TIMES model is a global multi-regional energy model mainly characterised by a rich-technology description which includes future fusion power plants. The model gives an optimal solution for the global energy system within a time horizon of 2100.

Global multi-regional EFDA-TIMES model has been improved by means of database revision and update. A deep literature review has been carried out as well as an examination of major international projects and databases of techno-economic data for present and future energy technologies. As a result, a series of proposed data to substitute the existing ones was given to be incorporated to the model. (1)

VI.7.2. Improving the global multi-regional EFDA-TIMES model: revision and update of the data included in the residential and commercial sectors of the model

Residential and commercial sectors of the EFDA-TIMES model have been reviewed. Revision was related to technical, economic and environmental data of existing and new technologies, the structure of the model itself, user constraints, demand projections and elasticities and other specific issues. Also some changes related to other sectors were reported and integrated in the CIEMAT database version. Finally, some suggestions of decisions were proposed to be considered by the Steering Committee. (2)

VI.7.3. EFDA-TIMES Model: Resource Potential Update

The objective of the task are the review, validation, improvement and documentation of the fossil resource potentials (different forms of oil, gas and coal) for the different regions of the EFDA-TIMES based on recent literature and databases. This is an on-going task.

VI.7.4. Social Perception of Large R&D Programmes (TW5-TRE-FESS/C)

According with the Technical Specifications, two research stages were developed by Ciemat and Cardiff University. First, a "systematic review" was carried out on the existing knowledge on the social perception of large R&D programmes which is specific to fusion work (including previous SERF, and other relevant EFDA research); the available evidence on the social perception of comparative or "parallel" cases; and the wider social sciences research literature. Our interrogation of the evidence on the social perception of fusion and comparative technologies in the light of generic social science knowledge resulted in the identification of a number of knowledge 'gaps' or key research questions. Second, these knowledge gaps were addressed by means of the design of an empirical programme of work suitable to carry out a detailed investigation of the nature of social perception of fusion energy. This empirical programme of work was proposed to, and accepted by the EFDA Technology Programme 2006.

The final report of this task has been published as a Ciemat Document (ref. TW5-TRE-FESS/C_1), and the main findings of this research have been submitted to Fusion Engineering and Design (ref. TW5-TRE-FESS/C_1), and will be presented in the forthcoming Annual Meeting of the Society for Risk Analysis (ref. TW5-TRE-FESS/C_3).

VI.7.5. Investigating lay understanding and reasonning about fusion technology by means of a group-based methodology suitable to take lay participants through a learning process about fusion (TW6-TRE-FESS-B1)

There is a need to explore how lay perceptions of fusion change as citizens learn more about the technology and associated issues. This would contribute important insights into the dynamics of such learning and engagement processes. The overall objective of the work proposed here is to find practical ways of improving communication about fusion, and enhancing the quality of lay engagement with this information. The contract for this new task was singed by the Commission on December the 22nd, and will last 18 months since its beginning. The research will be carried out by Ciemat and Cardiff University.

(1) Task Deliverable: Sub Task TW4-TRE-FESO/C "Improving the global multi-regional EFDA-TIMES model: revision and update of the data included in the power generation sector of the model" Cabal H., Lechón Y., Sáez R.

(2) Task Deliverable: Sub Task TW5-TRE_FESO/C "Improving the global multi-regional EFDA-TIMES model: revision and update of the data included in the residential and commercial sectors of the model". Labriet M. Cabal H., Lechón Y.

VII. INERTIAL FUSION ENERGY KEEP-IN-TOUCH ACTIVITIES

INSTITUTE OF NUCLEAR FUSION (DENIM)

POLYTECHNICAL UNIVERSITY OF MADRID / SPAIN

with the collaboration of the following University Groups:

- University of Las Palmas de Gran Canaria.
- Open University (UNED) (two groups).
- Polytechnical University of Barcelona.

(according to the proposal on December 21, 2000 to encourage scientific collaboration among professor of the Spanish Universities out of DENIM).

VII.1. TARGET DESIGN AND RADIATION FLUID DYNAMICS

We have improved a design of a X ray laser amplifier based in High Armonics amplification (PhysRevA_74_045802.pdf). Changes in laser profile and timing could increase the gain if a hipergaussian spatial profile is used.

We have proposed (Velarde-PoP-Septiembre-2006.pdf, jp4133209.pdf) an experiment to measure the structure of a plasmas produced by the collision of a 2 shock waves similar to these ones found in forward shock waves in supernova explosions. By adjusting the density of a foam and material composition, we can get spatial structures that scales to that in supernova remnants. High temperature points have been identified that can be observed in a experiment [INRT_01], [INRT_02], [INRT_03].

International Collaboration:

We have european collaborations in IFE related topics with E. Dalimier (UPMC, France) and M. Shmatov (Ioffe Physical Technical Institute, Russia).

VII.2. ATOMIC PHYSICS

VII.2.1. Simulation and Code Development.

Main work has been focused on the determination of radiative properties of plasmas under NLTE conditions.

ATOM 3 code has been improved and now it has more possibilities than before, being extended to low temperature plasmas.

In this sense, the results of 4th Workshop on NLTE kinetics calculations held in Las Palmas in December 2005, has been used to compare results of ATOM3 with other codes. Also experimental results have been compared, using those obtained at École Politechnique under the Eu program for Large Facilities.

Finally, results were presented as an invited talk at the International Conference on Radiative Properties of Hot Dense Matter, that took place in September 2006 in Albufeira (Portugal).

New experiments of hot dense plasmas have been carried out in collaboration with École Polytechnique and University Paris VI, in several sessions during 2006.

International Collaboration:

With Laboratoire de l´Utilisation des Lasers Intense (LULI), Ecole Polytechnique (France), University of Reno, Nevada (USA) and Lawrence Livermore National Laboratory (USA).

VII.3. SAFETY AND ENVIRONMENT

Our main objective during this year has been to apply and demonstrate the capabilities of the computational system ACAB in predicting the isotopic inventory and performing safety and environmental (S&E) analysis for fusion facilities. The capability to estimate the impact of activation cross section data uncertainties on the prediction of inventory and inventory-related radiological quantities used in S&E analysis is emphasized, as a

singular feature of ACAB. We demonstrate the adequacy of this methodology to perform S&E analysis in inertial fusion experimental facilities (NIF) and in different IFE (dry-wall and thick-liquid) and MFE concepts. [INRT_04]

VII.3.1. Impact of activation cross section uncertainties on the waste management performance of irradiated steels under different neutron environments of IFE Thick-Liquid Concepts.

The subject of low-activation material selection for both magnetic (MFE) and inertial fusion energy (IFE) applications has been covered extensively. At this respect, the fusion community has made a lot of work on activation calculations to select low activation materials, and the acceptable low activation concentration levels for intended and impurity elements have been set. However, very few works have addressed uncertainty analysis to draw conclusions on the reliability of the calculations of those acceptable levels under the potential impact of activation cross section uncertainties. The uncertainty analysis we have performed allows us to draw some relevant conclusions on the reliability of the present calculations of low-activation acceptable levels for the different elements, leading to some important practical implications. [INRT_05]

VII.3.2. Safety and environmental considerations for laser IFE chambers.

The US High Average Power Laser (HAPL) program is carrying out a coordinated effort to develop inertial fusion energy (IFE) based on lasers, direct-drive targets and a dry wall chamber. A primary focus of the study is the protection of the first wall (FW) from target emanations. The dry wall must accommodate the ion and photon threat spectra from the fusion micro-explosion over its required lifetime. The current HAPL strategy focuses on an armor/FW configuration based on tungsten and ferritic steel F82H as preferred armor and structural materials, respectively. [INRT_06]

VII.3.3. III.3. Comparison of Monte Carlo neutron transport codes and Nuclear Data Libraries for neutron calculations in different IFE concepts

A comparison of Monte Carlo neutron transport codes and evaluated nuclear data libraries in different Inertial Fusion Energy (IFE) neutron environments has been performed: HYLIFE-II (thick-liquid) and HAPL (dry-wall). The results of this analysis are very helpful in assessing if current neutron transport codes and evaluated nuclear data libraries are allowable for acceptable waste management options. In addition, a comprehensive uncertainty analysis for CL in SLB due to the overall effect of the complete set of cross-section uncertainties has been performed. [INRT 07]

International Collaboration:

Some of the efforts were done in collaboration first of all with Lawrence Livermore National Laboratory (LLNL), but also with University of California-Los Angeles, University of Wisconsin in the USA, and collaborations with CIEMAT (Spain).

VII.4. IFE REACTOR CHAMBERS

VII.4.1. Materials Damage: Multiscale Modeling

Amorphous Silica is a key component in Final Focusing of Lasers in Inertial Fusion. The energy spectra and fluxes of neutrons have been updated for different inertial fusion conceptual systems (HYLIFE-II, SOMBRERO) and magnetic fusion facilities such as ITER and IFMIF, and HFR-Petten and BOR-60. Primary Knock-on Atoms (PKA) energy spectra have been obtained using SPECTER code for Silica, and a systematic analysis of primary damage was done with TRIM and MARLOWE codes for high-energy recoils, in order to get distribution of cascades and subcascades ([INRT 08], accepted for publication in Journal Nuclear Materials in 2006).

Molecular dynamics simulations are performed to obtain the damage produced during irradiation of fused silica for energies between the threshold displacement energy and 3.5 keV. The interatomic potential developed by Feuston and Garofalini specifically for amorphous SiO_2 is used in these calculations. The effect of Hydrogen in damage accumulation is also studied for an initial H concentration of 1%. Calculations show the formation of predominately four types of defects: Si3, Si5, O1 and O3 where the numbers denote their coordination . In the presence of H new defects appear while others are reduced. In particular, as expected, O-H complexes are formed, therefore reducing the number of oxygen atoms with coordination one. [INRT 09], [INRT 10]

We have explored hcp α-Zirconium (very similar to hcp α-Titanium (c/a 1.5873 for Ti and 1.593 for Zr)). It has been observed experimentally that damage produced in Zr is qualitatively similar to that in Ti. We have been researching the defect energetics and cascade damage, by using the input data obtained from molecular dynamics (MD) simulations. A systematic generation of results has been produced on irradiation of hcp α-Zr under different conditions with a kinetic Monte Carlo model. Using 25 keV cascades we have studied the evolution of the microstructure during irradiation under environment conditions of 600K, dose rate 10^{-6} dpa/s, final dose of 0.5 dpa, and isotropic motion for vacancies. How the accumulation of damage is affected considering interstitial movement from one dimension to three-dimension has also been studied. A new code has been developed in collaboration with CRIEPI (Japan) to consider starin effects [INRT 11], [INRT 12].

Concerning ferritic steeels, new diffusion parameters from *ab-initio* calculations were implemented in kinetic MonteCarlo BIGMAC code. 150 keV Fe^{+} ion irradiation in UHP-Fe were developed. Simulations were performed using the new activation energies and 3D motion for the diffusion of interstitial defects. New vacancy's migration energies for 3-4 vacancy clusters and last *ab-initio* diffusion parameters for impurities were also implemented. TEM observations at CIEMAT were developed to quantify the defect concentration and the defect type. Large differences between old and new parameters and between simulations and experiments have been observed (from 350 nm in experiments to 8 nm in simulations). New mechanisms have been proposed to explain those differences, such as new reaction probabilities and surface effects. Work on Dislocation Dynamics and Parallelization of Kinetic MonteCArlo for defscts diffusion has been already done under EFDA tasks.

International Collaborations:

Lawrence Livermore National Laboratory (USA); University of Berkeley (USA); SCK-CEN Mol (Belgium); CEA Saclay (France); University Middlesborough (U.K.); University of Liverpool (U.K.); PSI (Switzerland); FZK Karlsruhe (Germany); CIEMAT (Spain); Universidad Alicante (Spain).

VII.4.2. TRITIUM: Environmental impact in IFE reactors

In this state of studies about tritium needs an important experimental contribution that corroborates the results obtained theoretically by means of the simulation computacional. The concentrations vary always depending on the process that takes place.

The tritium cycle, technologies of process and control of the tritium in the plant will constitute a fraction of the environmental impact of the first generation of DT fusion reactors. At the present time, the efforts of conceptual development of the tritium cycle are centered in the Internal Regenerator Cycle, which is a part of a power reactor.

The impact evaluations will be performed with the computational tools for dosimetric evaluations of tritiated effluents in operational conditions and in incident and hipotetic accident scenarios.

The most common different chemical forms of tritium present in the plant: HT, HTO have different pathway in the environment after release to the atmosphere. To simulate these behavior and being based on the mentioned experiments, the diffusion processes were simulated, and the deposition processes were developed in the soil and vegetables, penetration in the underground and re-emission to atmosphere needs a real metereological and topographics scenarios. Early (without growing vegetables) and chronic doses have been evaluated in 3 forms of tritium: elementary tritium, water vapour tritium and conversion to organically bound tritium.

The importance of dose assessment by ingestion is more than 2 orders of magnitude if the atmospheric emission is from HTO. It is necessary to remarks that the doses for the elementary tritium are very diminished in comparison with results from the incorporate concentration to the vegetables and animals. This is due to the Dose Conversion Factors which are four orders of magnitude smaller than those recommended in the regulatory guides for the HTO. This conservative overestimates the doses for the HTO, but it underestimates HT, [INRT 13].

As conclusion was carried out to the dosimetric analysis of the supposed contamination for all the ways: inhalation, re-emission and ingestion, in special the organic form of tritium (OBT). As it was necessary to wait the doses for ingestion they are important when the tritium incorporates to the vegetables in development but not in the times outside of this time of vegetable growth.

International Collaborations:

Lawrence Livermore National Laboratory (USA); FZK Karlsruhe (Germany); CIEMAT (Spain).

VII.5. ALTERNATIVE CONCEPTS FOR IFE - INTENSE NEUTRON SOURCES

Intense neutron sources based on spallation targets are analysed following a systematic approach, in order to point out the main problems regarding the thermal-hydraulic limits. Those limits pose upper bounds to the neutron yield of the target. In turn, the limits depend on the features of the impinging particle beam and the material composition and geometry of the target. Although the potential design window for spallation targets is rather wide, the analysis presented in this paper identifies specific topics that must properly be covered in the detailed project of a spallation source, in order to avoid unacceptable temperatures and mechanical stresses in the most critical parts of the source. [INRT_14]

International Collaborations have been resumed with the (Prof. Emmanuel Sarris), Laboratory of Electromagnetism and Space Research of the Democritus University of Thrace (Greece).

VIII. PUBLICATIONS

VIII.1. JOURNALS, BOOKS AND TECHNICAL REPORTS

VIII.1.1. Journals

Two-Dimensional Turbulence Analysis Using High-Speed Visible Imaging in TJ-II Edge Plasmas
J. A. Alonso, S. J. Zweben, J. L. de Pablos, E. de la Cal, C. Hidalgo, T. Klinger, B. Ph. Van Milligen, M. A. Pedrosa, C. Silva, H. Thomsen
Fusion Science and Technology **50(2)** (August 2006) 301-306

H-mode access in the low density regime on JET.
Y. Andrew, R. Sartori, E. Righi, E. de la Luna, S. Hacquin, D.F. Howell, N.C. Hawkes, L.D. Horton, A. Huber, A. Korotkov, M.G. O'Mullane and JET-EFDA contributors.
Plasma Phys. Control. Fusion **48** (2006) 479 - 488

PXI-based architecture for real-time data acquisition and distributed dynamical data processing.
E. Barrera, M. Ruiz, S. López, D. Machón, J. Vega.
IEEE Transactions on Nuclear Science. **53**, 3 (2006) 923-926.

Real-time data acquisition and parallel data processing solution for TJ-II bolometer array diagnostic.
E. Barrera, M. Ruiz, S. López, D. Machón, J. Vega, M. Ochando.
Fusion Engineering and Design. **81** (2006) 1863-1867.

Doppler reflectometry studies using a two-dimensional full-wave code
E. Blanco, T. Estrada and J. Sánchez
Plasma Phys. Control. Fusion **48** (2006) 699-714

A charge-exchange spectroscopic diagnostic for the TJ-II stellarator
J. M. Carmona, K. J. McCarthy, R. Balbín, S. Petrov,
Accepted in Rev. Sci. Instrum.

The NBI control systems for the TJ-II
R. Carrasco, M. Liniers, L. Pacios, A. de la Peña, F. Lapayese, G. Wolfers, J. Alonso, G. Marcon, C. Fuentes
Fusion Engineering and Design **81** (2006) 1813-1816

Thermographic calorimetry of the NBI Heating Beam at TJ-II
C. Fuentes, M. Liniers, J. Guasp, J. Doncel, J. Botija, G. Wolfers, J. Alonso , M. Acedo, E. Sánchez, G. Marcon, M. Weber, R. Carrasco, X. Sarasola, B. Zurro, J.Tera
Rev. Sci. Instrum. **77** (2006) 10E519

On the use of critical gradient models in fusion plasma transport studies,

B.A. Carreras, V.E. Lynch, B.Ph. van Milligen, and R. Sánchez,
Phys. Plasmas **13** (2006) 062301

An authentication and authorization infrastructure: the PAPI system.
R. Castro, D. R. López, J. Vega.
Fusion Engineering and Design **81** (2006) 2057-2061.

Search and retrieval of plasma waveforms: structural pattern recognition approach
S. Dormido-Canto, G. Farias, J. Vega, R. Dormido, J. Sánchez, M. Santos, J. A. Martín, G. Pajares.
Aceptado en Rev. Sci. Ins.

Automated clustering procedure for TJ-II experimental signals.
N. Duro, J. Vega, R. Dormido, G. Farias, S. Dormido-Canto, J. Sánchez, M. Santos, G. Pajares.
Fusion Engineering and Design **81** (2006) 1987-1991.

Electron Internal Transport Barriers and Magnetic Topology in the Stellarator TJ-II
T. Estrada, D. López-Bruna, A. Alonso, E. Ascasíbar, A. Baciero, A. Cappa, F. Castejón, A. Fernández, J. Herranz, C. Hidalgo, J.L. De Pablos, I. Pastor, E. Sánchez, J. Sánchez, L. Krupnik, A.A. Chmyga, N. Dreval, S.M. Khrebtov, A.D. Komarov, A.S. Kozachok, V. Tereshin, A.V. Melnikov and L. Eliseev
Fusion Science and Technology **50(2)** (August 2006) 127-135

Velocity shear layer measurements by reflectometry in TJ-II
T. Estrada, E. Blanco, L. Cupido, M.E. Manso and J. Sánchez
Nuclear Fusion **46** (September 2006) S792-S798

Searching patterns in TJ-II temporal evolution signals with Support Vector Machines.
G. Farias, S. Dormido-Canto, J. Vega, J. Sánchez, N. Duro, R. Dormido, M. Ochando, G. Pajares, M. Santos.
Fusion Engineering and Design **81** (2006) 1993-1997.

Efficiency of tritium removal techniques in castellated structures
J.A. Ferreira, F.L. Tabarés and D. Tafalla
Submitted to J. Nuc. Materials

The quest for a divertor effect in TJ-II
I. García-Cortés, F.L. Tabarés et al.
Fusion Science and Technology **50(2)** (August 2006) 307-312

Role of Turbulence on Edge Momentum Redistribution in the TJ-II Stellarator
B. Gonçalves, C. Hidalgo, M. A. Pedrosa, R. O. Orozco, E. Sánchez, and C. Silva
Phys. Rev. Lett. **96**, 145001 (2006)

Radiation resistant bolometers using platinum on alumina and AlN
M. Gonzalez and E.R. Hodgson
Fusion Engineering and Design, **74** (2005) 875-878.

Microstructural and Optical Features of a Eu-Monazite.
T. Hernández and P. Martín

J. Eur. Cer. Soc. **27(1)** (2007) 109-114

Testing of the collisional-radiative model by laser-induced perturbation of a supersonic He beam in TJ-II plasmas
A.Hidalgo, F.L. Tabarés and D.Tafalla
Plasma Phys. and Control. Fusion **48** (2006) 527-536

Physics of sheared flow development in the boundary of fusion plasmas
C. Hidalgo, M.A. Pedrosa, E. Sánchez, B. Gonçalves, J.A. Alonso, E. Calderón, A.A. Chmyga, N.B. Dreval, L. Eliseev, T. Estrada, L. Krupnik, A.V.Melnikov, R.O. Orozco, J.L. de Pablos, C. Silva
Plasma Phys. Control. Fusion **48**, S169 (2006)

A note on asymmetry effects in x-mode reflectometry
E. Holzhauer and E. Blanco
Nuclear Fusion **46** (September 2006) S824-S828

Localized electromagnetic modes in MHD stable regime of the TJ-II Heliac
J. A. Jiménez, E. De la Luna, I. García-Cortés and S. V. Shchepetov
Plasma Phys. Control. Fusion **48** (2006) 515-526

Breeding Blanket Design and Systems Integration for a Helium-Cooled Lithium-Lead Fusion Power Plant.
A. Li Puma, J.L. Berton, B. Brañas, L. Buhler, J. Doncel, U. Fischer, W. Farabolini, L. Giancarli, D. Maissonnier, P. Pereslavtsev, S. Raboin, J-F. Salavy, P. Sardain, J. Szczezepanski, D. Ward.
Fusion Engineering and Design **81** (2006) 469-476

Up-down and in-out asymmetries monitoring based on broadband radiation detectors
M. A. Ochando, F. Medina, B. Zurro, A. Baciero, K. J. McCarthy, M. A. Pedrosa, C. Hidalgo, E. Sánchez, J. Vega, A. B. Portas, L. M. Martínez-Fresno, HIBP Group, ECRH Group, NBI Group and TJ-II Team.
Fusion Science and Technology **50(2)** (August 2006) 313-319

Effect of suprathermal electrons on the impurity ionization state.
M. A. Ochando, F. Medina, B. Zurro, K. J. McCarthy, M. A. Pedrosa, A. Baciero, D. Rapisarda, J. M. Carmona and D. Jiménez
Plasma Phys. and Control. Fusion 48 (November 2006) 1573-1583

Synchronization resources in heterogeneous environments: time-sharing, real-time and JAVA
A. Pereira, J. Vega, L. Pacios, E. Sánchez, A. Portas.
Fusion Engineering and Design. **81** (2006) 1869-1872.

Study of runaway electron generation during major disruptions in JET.
V.V. Plyusnin, V. Riccardo, R. Jaspers, B. Alper, V. Kiptily, J. Mlynar, S. Popovichev, E. de la Luna, D. Andersson and JET EFDA contributors.
Nuclear Fusion **46** (2006) 277-284

Novel passive spectroscopy system for absolutely referenced plasma rotation measurements in clean plasmas

D. Rapisarda, B. Zurro, A. Baciero and V. Tribaldos
Rev. Sci. Instrum. **77** (2006) 33506.

A numerical procedure to simulate cord-integrated passive spectroscopy measurements in TJ-II plasmas
D. Rapisarda, B. Zurro, V. Tribaldos, A. Baciero, and TJ-II Team
Fusion Science and Technology **50(2)** (August 2006) 320-325

A new technique to observe the emission of fast protons from the plasma bulk with improved sensitivity
D. Rapisarda, B. Zurro, A. Moroño, A. Baciero
Rev. Sci. Instrum. **77** (October 2006) 10F519

The effect of carbon additives on the dielectric behaviour of alumina ceramics
R. Román, M.T. Hernández, A. Ibarra, R. Vila, J. Mollá, P. Martín, M. González
Acta Materialia **54** (2006) 2777–2782

Efecto conjugado de impurezas C y ZrO_2 en el comportamiento dieléctrico del Al_2O_3
R. Román, M.T. Hernández, M. González, R. Vila, J. Mollá, P. Martín, A. Ibarra
Bol. Soc Cer Vidrio

Applying a message oriented middleware architecture to the TJ-II remote participation system
E. Sánchez, A. Portas, J. Vega, A. Pereira.
Fusion Engineering and Design **81** (2006) 2063-2067.

Status and prospects for mm-wave reflectometry in ITER
G Vayakis, C I Walker, F Clairet, R Sabot, V Tribaldos, T Estrada, E Blanco, J Sánchez, G G Denisov, V I Belousov, F Da Silva, P Varela, M E Manso, L Cupido, J Dias, N Valverde, V A Vershkov, D A Shelukhin, S V Soldatov, A O Urazbaev, E Yu Frolov and S Heuraux
Nuclear Fusion **46** (September 2006) S836-S845

Overview of the TJ-II remote participation system
J. Vega, E. Sánchez, A. Portas, A. Pereira, A. Mollinedo, J. A. Muñoz, M. Ruiz, E. Barrera, S. López, D. Machón, R.Castro, D. López.
Fusion Engineering and Design **81** (2006) 2045-2050.

TJ-II operation tracking from Cadarache
J. Vega, E. Sánchez, A. Portas, A. Pereira, A. López, E. Ascasíbar, S. Balme, Y. Buravand, P. Lebourg, J. M. Theis, N. Utzel, M. Ruiz, E. Barrera, S. López, D. Machón, R. Castro, D. López, A. Mollinedo, J. A. Muñoz..
Fusion Science and Technology 2006 (in press)

Common Features of Core "Electron-Root" Confinement in Helical Devices
M. Yokoyama, H. Maassberg, C.D. Beidler, V. Tribaldos, K. Ida, F. Castejón, T. Estrada, A. Fujisawa, T. Minami, T. Shimouzuma, Y. Takeiri, J. Herranz, S. Murakami and H. Yamada
Fusion Science and Technology **50-3** (October 2006) 327-342

Comparison of Impurity Poloidal Rotation in ECRH and NBI Discharges of the TJ-II Heliac

B Zurro, A Baciero, D Rapisarda, V Tribaldos and TJ-II Team
Fusion Science and Technology **50-3** (October 2006) 419-427

Charge-exchange spectroscopic diagnostic for the TJ-II stellarator
J. M. Carmona, K. J. McCarthy, R. Balbín, S. Petrov,
Review of Scientific Instruments 77, 10F107 (2006)..

Thermographic calorimetry of the NBI Heating Beam at TJ-II
C. Fuentes, M. Liniers, J. Guasp, J. Doncel, J. Botija, G. Wolfers, J. Alonso , M. Acedo, E. Sánchez, G. Marcon, M. Weber, R. Carrasco, X. Sarasola, B. Zurro, J.Tera
Rev. Sci. Instrum. **77** (2006) 10E519

Search and retrieval of plasma waveforms: structural pattern recognition approach
S. Dormido-Canto, G. Farias, J. Vega, R. Dormido, J. Sánchez, M. Santos, J. A. Martín, G. Pajares.
Rev. Sci. Instruments, 77, 10F514 (2006)

Removal of carbon deposits in narrow gaps by oxygen plasmas at low pressure
J.A. Ferreira, F.L. Tabarés and D. Tafalla
J. Vac. Sci.Technol

Tritium retention in next step devices and the requirements for mitigation and renoval techniques
G Counsell, P Coad, C Grisola, C Hopf, W Jacob, A Kirschner, A Kreter, K Krieger, J. Likonen, V Philipps, J Roth, M Rubel, E Salancon, A. Semerok, FL Tabares, A Widdowson and JET EFDA contributors
Plasma Phys.Control.Fusion **48**(2006) B189-B199

Studies of film formation and erosion by hydrocarbon injection at the plasma edge of TJ-II.
D. Tafalla, F.L. Tabarés, I. García-Cortés, E.de la Cal, J.A. Ferreira and A. Hidalgo.
Journal of Nuclear Materials xxx (2007) xxx–xxx

On the mechanism of carbon film deposition by PACVD in the presence of nitrogen. Cryo-Trapping Assisted Mass Spectrometric Study
F. L Tabarés, JA Ferreira, and D. Tafalla.
Chem Vap Depos

Effect of suprathermal electrons on the impurity ionization state
M. A. Ochando, F. Medina, B. Zurro, K. J. McCarthy, M. A. Pedrosa, A. Baciero, D. Rapisarda, J. M. Carmona and D. Jiménez
Plasma Phys. and Control. Fusion 48 (November 2006) 1573-1583

New technique to observe the emission of fast protons from the plasma bulk with improved sensitivity
D. Rapisarda, B. Zurro, A. Moroño, A. Baciero
Rev. Sci. Instrum. **77** (October 2006) 10F519

TJ-II operation tracking from Cadarache

J. Vega, E. Sánchez, A. Portas, A. Pereira, A. López, E. Ascasíbar, S. Balme, Y. Buravand, P. Lebourg, J. M. Theis, N. Utzel, M. Ruiz, E. Barrera, S. López, D. Machón, R. Castro, D. López, A. Mollinedo, J. A. Muñoz..
Fusion Science and Technology, 50, 2006, 464-471

Common Features of Core "Electron-Root" Confinement in Helical Devices
M. Yokoyama, H. Maassberg, C.D. Beidler, V. Tribaldos, K. Ida, F. Castejón, T. Estrada, A. Fujisawa, T. Minami, T. Shimouzuma, Y. Takeiri, J. Herranz, S. Murakami and H. Yamada
Fusion Science and Technology **50-3** (October 2006) 327-342

Comparison of Impurity Poloidal Rotation in ECRH and NBI Discharges of the TJ-II Heliac
B Zurro, A Baciero, D Rapisarda, V Tribaldos and TJ-II Team
Fusion Science and Technology **50-3** (October 2006) 419-427

Impact of different confinement regimes on the two-dimensional structure of edge turbulence.
J A Alonso, S J Zweben, P Carvalho, J L de Pablos, E de la Cal1,
C Hidalgo, T Klinger, B Ph van Milligen, R J Maqueda, M A
Pedrosa, C Silva, M Spolaore, H Thomsen and the TJ-II team. Plasma Phys. Control. Fusion **48** (2006) B465–B473

Two-Dimensional Turbulence Analysis Using High-Speed Visible Imaging in TJ-II J. A. Alonso, S. J. Zweben, J. L. de Pablos, E. de la Cal, C. Hidalgo, T. Klinger, B. Ph. Van Milligen, M. A. Pedrosa, C. Silva, H. Thomsen. Stellarator News, 103, 2006

H_α measurement and neutral particle transport in Heliotron J
S. Kobayashi, H. Yabutani, Y. Nakashima, Y. Higashizono, K. Nagasaki, T. Mizuuchi, H. Okada, F. Sano, **A. Cappa**, K. Kondo, Y. Nakamura, Y. Suzuki
Review of Scientific Instruments, 77, 10E527 (2006)

Critical transition for the edge shear layer formation: Comparison of model and experiment.
B.A. Carreras, L. García, M.A. Pedrosa and C. Hidalgo
Phys. of Plasmas **13**, 122509 (2006)

Intermittency and structures in edge plasma turbulence
C. Hidalgo, B.Ph. van Milligen, and M.A. Pedrosa
Comptes Rendus Physique **7**, 6 (2006) 679

A study of pulse propagation in a simplified critical gradient model
B. van Milligen
Stellarator News, publicado por Fusion Energy Division, Oak Ridge National Laboratory.

Renormalization of tracer turbulence leading to fractional differential equation.
R. Sánchez, B.A. Carreras, D.E. Newman, V.E. Lynch and B.Ph. van Milligen.
Phys. Rev. E **74** (2006) 016305

Alternative Cleaning Technique for the Removal of Carbon Deposits
J.A. Ferreira, F.L. Tabarés, D. Tafalla
Journal of Nuclear Materials (2007)

Hydrogen recycling and puffing at a poloidal limiter of TJ-II

E. de la Cal, J. Guasp, F.L. Tabarés, D. Tafalla, A. Alonso, P. Carvalho, A. Salas, B. Zurro, TJ-II Team
Journal of Nuclear Materials (2007), doi: 10.1016/j.jnucmat.2007.01.061

Plasma Breakdown using Second-Harmonic EC Waves in Helical Devices
K. Nagasaki,_ T. Mizuuchi, F. Sano, H. Okada, S. Kobayashi and Heliotron J Team
A. Cappa, F. Castejón, A. Fernández, E. de la Cal,
T. Estrada, V. Tribaldos, F. Tabarés, D. Tafalla and TJ-II Team
Y. Yoshimura and CHS Team
K. Kondo and K. Takahashi. H. Shidara
Journal of the Korean Physical Society, Vol. 49, December 2006, pp. S18_S24

Relativistic plasma dielectric tensor evaluation based on the exact plasma dispersion functions concept.
F. Castejón and S. S. Pavlov
Physics of Plasmas **13** (2006) 072105

Ion orbits and ion confinement studies on ECRH plasmas in TJ-II stellarator.
F. Castejón, J. M. Reynolds, J. M. Fontdecaba, R. Balbín, J. Guasp, D. López-Bruna, I. Campos, L. A. Fernández, D. Fernández-Fraile, V. Martín-Mayor, and A. Tarancón.
Fusion Science and Technology **50** (2006) 412.

Ion kinetic transport in the presence of collisions and electric field in TJ-II ECRH plasmas.
F. Castejón, L. A. Fernández, J. Guasp, V. Martín-Mayor, A. Tarancón, and J. L. Velasco.
Submited to Plsma Physics and Controlled fusion, 2006.

Recommended data for capture cross sections in B5+ + H collisions
L. F. Errea, F Guzmán, Clara Illescas, L Méndez, B Pons, A Riera and J Suárez
Plasma Phys. Control. Fusion **48** (2006) 1585–1604

Precision control of gyrotron frequency by feedback loop
A. Fernandez Curto, Golubyatnikov G. et al.
Letters to Journal of Technical Physics 32(15) (2006) 13-18 (in Russian).

Reflectometría de microondas como técnica de diagnosis en plasmas de fusión y su aplicación en el stellarator TJ-II
T. Estrada
Revista Española de Física **20(2)** (2006) 35-40

VIII.1.2. Books

Quasi-optical transmission lines at CIEMAT and at GPI
A.Fernández, K.Likin, G.Batanov, L.Kolik, A.Petrov, K.Sarksyan, N.Kharchev, W.Kasparek and R. Martin
in *"Quasi-optical control of intense Microwave Transmission"*
NATO Science Series II. Matemathics, Physics and Chemistry – Vol.203
Published by Springer. The Netherlands ISBN-13 978-1-4020-3637-8 (PB) 2005

VIII.1.3. Technical reports

Experimental electron heat diffusion in TJ-II ECRH plasmas
V. I. Vargas. D. López-Bruna, J. Herranz, F. Castejón
Technical report, Ciemat, 1079, Julio 2006

Cost Evaluation And Time Schedule Of The Superconducting DTL Alternative For IFMIF.In-If-Acel-001.
J. Lucas, B. Brañas.
Final report of EFDA Task TW5-TTMI-001, deliverable 5. Junio, 2006. 51 p

Residual Magnetics Field Coils For The Neutral Beam Test Facility (NBTF).
A. López-Fraguas, J. Alonso, G. Barrera, J. Botija, A. Soleto, M. Liniers
Final report of EFDA Task TW4-THHN-IITF2

Energy Storage System For A Pulse DEMO.
J. Lucas, M. Cortés.
Final report of EFDA Task TW5-TRP-007. Mayo, 2006. 95 p.

DEMO Conceptual Studies. Segmentation And Maintenance.
J. Lucas, M.Pinilla.
Final report of EFDA Task, TW5-TRP-003. Julio 2006. 98 p.

State-of-the-art of high temperature innovative processes for H_2 production.
TW5-TRP-008-Del1.
M.Romero, A.Vidal.
Report number: IN-DM-H2Pr-001

Study of oxidizing agents for tritium removal in iter compatible conditions: alternatives to oxygen and ozone
F.L. Tabarés
Report on the work done on the EFDA task 04-1175

VIII.2. CONFERENCES AND WORKSHOPS

Pedestal Physics Working Session, ITM-IMP3 Project, Cadarache, 3-5 April 2006.

Overview of the JET New Diagnostic Capability for Edge Pedestal Measurements

E. de la Luna

16th Topical Conference on High-Temperature Plasma Diagnostics, Williamsburg (Virginia, USA), 7-11 May 2006

1.A new diagnostic neutral beam injector and associated diagnostics for the TJ-II stellarator
J. M. Carmona, K. J. McCarthy, R. Balbín, S. Petrov,

2. Absolute response of luminescent screens to low energy ions

D. Jiménez-Rey, B. Zurro, G. Garcia, A. Baciero, L. Rodríguez-Barquero, K.J. McCarthy.

3. Approach to real-time event detection in continuous data flows based on neuro-fuzzy models

J. A. Martin, M. Santos, G. Pajares, G. Farias, N. Duro, J. Sánchez, R. Dormido, S. Dormido-Canto, J. Vega, M Ruiz, E. Barrera, S. López.

4. A new technique to observe the emission of fast protons from the plasma bulk with improved sensitivity

D. Rapisarda, B. Zurro, A. Moroño, A. Baciero

5. Thermographic calorimetry of the NBI Heating Beam at TJ-II

C. Fuentes, M. Liniers, J. Guasp, J. Doncel, J. Botija, G. Wolfers, J. Alonso , M. Acedo, E. Sánchez, G. Marcon, M. Weber, R. Carrasco, X. Sarasola, B. Zurro, J.Tera

14th Joint Workshop on Electron Cyclotron Emission and Electron Cyclotron Resonance Heating, Santorini (Greece), 9 - 12 May 2006

http://ec14.conferences.gr/

1. Relativistic effects on EBW heating TJ-II Stellarator

F. Castejón, A. Cappa, M. Terechshenko, S. S. Pavlov and A. Fernández

http://ec14.conferences.gr/fileadmin/dtemplates/ec14/latest_abstracts/47.pdf

2. The Electron Bernstein Wave Emission Radiometer System for the TJ-II Stellarator

J.B.O. Caughman, A.Fernández, F.Castejón, A.Cappa, M.C. Carter, D.A. Rasmussen and J.B. Wilgen

http://ec14.conferences.gr/fileadmin/dtemplates/ec14/latest_abstracts/88.pdf

3. Experimental ECCD Efficiency in the TJ-II Stellarator

A.Fernández, K.Nagasaki, A.Cappa, F.Castejón, J.M.Fontdecaba

http://ec14.conferences.gr/fileadmin/dtemplates/ec14/latest_abstracts/81.pdf

4. High Power Measurements on a Remote Steering Upper Port Launcher mock-up for ITER

M.F. Graswinckel, W.A. Bongers, Á. Fernández , I. Danilov, B.S.Q. Elzendoorn, R. Heidinger, O. Kruyt,B. Lamers, B. Piosczyk, D.M.S. Ronden, M. Schmid, A.G.A. Verhoeven

http://ec14.conferences.gr/fileadmin/dtemplates/ec14/latest_abstracts/31.pdf

5. Measurement of single pass EC absorption using transmitted waves in Heliotron J

K.Nagasaki, t.Tsuji, M.Nosaku, N.Shimazaki, T.Mizuuchi, H.Okada, S.Kobayashi, K.Sakamoto, Z.Feng, Y.Torii, K.Kondo, M.Kaneko, G.Motojima, S.Watanabe, A.Cappa and F.Sano.

http://ec14.conferences.gr/fileadmin/dtemplates/ec14/latest_abstracts/46.pdf

6. The multichannel Extension of the Martin-Puplett Interferometer for perpendicular and oblique ECE measurements on JET
C. Sozzi, A. Simonetto, S. Garavaglia, E. de la Luna, J. Fessey, S.Nowak1, M. Zerbini4 and JET-EFDA contributors
http://ec14.conferences.gr/fileadmin/dtemplates/ec14/latest_abstracts/41.pdf

7. Design of the Remote-Steering ITER ECRH Upper-Port Launcher
A.G.A. Verhoeven, W.A. Bongers, A. Bruschi, S. Cirant, I. Danilov, B.S.Q. Elzendoorn, Á. Fernández, M.F. Graswinckel, R. Heidinger, M. Henderson, J.Jamar, W. Kasparek, O.G. Kruijt, B. Lamers,B. Plaum, D.M.S. Ronden, G. Saibene, F.C. Schüller, E. Westerhof and H. Zohm
http://ec14.conferences.gr/fileadmin/dtemplates/ec14/latest_abstracts/24.pdf

17th International Conference on Plasma Surface Interaction, Hefei, China, 22-26 May 2006

http://202.127.205.20/

1. Hydrogen recycling and puffing at a poloidal limiter of TJ-II

E. de la Cal, J. Guasp, F.L. Tabarés, D. Tafalla, A. Alonso, P. Carvalho[a], A. Salas, B. Zurro and TJ-II Team
http://202.127.205.20/manage/article/4/edelacal/abs_PaperJNM.pdf

2. Atomic chemical reactions for the removal of carbon deposits in ITER

J. A. Ferreira, F. L. Tabarés, D. Tafalla

http://202.127.205.20/manage/article/6/ferreira/abs_Ferreira17PSI.pdf

3. Tritium Inventory Control Through Chemical Reactions
F.L. Tabarés, J.A. Ferreira and D. Tafalla
http://202.127.205.20/manage/article/6/tabares/abs_Tabares17PSI.pdf

4. Studies of film formation and erosion by hydrocarbon injection at the plasma edge of TJ-II.
D. Tafalla, F.L. Tabarés, I. García-Cortés, E.de la Cal, J.A. Ferreira and A. Hidalgo.
http://202.127.205.20/manage/article/5/tabares/abs_Studies of HC injection.pdf

8th Workshop on Hydrogen Isotopes, Huangshan, China, 29-30 May 2006
http://202.127.205.20/

Deuterium ICRF conditioning for tritium removal and surface isotope exchange
E. de la Cal.
http://202.127.205.20/HWorkshopPresentation/S2T1.pdf

ELECTROCERAMICS X, Toledo (Spain), 18-22 Junio 2006

Microstructural and Electrical Features of Lithium doped Ce-Monazite
M.T. Hernández, R.Vila, J.R.Jurado, E. Chinarro, J. Molla and P. Martín

33rd EPS Conference on Controlled Fusion and Plasma Physics, Rome (Italy), 19-23 June 2006
http://eps2006.frascati.enea.it/index.htm

Impact of different confinement regimes on the two-dimensional structure of edge turbulence
J.A. Alonso, S.J. Zweben, J.L. de Pablos, E. de la Cal, C. Hidalgo, T. Klinger, B.Ph. van Milligen, M.A. Pedrosa , M. Spolaore, H. Thomsen

Proceedings of the Conference, I5.004

http://eps2006.frascati.enea.it/presentazioni_finali/Aula_Mayor/Friday/Alonso/Alonso/AlonsoEPS2006_Talk.pdf

Study of Doppler reflectometry capability to determine the perpendicular velocity and the k-spectrum of the density fluctuations using a 2D full-wave code
E. Blanco, T. Estrada, E. Holzhauer, and J. Sánchez.

Proceedings of the Conference, P 4.195

http://eps2006.frascati.enea.it/pdf_packs/P4.pdf

First results from the new diagnostic neutral beam injector and charge-exchange diagnostic system on the TJ-II stellarator
J. M. Carmona, K. J. McCarthy, R. Balbín

Ion kinetic transport in presence of collisions and electric field in TJ-II ECRH plasmas.
F. Castejón1,4, L. A. Fernández2,4, J. Guasp1, V. Martín-Mayor2,4, J. M. Reynolds3,4, A. Tarancón3,4, and J. L. Velasco3,4

Proceedings of the Conference, P 1.135

Influence of low order rational magnetic surfaces on electron internal transport barriers in the stellarator TJ-II
T. Estrada, D. López-Bruna, F. Medina, E. Ascasíbar et al.

Proceedings of the Conference, P 1.140

Characterization of the quasi-coherent oscillations by HIBP diagnostic in the TJ-II stellarator
L. Krupnik, A.A. Chmyga, N. Dreval, L. Eliseev*, S.M. Khrebtov, A.D. Komarov, A.S. Kozachok, A.Melnikov*, S. V. Perfilov*, R. Jiménez-Gómez, , A. Alonso, M.A. Pedrosa, J. L. de Pablos, C. Hidalgo, T. Estrada

Heavy Ion Beam Probe investigations of plasma potential in ECRH and NBI in the TJ-II stellarator
A.V. Melnikov, L. Eliseev, S. V. Perfilov, A.A. Chmyga, S.M. Khrebtov, A.D. Komarov, A.S. Kozachok, L. Krupnik, A. Alonso, J. L. de Pablos, A. Cappa, A. Fernández, C. Fuentes, C. Hidalgo, M. Liniers, M.A. Pedrosa

Proceedings of the Conference, O3.017

http://eps2006.frascati.enea.it/pdf_packs/Contr_Or.pdf

On the time scales and statistical properties of turbulence during ExB sheared flow development in the TJ-II stellarator
M.A. Pedrosa, O. Orozco, C. Hidalgo, J.A. Alonso, J.L. de Pablos

A study of ion heating by means of spectroscopic techniques in the TJ-II stellarator
D. Rapisarda, B. Zurro, A. Baciero, V. Tribaldos and TJ-II team
Proceedings of the Conference, P 1.133

He emission profiles in TJ-II edge plasmas and their simulation by EIRENE
F.L. Tabarés, A. Hidalgo, D. Tafalla, J. Guasp, A. Salas, I. Pastor and J. Herranz

Dependencies of electron heat diffusion in TJ-II ECRH plasmas
V. I. Vargas, D. López-Bruna, J. Herranz, F. Castejón
Proceedings of the Conference, P 1.134

A study of the electron to ion root transition in the TJ-II stellarator by means of impurity poloidal rotation measurements
B. Zurro, A. Baciero, D. Rapisarda, V. Tribaldos and TJ-II Team
Proceedings of the Conference, P 1.132

Workshop on Remote Participation for Fusion Research, Riga (Latvia) 20-21 June 2006
TJ-II remote participation model: towards thin client environments
J. Vega

9th Workshop on the Electric Fields, Structures, and Relaxation in Edge Plasmas 2006, Rome (Italy), 26-27 June 2006
http://www.ipp.cas.cz/Tokamak/conf/efsrep06/

On the relaxation physics of plasma potential and perpendicular flows in the boundary of stellarator and tokamak plasmas

M.A. Pedrosa, C. Silva, C. Hidalgo, P. Carvalho, A. Alonso, J.L. de Pablos, R.O. Orozco, and the TJ-II team

Vacuum Measurement, Leak Detection and Calibration. Quality Control in Advanced Industries, Salamanca (Spain) June 26-28, 2006

http://www.icmm.csic.es/aseva/ws18_home.html

Mass Spectrometric Análisis of Complex Gas Mixtures by using a Cryogenic Trap: Application to H_2:CH_4:N_2 plasmas

J. A. Ferreira, F. L. Tabarés

VIII.3. PH. D. THESIS AND MASTER DIPLOMAS

VIII.3.1. Thesis

Emilio Blanco
Desarrollo de un código de onda completa en dos dimensiones y su aplicación al estudio de la reflectometría de microondas como técnica de diagnosis en plasmas de fusión
Universidad Complutense de Madrid. Facultad de Ciencias Físicas.
July 2006

VIII.3.2. Master Diplomas (Diploma de Estudios Avanzados)

David Jiménez Rey
Ionoluminiscencia y su aplicación a plasmas de fusión
Departamento de Física de los Materiales de la Universidad Nacional de Educación a Distancia (UNED)
January 2006

J. A. Ferreira
Métodos químicos de limpieza de co-depósitos en dispositivos de Fusión
Universidad Complutense de Madrid. Facultad de Ciencias Físicas.
July 2006

VIII.4. PUBLICATIONS ON INERTIAL FUSION

VIII.4.1. Chapter in Books

1.- "Key Aspects on the Non-Proliferation Measures".
G. Velarde, N.C. Santamaria
in *Coutering Nuclear and Radiological Terrorism*. S. Apikyan and d. Diamond (eds.), pp. 85-94. Springer (2006). ISBN 1-4020-4920-X.

2.- "Radiation damage in metals, and amorphous silica in inertial fusion reactors: Modeling and experiments".
J.M. Perlado, M. Victoria, M.J. Caturla, J. Marian, M.L. Gámez, C. Arévalo, E. Martínez, F. Mota, M. Velarde, G. Velarde and P. Cepas
in *Inertial Fusion Sciences and Applications 2005*. J.C. Gauthier, B. Hammel, H. Azechi, C. Labaune (Eds.), pp. 805-809. EDP Sciences. (2006). ISBN 2-86883-929-0.

3.- "Sensitivity of Shallow Land Burial to neutron environment and activation cross sections in IFE thick-liquid concepts".
O. Cabellos, J. Sanz, S. Reyes, J. Latkowski and N. García-Herranz
in *Inertial Fusion Sciences and Applications 2005*. J.C. Gauthier, B. Hammel, H. Azechi, C. Labaune (Eds.), pp. 821-823. EDP Sciences. (2006). ISBN 2-86883-929-0.

4.- *"*Behaviour of three chemical forms of tritium in the environment after release from inertial fusion reactors".
M. Velarde, J.M. Perlado and L. Sedano
in *Inertial Fusion Sciences and Applications 2005*. J.C. Gauthier, B. Hammel, H. Azechi, C. Labaune (Eds.), pp. 849-851. EDP Sciences. (2006). ISBN 2-86883-929-0.

5.- "Code to calculate optical properties for plasmas in a wide range of densities".
R. Rodríguez, J.M. Gil, R. Florido, J.G. Rubiano, P. Martel and E. Mínguez
in *Inertial Fusion Sciences and Applications 2005*. J.C. Gauthier, B. Hammel, H. Azechi, C. Labaune (Eds.), pp. 981-984. EDP Sciences. (2006). ISBN 2-86883-929-0.

6.- "Line photon transport in a non-homogeneous plasma using radiative coupling coefficients".
R. Florido, J.M. Gil, R. Rodríguez, J.G. Rubiano, P. Martel and E. Mínguez
in *Inertial Fusion Sciences and Applications 2005*. J.C. Gauthier, B. Hammel, H. Azechi, C. Labaune (Eds.). Journal de Physique IV, vol. 133, pp. 993-996. EDP Sciences. (2006). ISBN 2-86883-929-0.

7.- "Calculation of optical properties for hot plasmas using a screened hydrogenic model".
J.G. Rubiano, R. Rodríguez, R. Florido, M.A. Mendoza, J.M. Gil, P. Martel and E. Mínguez
in *Inertial Fusion Sciences and Applications 2005*. J.C. Gauthier, B. Hammel, H. Azechi, C. Labaune (Eds.), pp. 997-1000. EDP Sciences. (2006). ISBN 2-86883-929-0.

8.- "Calculation of opacities and emisivities for carbon plasmas under NLTE and LTE conditions".
J.M. Gil, R. Rodríguez, R. Florido, J.G. Rubiano, P. Sauvan, P. Martel and E. Mínguez
in *Inertial Fusion Sciences and Applications 2005*. J.C. Gauthier, B. Hammel, H. Azechi, C. Labaune (Eds.). Journal de Physique IV, vol. 133, pp. 1005-1008. EDP Sciences. (2006). ISBN 2-86883-929-0.

9.- "Interaction of supernovae remnants: From the circumstellar medium to the terrestrial laboratory".
P. Velarde, D. García-Senz, E. Bravo, F. Ogando, A. Relaño, C. García, E. González, M. Lachaise and E. Oliva
in *Inertial Fusion Sciences and Applications 2005*. J.C. Gauthier, B. Hammel, H. Azechi, C. Labaune (Eds.), pp. 10351037-. EDP Sciences. (2006). ISBN 2-86883-929-0.

VIII.4.2. Articles in refereed International Journals:

1.- *Interaction of supernova remnants: From the circumstellar medium to the terrestrial laboratory.*
P. Velarde, D. García-Senz, E. Bravo, F. Ogando, A. Relaño, C. García, E. Oliva
Physics of Plasmas, 13 (2006) 092901-1/10.

2.- *Transverse spatial improvement of a transiently pumped soft-x-ray amplifier.*
K. Cassou, Ph. Zeitoun, P. Velarde, F. Roy, F. Ogando, M. Fajardo, G. Faivre,and D. Ros
Physical Review A, 74. págs. 4. (2006)

3.- *Effect of Activation Cross Section Uncertainties on the Radiological Assessment of the MFE/DEMO First Wall*
O. Cabellos, S. Reyes, J. Sanz, A. Rodriguez, M. Youssef, M. Sawan
Fusion Engineering and Design, Vol. 81, 1561-1565 (2006)

4.- *Innovative ignition scheme for ICF-impact fast ignition.*
M. Murakami, H. Nagatomo, H. Azechi, F. Ogando, M. Perlado, S. Eliezer
Nuclear Fusion, 46, pp. 99-103 (2006)

5.- *Radiation damage in metals, and amorphous silica in inertial fusion reactors: Modeling and experiments*.
J.M. Perlado, M. Victoria, M.J. Caturla, J. Marian, M.L. Gámez, C. Arévalo, E. Martínez, F. Mota, M. Velarde, G. Velarde and P. Cepas
Journal de Physique IV, vol. 133, pp. 805-809. EDP Sciences. (2006).

6.- *Sensitivity of Shallow Land Burial to neutron environment and activation cross sections in IFE thick-liquid concepts.*
O. Cabellos, J. Sanz, S. Reyes, J. Latkowski and N. García-Herranz
Journal de Physique IV, vol. 133, pp. 821-823. EDP Sciences. (2006).

7.- *Behaviour of three chemical forms of tritium in the environment after release from inertial fusion reactors.*
M. Velarde, J.M. Perlado and L. Sedano
Journal de Physique IV, vol. 133, pp. 849-851. EDP Sciences. (2006).

8.- *Code to calculate optical properties for plasmas in a wide range of densities.*
R. Rodríguez, J.M. Gil, R. Florido, J.G. Rubiano, P. Martel and E. Mínguez
Journal de Physique IV, vol. 133, pp. 981-984. EDP Sciences. (2006).

9.- *Line photon transport in a non-homogeneous plasma using radiative coupling coefficients.*
R. Florido, J.M. Gil, R. Rodríguez, J.G. Rubiano, P. Martel and E. Mínguez
Journal de Physique IV, vol. 133, pp. 993-996. EDP Sciences. (2006).

10.- *Calculation of optical properties for hot plasmas using a screened hydrogenic model.*
J.G. Rubiano, R. Rodríguez, R. Florido, M.A. Mendoza, J.M. Gil, P. Martel and E. Mínguez
Journal de Physique IV, vol. 133, pp. 997-1000. EDP Sciences. (2006).

11.- *Calculation of opacities and emisivities for carbon plasmas under NLTE and LTE conditions.*
J.M. Gil, R. Rodríguez, R. Florido, J.G. Rubiano, P. Sauvan, P. Martel and E. Mínguez
Journal de Physique IV, vol. 133, pp. 1005-1008. EDP Sciences. (2006).

12.- *Interaction of supernovae remnants: From the circumstellar medium to the terrestrial laboratory.*
P. Velarde, D. García-Senz, E. Bravo, F. Ogando, A. Relaño, C. García, E. González, M. Lachaise and E. Oliva
Journal de Physique IV, vol. 133, pp. 10351037-. EDP Sciences. (2006).

13.- *Safety issues of Nuclear Production of Hydrogen.*
M. Piera, J.M. Martínez-Val, M.J. Montes
Journal of Energy Conversion and Management, 47, pp. 2732-2739. (2006).

14.- *PKA Energy Spectra and Primary Damage Identification in Amorphous Silica under Different Neutron Energy Spectra*
M.L. Gámez, M. Velarde, F. Mota, J.M. Perlado, M. León, A. Ibarra
Accepted for publication in Journal of Nuclear Materials (Elsevier) (2006)
In press, doi: 10.1016/j.jnucmat.2007.03.050.

15.- *Transmutation analysis of realistic low-activation steels for magnetic fusion reactors and IFMIF*
O. Cabellos, J. Sanz, N. García-Herranz, S. Díaz, S. Reyes, S. Piedloup
Accepted for publication in Journal of Nuclear Materials (Elsevier) (2006)
In press, doi: 10.1016/j.jnucmat.2007.04.023

16.- *Temperature dependence of damage accumulation in α-Zirconium*
C. Arévalo, M.J. Caturla, J.M. Perlado
Accepted for publication in Journal of Nuclear Materials (Elsevier) (2006)
In press, available on line

17.- *Identification and characterization of defects produced in irradiated fused silica through molecular dynamics.*
F. Mota, M.J. Caturla, J.M. Perlado, A. Ibarra, M. León, J. Mollá
Accepted for publication in Journal of Nuclear Materials (Elsevier) (2006)
In press, available online

18.- *The Role of the Fused Silica Stoichiometry on the Intrinsic Defects Concentration.*
J. Mollá, F. Mota, M. León, A. Ibarra, M.J. Caturla, J.M. Perlado
Accepted for publication in Journal of Nuclear Materials (Elsevier) (2006)
In press, available online

19.- *Atomistically-informed Dislocation Dynamics in fcc Crystals*
E. Martínez, J. Marian, A. Arsenlis, M. Victoria, J.M. Perlado
Accepted for publication in Journal of the Mechanics and Physics of Solids (Elsevier Science). (September 2006).

20.- *Synchronous Parallel Kinetic Monte Carlo*
E. Martínez, J. Marian, M.H. Kalos, J.M. Perlado
Accepted for publication in Journal of Computational Physics (Elsevier Science). (December 2006).

21.- *Damage in Fe using Kinetic MonteCarlo: modeling neutron irradiation*
L. Gámez, E. Martínez, J.M. Perlado, P. Cepas, M.J. Caturla, M. Victoria, J. Marian, C. Arévalo, M. Hernández, D. Gómez
Accepted for publication in Fusion Engineering and Design (Elsevier Science). (July 2006).

22.- *Modelling irradiation effects in fusion materials.*
M. Victoria, S. Dudarev, J. L. Boutard, E. Diegele, R. Lässer , A. Almazouzi, M. J. Caturla, C. C. Fu, J. Källne, L. Malerba, K. Nordlund, M. Perlado, M. Rieth, M. Samaras, R. Schaeublin , B. Singh, F. Willaime
Accepted for publication in Fusion Engineering and Design (2006)

23.- *Dose Assessments for Normal and Accidental Releases of Elemental Tritium and Tritiated Water Vapour.*
M. Velarde, J.M. Perlado
Accepted for publication in Journal of Nuclear Materials (2006)

24.- *The Analytic Coarse-Mesh Finite-Difference for Multigroup and Multidimensional Diffusion Calculations.*
J.M. Aragonés, C. Ahnert, N. García-Herránz
Accepted for publication in Nuclear Science & Engineering. ANS (2006)

VIII.4.3. Communications to refereed International Conferences

1.- *Influence of anisotropic defect diffusion on microstructure evolution in hcp-Zr.*
M.J. Caturla, C. Arévalo, J.M. Perlado
European Materials Research Society Annual Meeting (EMRS)
Niza (Francia) (29 Mayo – 2 Junio, 2006)

2.- *Damage accumulation in Fe under ion and electron irradiation conditions.*
M.J. Caturla, E. Martínez, M. Hernández-Mayoral, J.M. Perlado
European Materials Research Society Annual Meeting (EMRS)
Niza (Francia) (29 Mayo – 2 Junio, 2006)

3.- *Fission spectra for cladding formed by Zirconium alloys: application to MonteCarlo simulations.*
C. Arévalo, M.J. Caturla, J.M. Perlado
Computer Simulations of Radiation Effects in Solids (COSIRES) 2006
WA (EUA) (18-23 Junio, 2006)

4.- *Defects produced in irradiated fused silica: influence of hydrogen concentration.*
M. Mota, M.J. Caturla, J.M. Perlado, A. Ibarra, J. Mollá

Computer Simulations of Radiation Effects in Solids (COSIRES) 2006
WA (EUA) (18-23 Junio, 2006)

5.- *Damage in Fe using Kinetic Montecarlo and Dislocation Dynamics.*
E. Martínez, L. Gámez, P. Cepas, J.M. Perlado, M. Victoria, M.J. Caturla, J. Marian, M. Hernández, D. Gómez
24th Symposium on Fusion Technology
Varsovia (Polonia) (11-15 Septiembre, 2006)

6.- *Advances in Target Design and Materials Physics for IFE at DENIM.*
J.M. Perlado, G. Velarde, J.M. Martínez-Val, E. Mínguez, J. Sanz, M. Velarde, P. Velarde, C. Arévalo, E. Bravo, O. Cabellos, P. Cepas, M.J. Caturla, S. Eliezer, R. Florido, L. Gámez, C. García, N. García-Herranz, D. García-Senz, J.M. Gil, E. González, P.T. León, R. Manzini, J. Marian, P. Martel, E. Martínez, F. Mota, F. Ogando, E. Oliva, M. Piera, A. Relaño, S. Reyes, R. Rodríguez, J.G. Rubiano, P. Sauvan, M. Victoria
21st IAEA Fusion Energy Conference
Chengdu (China) (16 –21 Octubre, 2006)

7.- *Recent results on fast ignition jet impact scheme.*
P. Velarde, F. Ogando, C. García, E. Oliva, A. Kasperczuk, T. Pisarczyk, J. Ullschmied, S. Eliezer, M. Perlado
21st IAEA Fusion Energy Conference
Chengdu (China) (16 –21 Octubre, 2006)

8.- *Atomistic simulations of displacement cascades in fused silica: effect of H.*
F. Mota, M.J. Caturla, J.M. Perlado, J. Mollá, A. Ibarra, A. Kubota
Materials Research Society Fall Meeting (MRS)
Boston (EUA) (27 Noviembre – 1 Diciembre, 2006)

9.- *Behaviour of irradiated hcp Zirconium coupling molecular dynamics and MonteCarlo simulations.*
C. Arévalo, M.J. Caturla, J.M. Perlado
Materials Research Society Fall Meeting (MRS)
Boston (EUA) (27 Noviembre – 1 Diciembre, 2006)

VIII.4.4. Invited Communications to International Conferences

1.- *Inertial confinement fusion research in Spain: From a difficult beginning to a hopeful future.*
G. Velarde
29th European Conference on Laser Interaction with Matter (29th ECLIM)
Madrid (España) (11-16 Junio, 2006)

2.- *Advances in Materials Physics for IFE at DENIM.*

J.M. Perlado, J. Sanz, C. Arévalo, O. Cabellos, E.P. Cepas, M.J: Caturla, T. Díaz de la Rubia, B. Gámez, M.L. Gámez, N. García-Herránz, J. Juan, E. Martínez, J. Marian, F. Mota, S. Reyes, M. Velarde, M. Victoria
29th European Conference on Laser Interaction with Matter (29th ECLIM)
Madrid (España) (11-16 Junio, 2006)

3.- *Monte Carlo simulations of electron irradiation damage in hcp metals.*
C. Arévalo, M.J. Caturla, J.M. Perlado
29th European Conference on Laser Interaction with Matter (29th ECLIM)
Madrid (España) (11-16 Junio, 2006)

4.- *Atomistic simulations of displacement cascades in Fused Silica: It is compared with different concentration of H in the bulk.*
F. Mota, M.J. Caturla, J.M. Perlado, A. Ibarra, J. Molla
29th European Conference on Laser Interaction with Matter (29th ECLIM)
Madrid (España) (11-16 Junio, 2006)

5.- *Comparison of Monte Carlo neutron transport codes and Nuclear Data Libraries for neutron calculations in different IFE concepts.*
O. Cabellos, N. García-Herránz, J. Sanz
29th European Conference on Laser Interaction with Matter (29th ECLIM)
Madrid (España) (11-16 Junio, 2006)

6.- *Safety and Environmental Analysis for Fusion Facilities: Methodologies and Applications.*
J. Sanz, O. Cabellos, S. Reyes, N. García-Herránz, J. Juan
29th European Conference on Laser Interaction with Matter (29th ECLIM)
Madrid (España) (11-16 Junio, 2006)

7.- *Impact of activation cross section uncertainties on the waste management performance of irradiated steels under different neutron environments of IFE Thick-Liquid Concepts..*
N. García-Herránz, O. Cabellos, S. Reyes, J. Sanz
29th European Conference on Laser Interaction with Matter (29th ECLIM)
Madrid (España) (11-16 Junio, 2006)

8.- *Safety and environmental considerations for laser IFE chambers.*
S. Reyes, J.F. Latkowski, W.R. Meier, J. Sanz, O. Cabellos
29th European Conference on Laser Interaction with Matter (29th ECLIM)
Madrid (España) (11-16 Junio, 2006)

9.- *Hydrodynamic simulation of laser plasma generation for transiently pumped soft x-ray amplifier.*
K. Cassou, Ph. Zeitoun, P. Velarde, E. Oliva, C. García, F. Ogando, F. Roy, D. Ros
29th European Conference on Laser Interaction with Matter (29th ECLIM)
Madrid (España) (11-16 Junio, 2006)

10.- *Atomic physics and plasmas optical properties at DENIM..*

E. Mínguez, R. Florido, J.M. Gil, P. Martel, M.A. Mendoza, R. Rodríguez, J.G. Rubiano, P. Sauvan
29th European Conference on Laser Interaction with Matter (29th ECLIM)
Madrid (España) (11-16 Junio, 2006)

11.- *Fast ignition by jet impact..*
P. Velarde, C. García, E. Oliva, M. Lachaise, E. González, F. Ogando, E. Pérez
29th European Conference on Laser Interaction with Matter (29th ECLIM)
Madrid (España) (11-16 Junio, 2006)